Spring 5-9-2020

Novel regulatory roles of endocytic membrane trafficking proteins in mitochondrial homeostasis

Trey Farmer
University of Nebraska Medical Center

Novel regulatory roles of endocytic membrane trafficking proteins in mitochondrial homeostasis

By

Trey Farmer

A DISSERTATION

Presented to the Faculty of

the University of Nebraska Graduate College

in Partial Fulfillment of the Requirements

for the Degree of Doctor of Philosophy

Biochemistry & Molecular Biology
Graduate Program

Under the Supervision of Professor Steve Caplan

University of Nebraska Medical Center
Omaha, Nebraska

May, 2020

Supervisory Committee:

Paul Sorgen, Ph.D.

Justin Mott, M.D., Ph.D.

Keith Johnson, Ph.D.

Novel regulatory roles of endocytic membrane trafficking proteins in mitochondrial homeostasis

Trey Farmer, Ph.D.

University of Nebraska, 2020

Supervisor: Steve Caplan, Ph.D.

Endocytic membrane trafficking is a basic cell process that is critical for regulating the transport of lipids and proteins. Our lab focuses on the cellular functions and mechanisms of the proteins that regulate these pathways. A key family of regulatory proteins is the C-terminal Eps15 Homology Domain (EHD) protein family. The EHD family includes EHD1-4, which are ubiquitously expressed in mammalian tissues. While these isoforms do have some overlapping functions, each protein also has distinct activities in regulating the shape and fission of membranes throughout the endocytic pathways. Specifically, EHD1 uses ATP hydrolysis to induce constriction and fission of endocytic membranes. EHD1 is recruited to tubular recycling endosomes (TREs) by interacting with Molecules Interacting with CAsL-Like 1 (MICAL-L1) and it performs fission to release cargo-containing vesicles from the TRE. Our lab demonstrated that upon EHD1 depletion, the TREs become elongated due to the lack of fission and the receptors that recycle through this pathway display impaired recycling to the plasma membrane. Furthermore, our lab and others have shown that EHD1 not only interacts with MICAL-L1, but also with a variety of other proteins, such as the retromer cargo selection complex (CSC), which is known to regulate the trafficking of membranes

and proteins between endosomes and the Golgi complex. Recently, the proposed role of VPS35, a core protein of the retromer complex, has expanded, and it was found to interact with and control the mitochondrial fission protein, Drp1. However, the connection between EHD1 and the retromer and their role in mitochondrial homeostasis is less clear. It was previously thought that endocytic regulatory proteins exclusively impacted membrane trafficking pathways, but recent studies suggest that endocytic regulatory proteins play a role in many other pathways including ciliogenesis, centrosome disengagement, and mitochondrial homeostasis. Herein, I describe a novel role for in endocytic regulatory proteins in controlling mitochondrial fission and mitochondrial-induced apoptosis. My studies led to a model by which EHD1 regulates the localization of the retromer within the cell; accordingly, when EHD1 is absent, the retromer no longer regulates the mitochondrial fission protein, Drp1. In addition, I demonstrate for the first time, a connection between endocytic proteins and apoptosis by proposing a model for an expanded role for the retromer complex in regulating mitochondrial-induced apoptosis through the trafficking of the anti-apoptotic protein, Bcl-xL.

TABLE OF CONTENTS

TABLE OF FIGURES

CHAPTER I

CHAPTER II

CHAPTER III

LIST OF ABBREVIATIONS

AAA+	ATPases Associated with diverse cellular Activities
ATCC	American Type Culture Collection
AP-2	Adaptor Protein-2
APPL	Adaptor protein containing PH domain
Arf	(ADP)-ribosylation factor 1
ATPase	Adenosine tri-phosphatase
BAR	BIN-Amphiphysin-Rvs
Bcl	B-cell lymphoma
CCP	Clathrin-coated pit
CCV	Clathrin-coated vesicle
Cdc42	Cell cycle dependent 42
CIE	Clathrin-independent endocytosis
CLASP	Clathrin-associated sorting proteins
CLICs	Cell surface-derived clathrin independent tubulovesicular intermediates
CME	Clathrin-mediated endocytosis

Crmp2	Collapsing response mediator protein-2
CTxβ	Cholera toxin β subunit
Drp1	Dynamin-related protein 1
Dyn2	Dynamin-2
EE	Early endosome
EEA1	Early endosome antigen 1
EGFR	Epidermal growth factor receptor
EHBP1	EH-domain-binding protein 1
EHD	Eps15 homology domain
ERC	Endocytic recycling compartment
ERMES	Endoplasmic reticulum mitochondria encounter structure
ESCRT	Endosomal sorting complexes required for transport
FBS	Fetal Bovine Serum
Fis1	Mitochondrial fission 1
GAP	Guanosine tri-phosphatase-activating proteins
GDI	Guanosine nucleotide dissociation inhibitors

GEEC	Glycosylphosphatidylinositol-anchor-linked protein-enriched early endosomal compartment
GEF	Guanine exchange factor
GPI	Glycosylphosphatidylinositol
GRAF1	Guanosine tri-phosphatase regulator associated with focal adhesion kinase-1
GTP	Guanine tri-phosphate
GTPase	Guanosine tri-phosphatase
h	Hour(s)
HOPS	Homotypic fusion and protein sorting
Hsc70	Heat shock protein 70
IL-2	Interleukin-2
ILV	Intraluminal vesicles
LDL	Low-density lipoprotein
LE	Late endosome
M6PR	Mannose-6 phosphate receptor
MDV	Mitochondrial derived vesicle
Mff	Mitochondria fission factor

Mfn	Mitofusin
MHC	Major Histocompatibility complex
MICAL-L1	Molecules interacting with CAsL-Like 1
μM	Micromolar
MiD	Mitochondrial dynamics protein
min	Minutes
mm	Micrometer
mM	Millimolar
MIM	Mitochondrial Inner Membrane
MMM1	Mitochondrial morphology protein 1
MOM	Mitochondrial Outer Membrane
MOMP	Mitochondrial outer membrane permeabilization
mtDNA	Mitochondria DNA
MVB	Multi-vesicular bodies
nm	Nanometer
nM	Nanomolar
NPF	Asparagine-Proline-Phenylalanine

NSF	N-ethylmaleimide-sensitive factor
OPA1	Optic atrophy 1
PA	Phosphatidic acid
PBS	Phosphate-buffered saline
PBST	Phosphate-buffered saline plus tween
PD	Parkinson's disease
PDZD8	PDZ domain containing protein 8
PH	Pleckstrin homology
PI(3,5)P2	Phosphatidylinositol 3,5 bisphosphate
PI(4,5)P2	Phosphatidylinositol 4,5 bisphosphate
PI3P	Phosphinositide 3-kinase
PI3K	Phosphatidylinositol 3-phosphate kinase
PI5K	Phosphatidylinositol 5-phosphate kinase
PM	Plasma membrane
PRD	Proline-rich domain
Px	Phox-homology domain
Rab	Ras-like guanosine tri-phosphatase

Rac1	Rac family small guanosine tri-phosphatase 1
RPE	Retinal Pigment Epithelial
RhoA	Ras homolog family member A
RILP	Rab7-interacting lysosomal protein
ROS	Reactive oxygen species
RTK	Tyrosine Kinase
s	Seconds
SE	Sorting endosome
SH3	Src homology 3
SIM	Structured Illumination microscopy
SNAP	Synaptosomal nerve-associated proteins
SNARE	Soluble N-ethylmaleimide-sensitive factor attachment receptor
SNX	Sorting nexin
STAM2	Signal transducing adaptor molecule 2
STORM	Stochastic Optical Reconstruction Microscopy
STS	Staurosporine
SV40	Simian virus 40

TfR	Transferrin receptor
TM	Transmembrane Domain
TGN	Trans-Golgi network
TRE	Tubular recycling endosome
UIM	Ubiquitin-interacting motifs
Vit1a	Vacuolar sorting protein 10p tail interactor 1
VPS	Vacuolar sorting protein
Z-VAD	Z-valine-alanine-aspartic acid-(OMe)-fluromethylketone

ACKNOWLEDGEMENTS

First off I would like to thank the Department of Biochemistry and Molecular Biology for allowing me to continue my education and pursue my doctorate degree at the University of Nebraska Medical Center. I would like to acknowledge the faculty, staff, and students in the department that provided support that allowed me to prosper and become a better scientist and human being. I would especially like to thank Dr. Steve Caplan and Dr. Naava Naslavsky for allowing me to rotate through their lab and eventually join the lab. Dr. Caplan and Dr. Naslavsky have equipped me with the necessary training and critical thinking skills that can be applied to any career path that I chose in the future and I am forever in their debt.

I would also like to thank my supervisory committee members; Dr. Paul Sorgen, Dr. Justin Mott, and Dr. Keith Johnson, for their encouragement, suggestions, and thoughtful conversations throughout my time at UNMC. Additionally, I would like to thank Dr. Andrew Trease and Dr. Gaelle Spagnol for helping deliver sequencing experiments and for allowing me to borrow miscellaneous lab equipment and supplies. I would like to thank the lab of Dr. Xu Luo for the guidance with Chapter III and for the GFP-HCT 116 cells that I used to complete experiments in Chapter III. I especially need to thank Dr. Xu Luo for his role as a co-sponsor on my NIH/NCI F31 fellowship. Without his help, I would not have been able to complete Chapter III or get my fellowship.

I appreciate all the members of Dr. Caplan's lab, previous and present, that have laid the foundation for my work so that I could branch off and explore mitochondria homeostasis. These members include Kanika Dhawan, Tyler Jones, Dr. Shuwei Xie, Dr. James Reinecke, Dr. Kriti Bahl, Dr. Bishuang Cai, Dr. Sai Srinivas Panapakkam Giridharan, Dr. Jing Zhang, Dr. Mahak Sharma, Dr. Marko Jovic, and Dr. Laura Simone. Without these lab members, I would not have been nearly as successful, nor would my time here be as enjoyable.

Personally, I am grateful to all my friends and family that have been a part of this journey with me. I would especially like to thank my wife and best friend, Tiffany Farmer, for supporting my scientific career over the last 5 years and directly dealing with me on a daily basis, no matter the outcome of my day. I would also like to thank my incredible parents, Rex and Melissa, for supporting my love for science growing up and allowing me to pursue an occupation that differs greatly from anyone else in the family. Without their constant support and guidance, I would not be where I am today. Thank you to my in-laws, Tim and Lori, for always asking how my education is going and genuinely careering about my success. Last but not least, I would like to thank my son, Walter Farmer. Thank you for reminding me why I am doing what I am doing and giving me a reason to finish strong.

Thank you to everybody that has been a part of my life during my time here at UNMC. I am forever grateful and will look back on this time fondly.

Chapter I

INTRODUCTION

With permission from Traffic, parts of this chapter were derived from: (Farmer, Naslavsky, & Caplan, 2018)

Farmer, T., N. Naslavsky, and S. Caplan. 2018. Tying trafficking to fusion and fission at the mighty mitochondria. *Traffic*. 19:569-577.

1. ENDOCYTIC TRAFFICKING

1.1 Overview

The plasma membrane (PM) is a lipid bilayer that forms a permeable barrier between the intracellular components of a cell and the extracellular environment (Conner & Schmid, 2003). The PM not only is responsible for the regulation of what comes in and out of the cell, such as ions or other various molecules, but also mediates the communication between neighboring cells, and has the ability to receive the extracellular cues needed for growth and survival. The dynamic connection between endocytic trafficking and endocytic events is critical for regulating and maintaining the surface area and protein composition of the PM (G. J. Doherty & McMahon, 2009).

Endocytic membrane trafficking refers to the process by which internalization of receptors, proteins, and nutrients along with extracellular fluid is enclosed in an invaginated portion of the PM, resulting in the pinching off of the membrane to form an endosome or vesicle (Conner & Schmid, 2003). Vesicle formation at the PM can occur through two distinct pathways, termed clathrin-dependent or clathrin-independent (described later in detail). No matter which way the lipids and proteins are internalized, the cargos are packaged into vesicles and delivered to an organelle, known as the early endosome (EE) or sorting endosome (SE) (Mayor, Presley, & Maxfield, 1993; Mellman, 1996a), where the cargo is initially sorted to determine its final fate. From the EE, the cargo can be destined for degradation by being transported to late endosomes (LE) and

eventually the lysosomes, the cargo can be recycled back to the PM, or transported to trans-Golgi network (TGN). (Figure 1.1)

Endocytic trafficking plays a crucial role in regulating many diverse cellular processes, including the uptake of nutrients, regulation of surface receptors, cellular signaling, cytokinesis (Conner & Schmid, 2003; Skop, Bergmann, Mohler, & White, 2001), maintenance of cell polarity, cell adhesion and cell migration (Caswell & Norman, 2008; E. Wang et al., 2000), and synaptic vesicle retrieval in neurons (Kjaerulff, Verstreken, & Bellen, 2002). Dysregulation of the endocytic pathways have been related to various diseases, such as different types of cancer, neurodegeneration, and heart disease (Conner & Schmid, 2003; Stein, Dong, & Wandinger-Ness, 2003). Additionally, studies have shown that pathogens can exploit distinct endocytic pathways in order for the host cell to internalize the pathogen more efficiently (Mercer et al., 2010). Understanding the mechanisms that regulate endocytic pathways will ultimately provide novel approaches for developing therapeutic strategies and drug development.

1.2 Modes of internalization

Internalization into a cell can occur through multiple pathways and is largely determined by the size of the molecule or particle that needs to be internalized. For example, smaller molecules like amino acids, sugars, and ions can enter through channels and protein pumps embedded into the PM. However, the macromolecules that are unable to fit through these channels or pumps undergo endocytosis through the invagination and budding of the PM. Endocytosis can be classified into two main types

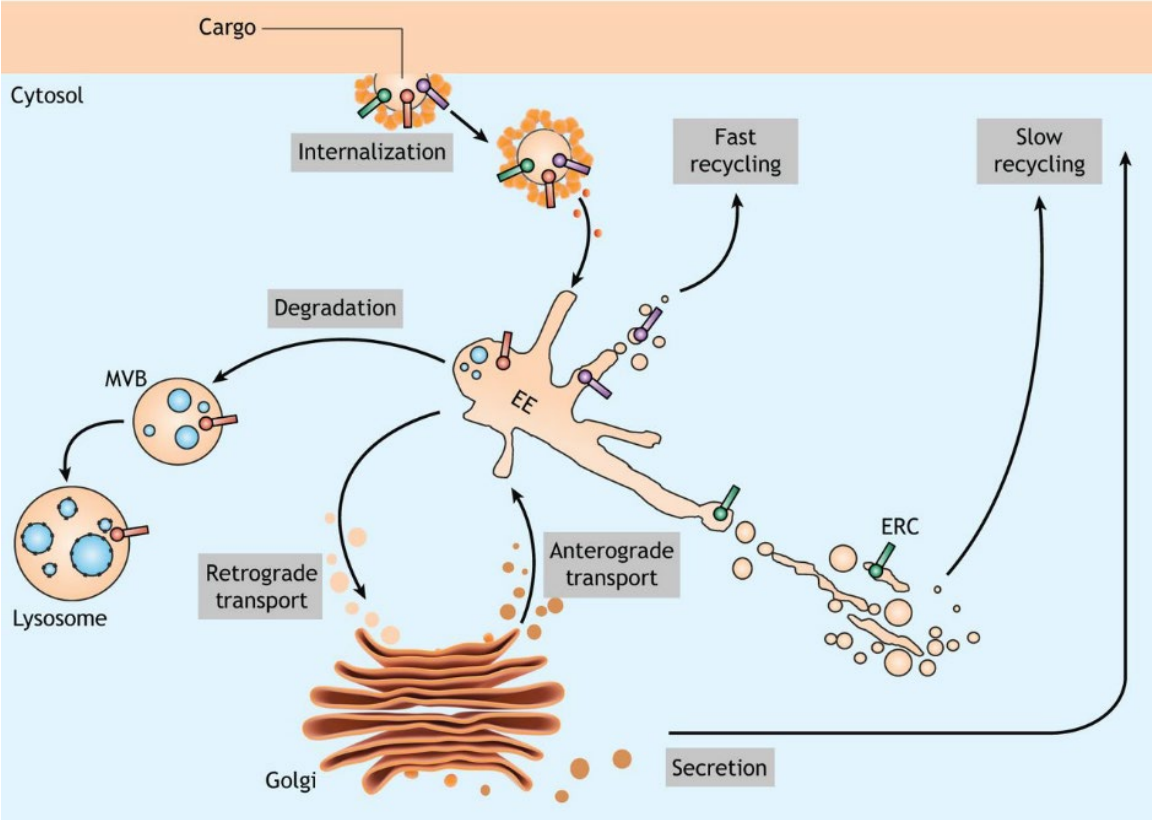

Figure 1.1

Overview of endocytic pathways. Once internalized from the plasma membrane, membrane-bound vesicles that carry receptors from the cell surface fuse with the EEs. The EE serves as a sorting station from which either tubulo-vesicular carriers deliver cargo to the endo-lysosomal system for degradation, or cargos are recycled directly or indirectly to the plasma membrane via the endocytic recycling compartment. Used with permission from JCS (Naslavsky & Caplan, 2018).

based on the size of the internalized endocytic vesicle, phagocytosis or pinocytosis. Phagocytosis includes the internalization of larger molecules, such as microbial pathogens or cellular debris (Aderem & Underhill, 1999), while pinocytosis includes the internalization of fluid and low-molecular-weight solutes (Conner & Schmid, 2003). Pinocytosis can be further broken down into two categories based on the type of machinery that is needed at the PM during internalization, clathrin-mediated endocytosis (CME) (Figure 1.1) or clathrin-independent endocytosis (CIE). Furthermore, CIE can be subdivided into different types depending on whether caveolae is present (Conner & Schmid, 2003; Mayor & Pagano, 2007; Mayor, Parton, & Donaldson, 2014).

1.2.1 Clathrin-mediated endocytosis (CME)

CME is the most extensively studied pathway of internalization from the PM. The founding discoveries of clathrin and clathrin-coated vesicles (CCVs) have shaped the way we currently think about CME (Pearse & Crowther, 1987). Over the last few decades, the work of many scientists has shed light on the mechanism by which receptors bound to their ligands at the PM are internalized into clathrin-coated pits (CCPs) and eventually form the CCVs (Robinson, 2015; Sorkin, 2004). The formation of CCVs can be divided into a five-stage process: initiation, cargo selection, coat assembly, scission, and uncoating. Key to the formation of CCPs and CCVs is the clathrin itself. During formation of CCPs, the clathrin is unable to bind to the membrane directly and instead forms a scaffold to recruit a diverse array of clathrin-associated proteins to complete the downstream internalization events. One key protein that is recruited to the PM before the assembly of CCPs is Adaptor Protein-2 (AP-2), which acts as a hub for

interactions between both the cargo and the PM. AP-2 is a complex composed of two large adaptin subunits-α and β2, one medium-μ2 and one small σ2 subunit (Owen, Collins, & Evans, 2004). The AP-2 complex is able to recognize two types of motifs on the cytoplasmic tail of receptors or cargo: 1) tyrosine-based motifs with a consensus sequence YXXΦ, where Y is a tyrosine residue, X stands for any amino acid residue and Φ is a bulky hydrophobic amino acid residue, and 2) the dileucine-based sorting signals with a consensus sequence defined by DXXLL and [DE]XXXL[LI] with D being aspartate, E being glutamate, L being leucine, and I being isoleucine (Bonifacino & Traub, 2003; Janvier et al., 2003). The binding site for the tyrosine-based motifs is on the carboxyl terminus of the μ2 domain (Ohno et al., 1995), while the α/σ2 hemi-complex and potential β2 subunit bind to the dileucine-based sorting signal sequence (Chaudhuri, Lindwasser, Smith, Hurley, & Bonifacino, 2007; Doray, Lee, Knisely, Bu, & Kornfeld, 2007). Along with the AP-2 protein are other specialized adaptor proteins known as clathrin-associated sorting proteins (CLASPs), that recognize diverse sorting signals on the respective cargo receptors, thus facilitating a large range of distinct cargos that can be endocytosed (Traub & Bonifacino, 2013). Furthermore, post-translational modifications such as phosphorylation and ubiquitination can recruit CLASPs to receptor tails. Once the cargo is selected and packaged by AP-2 and CLASPs, the assembly of the clathrin coat is initiated. AP-2 and the accessory proteins recruit clathrin to the site of internalization at the PM. Clathrin is a trimer of dimers consisting of three heavy chains and three light chains assembled as a triskelion that has the intrinsic ability to build a cage-like structure upon invagination of the PM (Kirchhausen, 2000). Once the

clathrin is recruited to the PM and the cage-like structure begins to form, more accessory proteins are recruited to generate and stabilize the curvature of the maturing CCPs, such as the Bin-Amphiphysin-Rvs (BAR) containing proteins (Koch, Westermann, Kessels, & Qualmann, 2012). Towards the end of the formation of the CCP, a large and modular guanosine tri-phosphatase (GTPase) known as Dynamin, along with other curvature sensing proteins including Amphiphysin, Endophilins, and Sorting Nexin (SNX) 9 (SNX9), facilitates the release of CCVs from CCPs (A. Lee, Frank, Marks, & Lemmon, 1999; Vallis, Wigge, Marks, Evans, & McMahon, 1999; van der Bliek et al., 1993; Yoshida et al., 2004). The Dynamin GTPase oligomerizes around the neck of the CCPs in a collar-like structure and catalyzes guanosine tri-phosphate (GTP) hydrolysis to mediate membrane fission and generate independent CCVs. After the scission of the CCV from the PM, the clathrin coat around the vesicle is disassembled by an adenosine tri-phosphatase (ATPase) known as Heat shock cognate 70 (Hsc70) and its co-factor Auxillin (Braell, Schlossman, Schmid, & Rothman, 1984; Prasad, Barouch, Greene, & Eisenberg, 1993; Ungewickell, 1999). The low-density lipoprotein (LDL) receptor and the iron-laden transferrin receptor (TfR) are examples of signature cargo that are internalized by CME. (Figure 1.1)

1.2.2 Clathrin-Independent Endocytosis (CIE)

It is thought that CME is the dominant pathway of internalization of cargo into the cell, however cells are able to utilize a variety of non-CME pathways collectively termed CIE. A common theme connecting the CIE pathways is the need for a high

concentration of cholesterol at the PM upon invagination (Mayor & Pagano, 2007; Sandvig & van Deurs, 1994).

The caveolae-mediated pathway is the most well-known CIE pathway. The invaginations formed by caveolae are a flask-shape anywhere from 50-100 nm in size. These invaginations are usually concentrated at the PM in micro-domains containing cholesterol, sphingolipids, and phosphatidylinositol (4,5)-bisphosphate (PIP2) (Anderson, 1998; Pitto et al., 2000; Simone, Caplan, & Naslavsky, 2013). Caveolin-1 is a crucial membrane protein that oligomerizes to form a loop and inserts into the micro-domain of the PM in order to form the framework for the flask-shaped membrane that comprises the caveolae. Once the Caveolin-1 inserts itself into the PM, it recruits cavin proteins (cavin 1-4), which in turn help stabilize and build the budding caveolar vesicle (Hansen, Bright, Howard, & Nichols, 2009; Hill et al., 2008). In addition to Caveolin-1 and the cavin proteins, Syndapin2 (also known as Pacsin2), is recruited to the invagination. Syndapin2 is a BAR domain-containing protein that can regulate membrane curvature and helps shape the caveolar invagination (Koch et al., 2012; Senju, Itoh, Takano, Hamada, & Suetsugu, 2011). Syndapin2 also has a Src homology 3 (SH3) domain that allows it to bind the proline-rich domain (PRD) of the dynamin GTPase and a tripeptide sequence containing asparagine-proline-phenylalanine (NPF) motif that facilitates the binding of Syndapin2 with C-terminal Eps15 homology domain containing (EHD) protein 2 (EHD2). EHD2 is required for caveolar stabilization at the PM but previous studies in our lab have shown that whereas Syndapin2 is not required for EHD2 recruitment, PIP2 levels in the PM are critical for recruitment (Moren et al., 2012;

Simone et al., 2013; Stoeber et al., 2012). Certain cell types, such as smooth muscle cells, fibroblast, adipocytes, and endothelial cells, are enriched in caveolae-associated invaginations (Parton & Simons, 2007). Some examples of the cargo that can be internalized through the caveolae-mediated pathway include simian virus 40 (SV40) virions, cholera toxin β subunit (CTxβ), and glycosylphosphatidylinositol (GPI)-linked proteins (Cheng, Singh, Marks, & Pagano, 2006; Parton & Simons, 2007).

1.2.3 Clathrin-Independent Carriers/GPI-AP-enriched early endosomal compartment (GLIC/GEEC)

Proteins that are secured to the PM by GPI-anchor-linked proteins (GPI-AP) do not depend on clathrin or caveolin coats to be internalized but they still require the cholesterol enriched micro-domains that can be found at the PM (Lakhan, Sabharanjak, & De, 2009). GPI-APs are internalized through EE-like structures that are highly enriched in GPI-AP. These EE-like structures are called GPI-AP-enriched early endosomal compartments (GEEC). The GEECs are formed by the fusion process between cell surface-derived clathrin-independent tubulovesicular intermediates termed CLICs (Kirkham et al., 2005). In order to form CLICs, two small GTPases must be present: cell cycle dependent 42 (Cdc42) and adenosine di-phosphate (ADP)-ribosylation factor 1 (Arf1) (Kumari & Mayor, 2008). Unlike the pathways mentioned previously, these structures are dynamin-independent and the mechanism of budding in these vesicles remains unclear. However, recently a marker of these CLICs was identified as a protein called GTPase regulator associated with focal adhesion kinase-1 (GRAF1). GRAF1 has distinct domains that are critical for generating CLICs, such as a scission-

BAR domain for membrane curving, a pleckstrin homology (PH) domain that allows GRAF1 to directly bind to PIP2 in the PM, and an SH3 domain that can bind to the PRD of dynamin (Lundmark et al., 2008). Additionally, work from our lab has provided evidence for a model suggesting that GRAF1 forms a vesiculation complex that is comprised of Molecules Interacting with CAsL-Like 1 (MICAL-L1) and C-terminal Eps15 homology domain containing (EHD) protein 1 (EHD1) on tubular recycling endosomes (TRE), which in turn helps support TRE vesiculation (Cai, Caplan, & Naslavsky, 2012; Cai, Xie, Caplan, & Naslavsky, 2014). This may suggest that a vesiculation complex generated by GRAF1 could be the potential vesiculator of CLICs. GPI-APs, CTxβ, and fluid phase markers are some examples of known cargos that go through this pathway (Mayor & Pagano, 2007) (G. J. Doherty & McMahon, 2009).

1.2.4 Arf6 mediated pathway

Another pathway considered to be clathrin-independent is associated with the ATPase, ADP-ribosylation factor 6 (Arf6). Arf6 can be found at the PM where it regulates the rate of trafficking in and out of the cell as well as the dynamics of the actin cytoskeleton near the PM. The mechanism for Arf6 regulation of internalization is by activating phosphatidylinositol 4,5 kinase (PI5K), which in turn generates PIP2 at the PM, resulting in enriched PIP2 budding vesicles. Since Arf6 stimulates the production of PIP2, the latter is able to activate the machinery needed for actin polymerization, thus driving the endocytic pathway. GPI-APs, CD59, CD55, and major histocompatibility complex class I (MHC I) proteins are cargo known to internalize through this pathway (Naslavsky, Weigert, & Donaldson, 2003).

1.2.5 CIE of interleukin-2 receptor

Another less common CIE pathway is the mechanism used to internalize the interleukin-2 (IL-2) receptor. IL-2 concentration and internalization occurs through a small non-coated invagination that depends on RhoA and consequently ras-related C3 botulinum toxin substrate 1 (Rac1) (Gesbert, Sauvonnet, & Dautry-Varsat, 2004; Lamaze et al., 2001; Mayor et al., 2014). Internalization of IL-2 occurs in detergent-resistant microdomains of the PM and requires dynamin as well as proteins that regulate actin polymerization, such as phosphatidylinositol 3-kinase (PI3K), Rac1, Rac1's guanine exchange factor Vav2, kinases Pak1 and Pak2, endocytic adaptor cortactin, and Arp2/3 stimulator N-WASP (Basquin et al., 2013; Basquin & Sauvonnet, 2013; Grassart, Dujeancourt, Lazarow, Dautry-Varsat, & Sauvonnet, 2008; Lamaze et al., 2001). PI3K plays a key role as its regulatory subunit, p85, associates with the IL-2 receptor and activates the recruitment of its catalytic p110 subunit to produce PI(3,4,5)P3 (Cendrowski, Maminska, & Miaczynska, 2016). This induces that activation of Rac1 by Vav2, which in turn is recruited to the IL-2 receptor that is bound to the PI3K and stimulates Pak1 and Pak2 kinases (Cendrowski et al., 2016). The kinases promote actin polymerization through cortactin and N-Wasp (Basquin & Sauvonnet, 2013). The activation of these proteins likely occurs at the last step of internalization and is critical for vesicle scission from the PM.

1.3 Sorting at the Early Endosome (EE)/Sorting Endosome (SE)

The EE is responsible for receiving vesicles from the PM so that cargo can be sorted and directed to the correct cellular destination (Jovic, Sharma, Rahajeng, &

Caplan, 2010). While many proteins localize to EE and are required for proper function, Rab5, a member of the Ras-associated binding (Rab) small GTPases, marks EE and controls the function, dynamics, and subsequent organelle transport of EE (Woodman, 2000). Active Rab5 or GTP-bound Rab5 recruits a number of Rab5 effectors that include the phosphatidyl inositol-4-5 bisphosphate-3-kinase (PI3K), promoting the generation of phosphoinositol 4-phosphate (PI3P) at the EE. PI3P in the EE membrane allows recruitment of proteins that contain a FYVE domain (Stenmark, Aasland, & Driscoll, 2002). Examples of FYVE domain-containing proteins include Early Endosomal Autoantigen-1 (EEA1), Rabankyrin-5, and Rabenoysn-5, which also interact with Rab5 (Grosshans, Ortiz, & Novick, 2006), suggesting that more than a single mechanism exists to recruit these proteins to the EE.

EE have a mildly acidic lumen between pH 6.3-6.5 and the acidity is important for disrupting the coupling between the ligands and their receptors within the first few moments of internalization. This uncoupling of the ligand from the receptor is the first step in cargo sorting (Maxfield & McGraw, 2004). Additionally, the Rab-5-dependent recruitment of a diverse number of effector proteins encourages the differentiation of the EE from a small vesicular structure to a rather large structure that has both a vacuolar and tubular component to it (Huotari & Helenius, 2011). This differentiation is due to the fact that EE are highly dynamic and undergo homotypic fusion (Gruenberg et al. 1989). The formation of both vacuolar and tubular components provides subdomains within the EE that allow for efficient sorting of cargos (Mayor et al., 1993). For example, cargo clustered in the tubular areas of the EE is usually targeted for recycling back to the

PM, whereas cargo inside the more bulky vesicles is usually sent to the lysosome for degradation by way of multi-vesicular bodies (MVBs) (Mellman, 1996b). Frequently, the internalized receptor is recycled back to the PM to bind with another ligand, while the ligand is transported to the lysosome for degradation (Maxfield & McGraw, 2004). For instance, TfR and LDL receptors are recycled back to the PM upon entering the EE, while the transferin (Tf) and LDL itself are transported to the lysosome for degradation (Jovic, Kieken, Naslavsky, Sorgen, & Caplan, 2009). (Figure 1.1)

1.4 Sorting cargos to the LE/lysosome for degradation

As previously mentioned above, the EE is responsible for regulating the sorting of ligands and signaling receptors that have been internalized from the PM. The ligands that have uncoupled from their receptors and become soluble are typically sorted for degradation by a maturation pathway beginning with EE and advancing to LE. However, the transmembrane receptors must be sorted by their sorting signals located in the cytosolic domain of the receptor. A frequently studied receptor is the Epidermal Growth Factor Receptor (EGFR), a tyrosine kinase (RTK) that has a specific cytosolic domain recognized by sorting machinery that targets it to the degradation pathway (Haglund et al., 2003). The sorting of the EGFR is done by post-translational ubiquitination of one or more of the lysine residues in its cytoplasmic tail, in turn marking it for degradation through the lysosome (Haglund et al., 2003; Huang, Kirkpatrick, Jiang, Gygi, & Sorkin, 2006; Levkowitz et al., 1998; Umebayashi, Stenmark, & Yoshimori, 2008). Once the receptor is marked with ubiquitin, several proteins that interact with ubiquitin through ubiquitin-interacting motifs (UIM) recognize the

receptor. These proteins include the endosomal sorting complexes required for transport-0 (ESCRT-0), hepatocyte growth factor regulated tyrosine kinase substrate (Hrs), signal transducing adaptor molecule 2 (STAM2) and the ESCRT-I component, and tumor susceptibility gene 101 (TSG101) (Raiborg & Stenmark, 2002). In parallel, the ESCRT-1 component and Tsg101 promote the recruitment of the ESCRT-II complex. This event is needed to initiate the budding of MVBs. The ESCRT-II triggers the oligomerization of the ESCRT-III complex on the endosomal membrane, which allows for the capture of the cargo to novel MVB and also catalyzes the scission of the MVB (Babst, Katzmann, Estepa-Sabal, Meerloo, & Emr, 2002; Babst, Katzmann, Snyder, Wendland, & Emr, 2002). Upon completion of MVB formation, vacuolar sorting protein (VPS) 4 (VPS4), an ATPase, is recruited to catalyze the disassembly of the ESCRT-III complex from the newly formed MVB. The newly formed MVB can then fuse with the LE or lysosome, resulting in the degradation of the EGFR and other sorted receptors (Shestakova et al., 2010). Our lab has been able to establish a novel role for C-terminal Eps15 homology domain containing (EHD) protein 4 (EHD4) in the trafficking of receptors from the EE to the lysosomes (Sharma, Naslavsky, & Caplan, 2008).

1.5 Sorting cargos for recycling back to the PM

Cargos that are selected to return back to the PM can do so via two routes. The first route is through the "fast recycling" pathway. Fast recycling refers to the recycling of receptors back to the PM directly from the EE. However, most of the receptors travel from the EE to an additional organelle termed the endocytic recycling compartment (ERC). The ERC is localized near the microtubule organizing center (MTOC) in the

perinuclear area of the cell (B. D. Grant & Donaldson, 2009; Maxfield & McGraw, 2004). Rab4 and Rab11 are the most prominent markers for differentiating between the fast and slow recycling pathways, respectively (Ullrich, Reinsch, Urbe, Zerial, & Parton, 1996; Van Der Sluijs et al., 1991).

The composition, structure, and functional mechanism of the ERC in endocytic recycling are poorly understood despite the importance of the ERC in the recycling process. Recent studies from our lab took advantage of super resolution microscopy, Structured Illumination Microscopy (SIM), dual channel 2D-direct Stochastic Optical Reconstruction Microscopy (dSTORM), and 3D STORM, in order to address ERC morphology and cargo selection. The studies showed that the ERC is composed of an array of dynamic, densely situated but independent tubular and vesicular recycling endosomes coming from the MTOC (Xie et al., 2016). It has been established that due to the high surface area-to-volume ratio displayed in the ERC, this facilitates segregation of the integral membrane protein cargo from their luminal content (Maxfield & McGraw, 2004). However, studies in our lab show that the ERC maintains cargo separation that has occurred in the EE, suggesting that the ERC serves as a focal point for vesicular transport to the PM (Xie et al., 2016).

TREs, found within the ERC, are critical for the recycling of internalized receptors and lipids. Previous studies from our lab have shown that MICAL-L1-decorated TREs can be generated from areas of the EE that are enriched in a Rab-5 effector known as Rabenosyn-5 (Xie et al., 2016). Furthermore, our lab's current model suggests that the

fission of TREs leads to the formation of vesicle carriers that transport the receptor back to the PM (Cai et al., 2012; Cai et al., 2013; Cai et al., 2014). Adding to the significance of TREs, our lab as extensively studied the players involved in TRE generation, fission, fusion, and function. Previous studies from our lab have been able to demonstrate that MICAL-L1 localizes to TRE (Sharma, Jovic, et al., 2009) and acts as a hub that recruits and stabilizes multiple proteins that can impact the shape of the TREs. For example, the F-BAR domain containing protein Syndapin2 interacts with MICAL-L1 and bends endosomal membranes to generate TREs (Giridharan, Cai, Vitale, Naslavsky, & Caplan, 2013). MICAL-L1 also interacts with the C-terminal Eps15 homology domain containing (EHD) protein 3 (EHD3) and EHD1 (Kieken et al., 2010; Sharma, Jovic, et al., 2009). EHD3 and EHD1 are responsible for the stabilization and vesiculation of the TREs, respectively (Bahl et al., 2016; Cai et al., 2013). Another critical aspect to TREs is the high concentration of phosphatidic acid (PA), an essential lipid component of the TRE membrane that allows for the binding with MICAL-L1 and Syndapin2. EHD1 subsequently binds to the MICAL-L1 and Syndapin2 complex on the TRE, and induces scission of these membranes, generating a newly synthesized vesicle (Cai et al., 2013; Cai et al., 2014; Giridharan et al., 2013). (Figure 1.2)

1.6 Sorted cargos destined for the trans-Golgi network (TGN)

EEs are not only important for sorting receptors and ligands to the recycling or degradation pathway but are also important for the tethering of various endocytic and biosynthetic pathways. Transport from the EE to the TGN is known as retrograde transport. (Figure 1.1) While retromer-mediated tubulation is required for retrograde

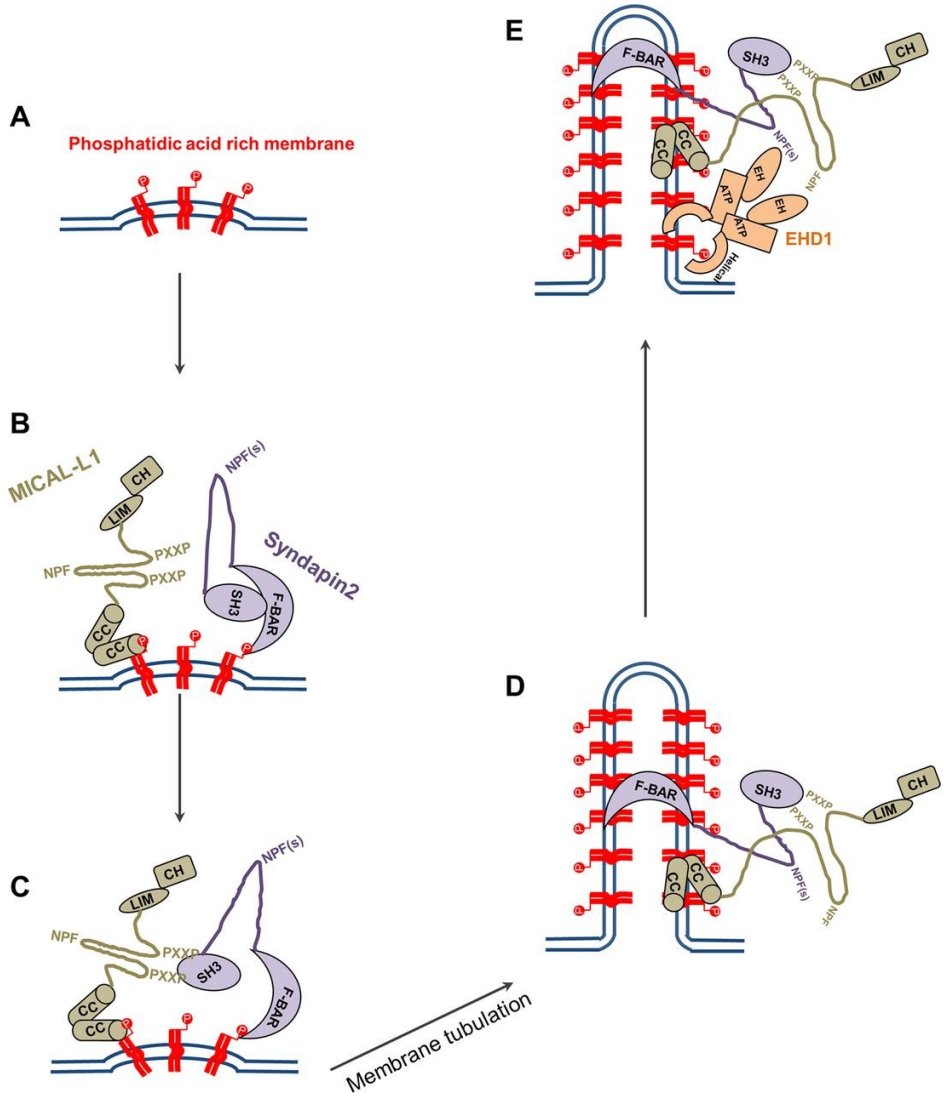

Figure 1.2

Model for biogenesis of tubular recycling endosomes. (A) Phosphatidic acid is generated or enriched on membranes. (B) MICAL-L1 (via its CC domain) and Synd2 (via its F-BAR domain) are recruited to PA-enriched membranes. (C) The MICAL-L1 PXXP motifs interact with the SH3 domain of Synd2 to stabilize both proteins on the membranes and (D) facilitate the generation of tubular endosomes by Synd2. (E) Synd2 and MICAL-L1 bind to the EH domain of EHD1 via their NPF motifs and recruit EHD1 to these tubular membranes, potentially facilitating vesiculation. Used with permission from MBoC (Giridharan et al., 2013).

transport, these tubules are distinct from the TREs that facilitate the recycling process previously described (Bonifacino & Rojas, 2006). The machinery that is necessary for retrograde transport is recruited to EEs that are in the process of maturation and evolving into LE and therefore contain a higher concentration of phosphatidylinositol 3,5, bisphosphate (PI(3,5)P2) and have an increasing number of intraluminal vesicles (ILVs).

Initial studies by Seaman and coworkers in the yeast endolysosomal system were instrumental in the identification of the protein complex called the "retromer" (Seaman, McCaffery, & Emr, 1998). The retromer was proposed to mediate the endosome-to-TGN retrieval of the vacuolar hydrolase receptor, Vps10p, which is the yeast equivalent of the mannose 6-phosphate (M6PR) receptor. The retromer consists of a hetero-pentameric complex consisting of a SNX dimer composed of SNX1/2 or Snx5/6 and a trimer consisting of vacuolar protein sorting 35 (VPS35), vacuolar protein sorting 26 (VPS26), and vacuolar protein sorting 29 (VPS29) (Bonifacino & Hurley, 2008; Bonifacino & Rojas, 2006; Rojas et al., 2008; Seaman, 2005). Initially the trimer of VPS35, VPS26, and VPS29 was thought to be involved in the cargo sorting, while the SNX dimer was responsible for binding to the EE membrane by the phox-homology (PX) domain contained within the SNX proteins, therefore acting as a scaffold (Bonifacino & Rojas, 2006). However, the structure of the retromer complex has recently been described using cryo-elctron tomography and subtomogram averaging to highlight the retromer as a structure that forms arches that extend away from the membrane surface (Kovtun et al., 2018). Based on these structures, it is thought that the trimer of VPS proteins forms a scaffold and the

distinct combination of SNX proteins associated with the retromer controls the cargo sorting function (Kovtun et al., 2018). While the exact mechanism detailing how the retromer sorts cargo destined for the TGN is yet to be determined, it has been established that the cargo within these endosomes contain at least one simple hydrophobic motif comprised of phenylalanine/tryptophan-leucine-methionine/valine (F/W-L-M/V) (Gokool, Tattersall, & Seaman, 2007). The most well studied cargos that are transported through the retrograde transport include the vacuolar hydrolase transport receptors, VPS10 in yeast or M6PR in mammals (Bonifacino & Rojas, 2006; Johannes & Popoff, 2008).

EHD1 is also an important regulator of the retromer-mediated transport of cargos from EEs to the TGN. EHD1 co-localizes and interacts with the VPS26 and VPS35 subunits of the retromer and impacts the retrieval of the M6PR back to the TGN (Gokool et al., 2007). While we have observed co-localization and interactions between EHD1, VPS35, and VPS26, it has yet to be determined if this interaction is direct or indirect. However, work from our lab suggests that Rabankyrin-5, a Rab5 effector that binds directly to EHD1 through a MPF motif, also interacts with the retromer complex, potentially mediating the interaction between EHD1 and the retromer (McKenzie et al., 2012; Zhang, Naslavsky, & Caplan, 2012; Zhang, Reiling, et al., 2012). It is also important to note that our lab found EHD3, the closest paralog of EHD1, mediates the transport of cargo from the EE to TGN (Naslavsky, McKenzie, Altan-Bonnet, Sheff, & Caplan, 2009).

2. REGULATORS OF ENDOCYTIC TRAFFICKING

2.1 Overview

Endocytic trafficking of cargos is very important and critical function for the cell to maintain homeostasis; therefore the process is highly regulated by multiple types of proteins, such as Rab GTPases, soluble N-ethylmaleimide-sensitive factor attachment protein receptors (SNARE) fusion machinery proteins, fission proteins such as EHD1, coat proteins, and many more. These proteins work together to actively internalize, sort, degrade, and recycle internalized cargo.

Rab GTPases are a family of more than 60 small Ras-related GTP-binding proteins that control endocytic trafficking steps and localize to the endocytic organelles, such as the EE or LE (Pfeffer & Aivazian, 2004). When a Rab is bound to GDP, the Rab usually becomes cytosolic and inactive, while GTP-bound Rabs are usually active and bound to the endocytic membranes. When Rab proteins are bound to the endocytic membranes they are able to recruit Rab effector proteins that regulate the membrane lipid content, membrane fusion/fission, and transport along the cytoskeleton (Pfeffer & Aivazian, 2004).

Another class of proteins that is critical for the transport of vesicles from one destination to another in the endocytic pathway is the SNARE family of proteins. SNARE proteins located on the vesicle are termed v-SNAREs and the vesicles target membrane are termed t-SNAREs. Together, the v-SNARE and t-SNARE provide the required energy for the fusion of the transport vesicle and the target membrane.

The EHD family of proteins consists of four highly homologous membrane-associated ATPases that are able to regulate membrane tubule and vesicle formation by means of their interaction partners. It has been well documented that if these EHD proteins are depleted or mutated, cargos are not efficiently transported between endocytic compartments (Naslavsky & Caplan, 2011). While the EHD1-4 family of proteins shares high sequence homology, each protein retains separate functionality in its regulation of the endocytic pathway.

2.2. Rab GTPases and their effector proteins

Among the various proteins needed to regulate endocytic trafficking, the small Rab proteins play a major role. During a Rab GTPase cycle, the GDP-bound Rab protein is considered inactive and associates with Guanosine nucleotide dissociation inhibitors (GDIs), which are located in the cytosol. In order for the Rab to unbind from the GDI in the cytosol, a GDI displacement factor (GDF) must release the Rab so it can be recruited to the endocytic membrane. Once the Rab becomes GTP-bound, it interacts with a series of specific protein effectors that include but are not limited to tethering molecules, kinases, phosphatases, adaptor proteins, and motor proteins that help the Rab carry out its function of fission, fusion, and tethering. A GTP-bound Rab can become inactive and disassociate from endocytic membranes by its specific GTPase-activating proteins (GAPs). GAPs work by facilitating GTP hydrolysis, making the Rab become GDP-bound and completing the Rab cycle. (Figure 1.3)

The Rab proteins that are associated with the EE mediate the function of post-internalization sorting and include Rab4, Rab5, Rab10, Rab11, and Rab22 (Babbey et al., 2006; Magadan, Barbieri, Mesa, Stahl, & Mayorga, 2006; Van Der Sluijs et al., 1991). As mentioned previously, Rab5 is the most extensively studied Rab on EE and commonly used as a marker of this organelle. (Barbieri, Roberts, Mukhopadhyay, & Stahl, 1996; Bucci et al., 1992; Gorvel, Chavrier, Zerial, & Gruenberg, 1991; Grosshans et al., 2006; Zerial & McBride, 2001). It is thought that Rab5 controls trafficking by regulating the composition of the membrane to include more PI3P (Christoforidis et al., 1999; Murray, Panaretou, Stenmark, Miaczynska, & Backer, 2002), promoting homotypic fusion (Gorvel et al., 1991) and facilitating the EE on cytoskeletal tracks (Nielsen, Severin, Backer, Hyman, & Zerial, 1999; Pal, Severin, Lommer, Shevchenko, & Zerial, 2006). For the Rab5 to become active and GTP-bound, the guanine exchange factor (GEF), Rabex-5, must be present at the EE to activate Rab5 (Horiuchi et al., 1997). GTP-bound Rab5 recruits Rab5 effector proteins to the membrane of the EE, where their specialized function in the sorting or trafficking of cargos can take place (Grosshans et al., 2006). Some of the key Rab5 effectors include PI3K (Christoforidis et al., 1999), EEA1 (Merithew, Stone, Eathiraj, & Lambright, 2003), Rabenosyn-5 (Nielsen et al., 2000) and Adaptor protein containing PH domain (APPL1 and APPL2) (Miaczynska et al., 2004). The PI3K leads to increased PIP2 in the endocytic membrane, which allows the recruitment of proteins (Gillooly et al., 2000; Siddhanta & Shields, 1998). EEA1 and

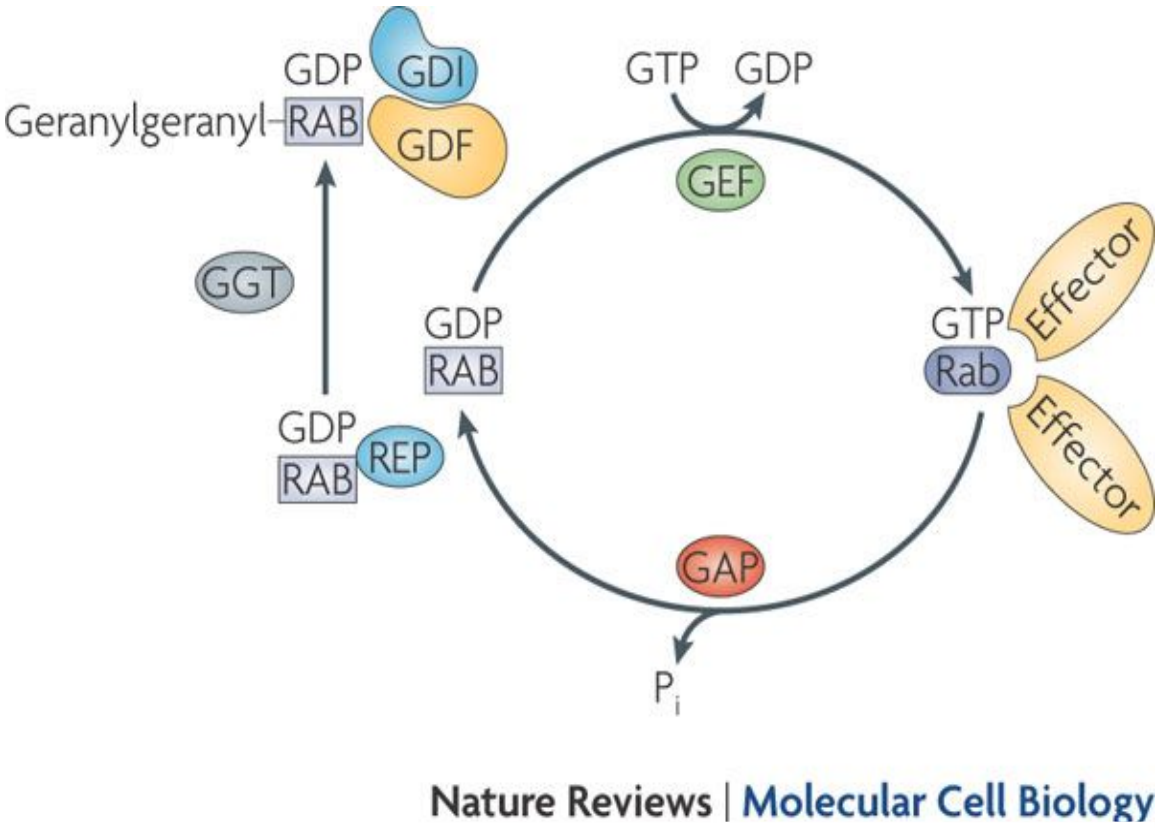

Figure 1. 3

The Rab switch and its circuitry. Conversion of the GDP-bound Rab into the GTP-bound form occurs through the exchange of GDP for GTP, which is catalysed by a guanine nucleotide exchange factor (GEF) and causes a conformational change. The GTP-bound 'active' conformation is recognized by multiple effector proteins and is converted back to the GDP-bound 'inactive' form through hydrolysis of GTP, which is stimulated by a GTPase-activating protein (GAP) and releases an inorganic phosphate (Pi). The newly synthesized Rab, in the GDP-bound form, is recognized by a Rab escort protein (REP). The REP presents the Rab to a geranylgeranyl transferase (GGT), which geranylgeranylates the Rab on one or two carboxy-terminal Cys residues. The geranylgeranylated, GDP-bound Rab is recognized by Rab GDP dissociation inhibitor (GDI), which regulates the membrane cycle of the Rab. Targeting of the Rab–GDI complex to specific membranes is mediated by interaction with a membrane-bound GDI displacement factor (GDF). Used with permission from Nature review (Stenmark, 2009).

Rabenosyn-5 both bind to PI3P in the membrane through their FYVE domain. EEA1 subsequently recruits Syntaxin13 and Syntaxin6, which facilitate EE fusion with other endocytic membranes later in the pathway (McBride et al., 1999; Simonsen, Gaullier, D'Arrigo, & Stenmark, 1999). Rabenosyn-5 on the endocytic membrane binds human vacuolar protein sorting 45 (hVPS45), which in turn binds to v-SNARE proteins and leads to fusion of the EE with target membranes (Naslavsky et al., 2009). Along with Rab5 and Rab5 effectors on EE, Rab4 is also localized to the EE (Van Der Sluijs et al., 1991). Rab4 is responsible for the direct exit of the recycling cargo containing vesicles from EE to the PM, known as fast recycling, as well as being able to sort these same cargos to the ERC (Sheff, Daro, Hull, & Mellman, 1999; Van Der Sluijs et al., 1991).

Upon maturation of the EE to a LE, the exchange of Rab5 with Rab7 is a key event (Peralta, Martin, & Edinger, 2010). Rab7 is recruited the EE membrane by homotypic fusion and by interacting with vacuole protein sorting (HOPS) subunit Vam6p/VPS39 (Caplan, Hartnell, Aguilar, Naslavsky, & Bonifacino, 2001; Wurmser, Sato, & Emr, 2000). The VPS39 protein interacts with a protein that binds to GTP-bound Rab5, Mon1, and displaces the Rabex-5 GEF protein from the membrane. The Mon1, along with its interaction partner, Czi1, can recruit Rab7 to the EE. The Mon1/Czi1 interaction prevents Rab5 from becoming activated again and also promotes the activation of the newly acquired Rab7, thus promoting the maturation of the EE to a LE (Nordmann et al., 2010). Similar to Rab5, Rab7 also has effector proteins that are recruited to the LE to perform specialized functions. Rab7-interacting lysosomal protein (RILP), is recruited to the LE and in turn recruits dynein-dynactin motor proteins that

allow for transport of the LE toward the minus end of the microtubules (Cantalupo, Alifano, Roberti, Bruni, & Bucci, 2001). The previously mentioned HOPs complex remains in contact with Rab7- positive LE and promotes tethering and fusion of the LE with target membranes through SNARE proteins.

A number of other Rab proteins play a role in regulating various steps in the endocytic pathway and include Rab11, Rab21, Rab 22, Rab8, Rab15, Rab35, (B. D. Grant & Donaldson, 2009; Grosshans et al., 2006; V. W. Hsu & Prekeris, 2010), and it was recently found that Rab10 associates with MICAL-L1 and localizes to TREs; however the function of Rab10 on the TRE is still being explored (Etoh & Fukuda, 2019). Not only are the Rab proteins present in the endocytic pathway, but the Rab effector proteins as well (Grosshans et al., 2006). Some of the Rab effector proteins are also able to interact with the aforementioned EHD1 protein (Naslavsky & Caplan, 2011). As previously mentioned, Rab4 is a well-known regulator of fast recycling from EE back to the PM, and Rab4 alone does not access the ERC. However, if Rab4 and Rab11 are both located on the EE, it can lead to the delivery of the cargo to ERC (Sonnichsen, De Renzis, Nielsen, Rietdorf, & Zerial, 2000). Rab11 binds to its effector proteins, Rab11 family-interacting protein 5 (FIP5) and Rab11-FIP2, which in turn recruit important players of the slow recycling pathway. These proteins include the kinesin II motor protein, KIF3B (Schonteich et al., 2008), myosin Vb (Roland, Kenworthy, Peranen, Caplan, & Goldenring, 2007), EHD1, and EHD3 (Naslavsky, Rahajeng, Sharma, Jovic, & Caplan, 2006). Similar to Rab4 function, Rab35 is able to promote the fast recycling of receptors (Allaire et al., 2010; Sato et al., 2008). However, Rab35 and its effector protein, MICAL-

L1, can localize to TRE and serve as scaffolding proteins to recruit various proteins that are critical to TRE homeostasis, such as EHD1 (Giridharan, Cai, Naslavsky, & Caplan, 2012). Besides these Rab proteins and their effectors, other types of Rab proteins play a role in the slow recycling pathway. For example, Rab8 is recruited to TRE by MICAL-L1 and is involved in the Rab11-Rab8-Myosin Vb complex that recycles cargos back to the PM (Huber et al., 1993; Roland et al., 2007). Rab22a is also found on tubules generated from the ERC and plays a role in mediating tubule generation and the fusion of recycling endosome membranes and the PM (Weigert, Yeung, Li, & Donaldson, 2004). Rab22a may also play a role in cargo selection within the slow recycling pathway as it preferentially traffics the MHC 1 protein and has little effect on the Tf receptor.

While Rab proteins play a major role in endocytic trafficking, there is another family of proteins that are also guanine nucleotide-binding proteins termed ADP-ribosylation factor (Arf) proteins. The Arf proteins regulate organelle dynamics and membrane trafficking in a similar manner to that of Rab proteins (Donaldson & Jackson, 2000). Arf proteins can be divided into different classes with the class 1 (Arf1-3) group of Arf proteins mediating the trafficking between the ER-to-Golgi (D'Souza-Schorey & Chavrier, 2006). On the other hand, the class III group of Arf proteins (Arf6) stimulates endocytosis by promoting the invagination of the PM (Naslavsky et al., 2003). As previously mentioned, Arf6 functions more as a lipid and cytoskeleton modifier by the activation of PI5K, which in turn enriches the membrane in PIP2. PIP2 enrichment at the PM promotes membrane trafficking and actin rearrangement (Czech, 2003; Yin & Janmey, 2003). Arf6 is responsible for the internalization of cargos such as MHCI, G

protein-coupled receptors, E-cadherin and β1-integrin (Brown, Campbell, & Sanderson, 2001; Houndolo, Boulay, & Claing, 2005; Naslavsky et al., 2003; Radhakrishna & Donaldson, 1997). Arf6 also coordinates with EHD1 to mediate the MHCI-containing TRE and the localization of Rab8 and MICAL-L1 to tubular membranes (Caplan et al., 2002; Rahajeng, Giridharan, Cai, Naslavsky, & Caplan, 2012).

2.3 v-SNARE and t-SNARE proteins

In general, the soluble N-ethylmaleimide-sensitive factor attachment receptor (SNARE) proteins mediate fusion events of two membranes by utilizing the SNARE motif that resides in each protein (Bennett, 1995; Fasshauer, 2003; Sollner, 1995). The SNARE motif consists of a helix-forming structure that has an evolutionarily conserved domain of 60-70 amino acids, along with heptad repeats. In order for two endocytic membranes to fuse using SNARE proteins, the vesicle membrane SNARE (v-SNARE) interacts with the target membrane SNARE (t-SNARE) by association with the SNARE motifs found in each protein. This association forms a four-helical bundle that is extremely stable and provides the energy to undergo fusion of the vesicle with the target membrane (Y. A. Chen & Scheller, 2001; Sutton, Fasshauer, Jahn, & Brunger, 1998). Some specific examples of SNARE proteins that are involved in the homotypic fusion of EE is syntaxin13, VPS10p tail interactor 1 (vit1a), syntaxin6, and VAMP4 (Brandhorst et al., 2006; Zwilling et al., 2007). The Rab5 effector, EEA1, plays a major role in recruiting SNARE proteins to the EE and if the recruitment of EEA1 is disrupted by PI3K inhibition, the activity of EEA1 is impaired, leading to EE that are unable to fuse properly (McBride et al., 1999; Simonsen et al., 1999). Like many other complexes, once

the fusion of homotypic EE is completed, the complex must be disassembled. The disassembly of the SNARE complex is regulated by AAA+ (ATPases Associated with diverse cellular Activities) protein N-ethylmaleimide-sensitive factor (NSF) (Hanson & Whiteheart, 2005; Mayer, Wickner, & Haas, 1996). The disassembly of the SNARE complex is initiated by the binding of 3 NSF attachment proteins (SNAP) with the four-helical bundle generated from the fusion of the v-SNARE and t-SNARE and uses the energy from ATP hydrolysis to break the bundle apart (Sollner, 1995). (Figure 1.4)

2.4 C-terminal Eps15 homology domain (EHD) protein family

The mammalian EHD family is comprised of four proteins, EHD1-4. This family of proteins has the ability to homo- and hetero-oligomerize and helps facilitate their function in the membrane trafficking pathway (B. D. Grant & Caplan, 2008; Pohl et al., 2000). The EHD proteins are highly conserved at the amino acid level across many species. For example, the EHD family member in *C. elegans*, RME-1, is 67% identical to the human EHD1 amino acid sequence. Furthermore, mammalian EHD1 and EHD3 share roughly 86% sequence identity, yet are able to perform specific functions (B. D. Grant & Caplan, 2008). No matter the species, the EHD proteins share a highly conserved domain architecture consisting of an N-terminal G-domain, a central helical region and a C-terminal EH domain. The EHD proteins became a highly interesting topic of study when EHD1 and RME-1 were found to be crucial in regulating endocytic recycling in human cells and in *C. elegans* (Caplan et al., 2002; B. Grant et al., 2001). (Figure 1.5)

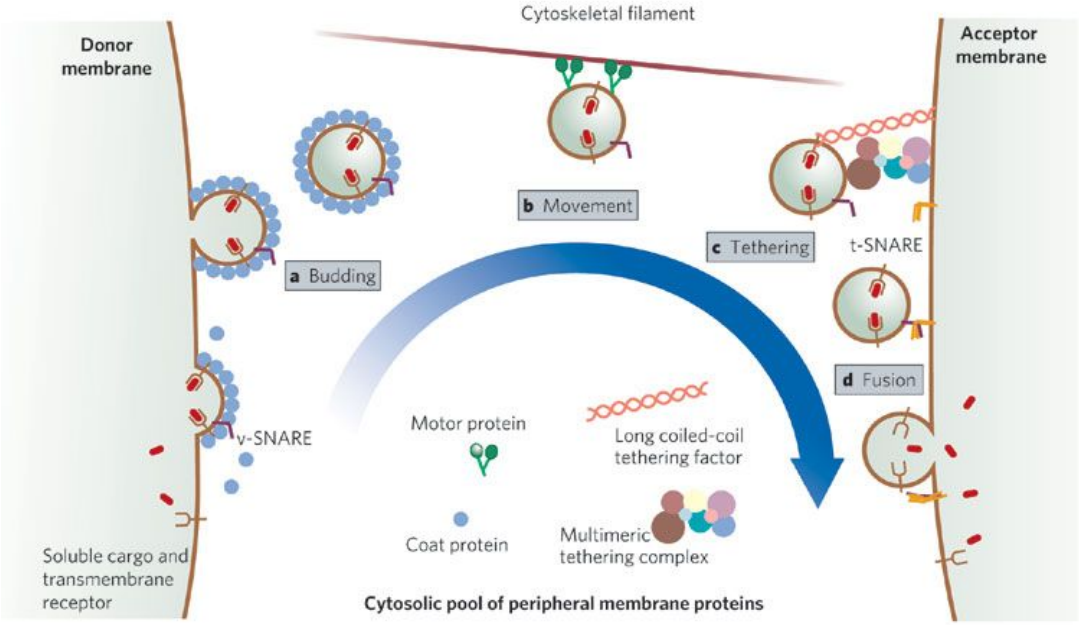

Figure 1.4

Schematic representation of the steps of vesicle transport. (A) Coat proteins are recruited to the cytosolic face of the donor membrane and induce the formation of a vesicle. The coat recruits SNAREs and transmembrane receptors bound to their cargo. (B) After uncoating, motor protein can be recruited to enable the vesicle to travel along microtubules or actin filaments. (c) Once at its destination, the vesicle becomes tethered to the acceptor membrane, probably by long coiled-coil proteins or multimeric tethering complexes. (D) The SNAREs on the vesicle and acceptor membrane form a complex which drives membrane fusion and hence delivery of the contents of the vesicle. Used with permission from Nature (Behnia & Munro, 2005).

2.4.1 EHD1

EHD1 is the best characterized EHD protein and is unique in its localization to TREs involved in endocytic recycling (B. D. Grant & Caplan, 2008; Naslavsky & Caplan, 2011). EHD1 regulates the recycling of many receptors that inter the cell through CME and CIE. Cargo that is regulated by EHD1 includes the transferrin receptor (TfR) (Lin, Grant, Hirsh, & Maxfield, 2001), major histocompatibility complex class I proteins (MHC I) (Caplan et al., 2002), the insulin-regulated GLUT4 transporters (Guilherme, Soriano, Furcinitti, & Czech, 2004), the cystic fibrosis transmembrane conductance regulator (Lin et al., 2001), AMPA type glutamate receptors (Park, Penick, Edwards, Kauer, & Ehlers, 2004), MHC class II molecules (Walseng, Bakke, & Roche, 2008), the hyperpolarization-activated cyclic nucleotide-gated (HCN) ion channel family members HCN1, HCN2 and HCN4 (Hardel, Harmel, Zolles, Fakler, & Klocker, 2008), G-protein-activated inwardly rectifying potassium channels (Chung, Qian, Ehlers, Jan, & Jan, 2009), and the calcium-activated potassium channel KCa2.3 (Gao et al., 2010), and other channels (Guilherme et al., 2004). EHD1 and the Rab11 effector protein, Rab11-FIP2, interacts and localizes to peripheral EE (Naslavsky et al., 2006). This relationship, along with Rab35, suggests a role for EHD1 in the transport of cargo from the EE to the ERC in some capacity (Allaire et al., 2010; Sato et al., 2008). It is known that EHD1 is linked with dynein motors via collapsing response mediator protein-2 (Crmp2), which in turn regulates the cargo trafficking from the EE to the ERC (Rahajeng, Giridharan, Naslavsky, & Caplan, 2010).

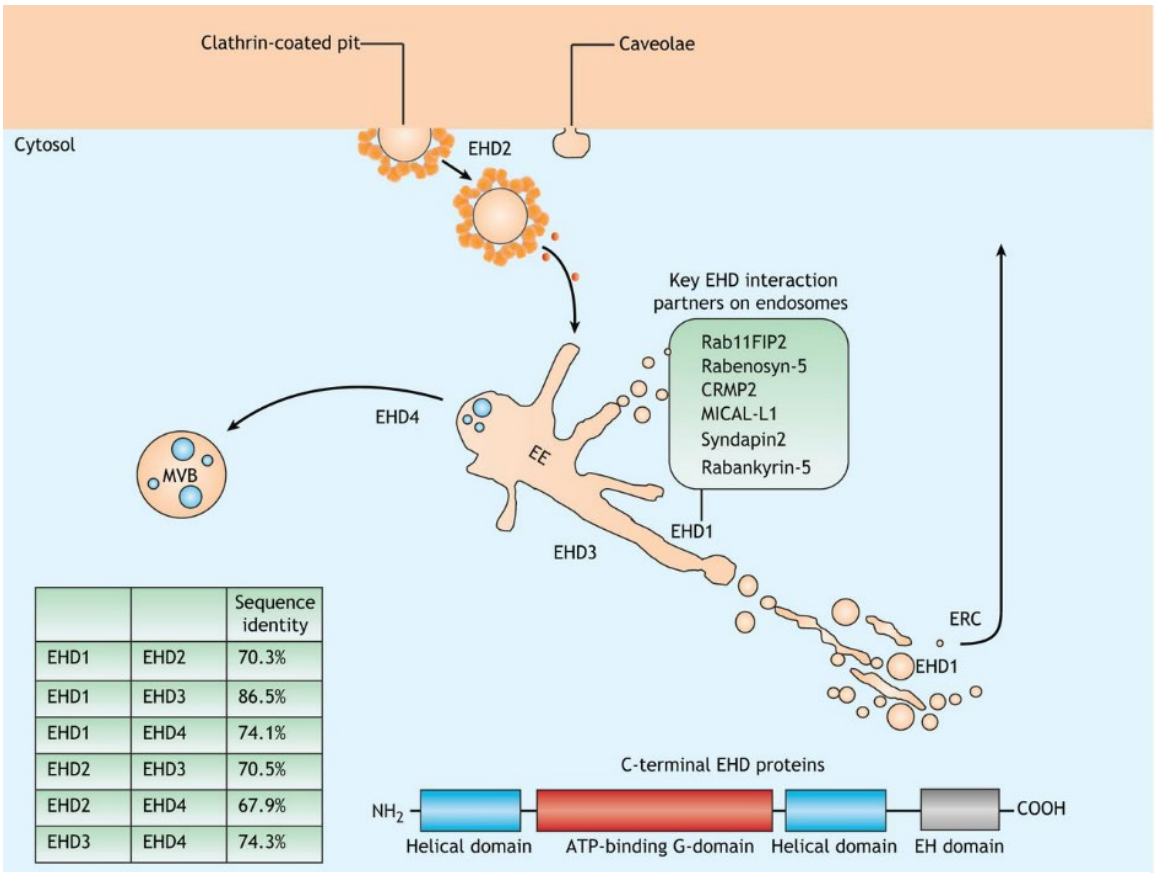

		Sequence identity
EHD1	EHD2	70.3%
EHD1	EHD3	86.5%
EHD1	EHD4	74.1%
EHD2	EHD3	70.5%
EHD2	EHD4	67.9%
EHD3	EHD4	74.3%

Figure 1.5

Role of EHD proteins in membrane trafficking. The four EHD proteins display considerable sequence identity, from ~68–87%, and have been implicated in membrane remodeling (table inset). EHD1, EHD3 and EHD4 have been characterized in the regulation of endosomal transport, primarily at the EE, with EHD1 additionally involved in the regulation of recycling from the ERC. EHD2, the most divergent of the EHD proteins, controls caveolar mobility and may influence internalization at the plasma membrane. Used with permission from JCS (Naslavsky & Caplan, 2018).

Studies have shown that EHD proteins induce lipid tubulation in vitro (Daumke et al., 2007), however studies done in cultured cells suggest that the EHD proteins play an opposite role and promote fission of lipid tubules. Previous studies of the EH domain and the structure of EHD2 provide evidence that they serve as dynamin-like ATPases in the fission of endocytic membranes (Cai et al., 2012; Daumke et al., 2007; Jakobsson et al., 2011; D. W. Lee et al., 2005). In support of EHD1's function as a fission protein, purified EHD1 can be added to an ATP-containing semi-permeable system and induce endosomal fission (Cai et al., 2013). Moreover, recent studies have elucidated the mechanism by which EHD1 forms oligomers around a tubule and induces fission (Deo et al., 2018). Additionally, the nuclear magnetic resonance solution structure of the EHD domain of EHD1 (Kieken, Jovic, Naslavsky, Caplan, & Sorgen, 2007) has led to the identification of novel interaction partners that contain an asparagine-proline-phenylalanine (NPF) motifs followed by acidic residues that selectively interact with the positively charged EH domain electrostatic surface area (Henry, Corrigan, Dineen, & Baleja, 2010).

Our lab discovered MICAL-L1 as a direct interaction partner of the EH domain of EHD1 (Giridharan et al., 2013; Sharma, Jovic, et al., 2009). The latter binds via the first of its two NPF motifs, and MICAL-L1 is required for TRE biogenesis and receptor recycling (Giridharan et al., 2013; Sharma, Jovic, et al., 2009). MICAL-L1 interacts with many essential regulators of TREs, including Rab8 (Sharma, Jovic, et al., 2009), proteins that contain a BAR domain (McMahon & Gallop, 2005; Zimmerberg & Kozlov, 2006), including the N-BAR protein Amphiphysin/Bin1 (Pant et al., 2009), and the F-BAR

protein Syndapin2 (or PACSIN2) (Braun et al., 2005; Giridharan et al., 2013). MICAL-L1 and Syndapin2 bind to the PA on the TRE membranes and subsequently recruit EHD1 to the TRE to facilitate fission, giving rise to newly formed endosomes that contain cargos traveling to and from the ERC.

In addition to the role that EHD1 plays in the recycling of cargos from the PM, EHD1 interacts with VPS26 and VPS35 and in turn can regulate the retrograde transport of cargo from EE to the TGN (Gokool et al., 2007). In recent years, the role of EHD1 has expanded beyond the realm of recycling and it has been revealed as an important player in mitosis and ciliogenesis (Lu et al., 2015; Reinecke, Katafiasz, Naslavsky, & Caplan, 2015), demonstrating that endocytic regulatory proteins may play a larger role in the cell than just controlling endocytic trafficking. This notion that endocytic regulatory proteins can play a role in other pathways, such as EHD1 playing a role in mitosis or ciliogenesis, has led to us identifying a novel role for EHD1 in mitochondrial fission.

2.4.2 EHD2

EHD2 displays the least amount of homology to EHD1, at only 70% identity. The structure of EHD2 has been solved and further supports its role in nucleotide-dependent membrane remodeling (Daumke et al., 2007). EHD2 is involved in the regulation of a variety of important functions such as sarcolemma repair (Marg, Schoewel), myoblast fusion (K. R. Doherty et al., 2008; Posey et al., 2011), and controls Rac1 and the actin cytoskeleton (Benjamin et al., 2011; Stoeber et al., 2012). EHD2 plays a very different role in regulating endocytic trafficking as compared to the other EHD proteins and is

recruited to the PM by preferentially binding to phosphatidylinositol (4,5)-bisphosphate (PI(4,5)P2) (Simone et al., 2013) and is able to regulate caveolar mobility at the PM (Moren et al., 2012). Previous studies from our lab suggest that the phenylalanine residue in the EHD2 NPF motif is crucial for its localization to the PM, while the proline plays a key role in EHD2 dimerization and binding (Bahl, Naslavsky, & Caplan, 2015). Furthermore, EHD2 is able to bind to the EH-domain-binding protein 1 (EHBP1) (Guilherme et al., 2004), which implies that there is functional redundancy with EHD1 (M. George et al., 2007), as well as a role for EHD2 with the internalization of TfR and GLUT4 (Guilherme et al., 2004).

2.4.3 EHD3

EHD3 and EHD1 share the highest percentage of amino acid identity at 86% (Galperin et al., 2002). However, EHD3 does not seem to play a major role in regulating the exit of cargos from the ERC back to the PM. Indeed, upon EHD3-depletion, the cargo accumulates in the EE and does not reach the ERC (Naslavsky et al., 2006). Additionally, EHD3 is involved in retrograde transport from the EE to the TGN and helps maintain the morphology of the Golgi membrane (Naslavsky et al., 2009). EHD3 has the capacity to hetero-dimerize with EHD1 and localizes to the tubulovesicular endosomes (Galperin et al., 2002). Similar to EHD1, EHD3 binds to Rab effectors, such as Rab11-FIP2, Rabenosyn-5, and MICAL-L1 (Naslavsky et al., 2006; Sharma, Jovic, et al., 2009). Studies from our lab have shown that upon knockdown of EHD3, fewer MICAL-L1-decorated TRE are observed, whereas EHD1-depletion leads to hyper-elongation of TRE. This finding was further supported by our semi-intact cell system utilizing purified EHD3,

which led to rapid induction of tubules (Cai et al., 2014). Our lab recently elucidated the mechanism by which EHD3 supports TRE stabilization, (Bahl et al., 2016)

2.4.4 EHD4

EHD4 localizes primarily to EE and may regulate cargo transport from EE to both the ERC and the lysosomal degradation pathway (M. George et al., 2007; Sharma et al., 2008). Studies performed in neuronal cells have shown that EHD4 functions upstream of EHD1 by regulating the internalization of TrkA and TrkB nerve growth factor receptors, along with Nogo-A, an inhibitor of axonal growth (Joset, Dodd, Halegoua, & Schwab, 2010; Shao et al., 2002; Valdez et al., 2005). However, recent studies in our lab have shown that EHD4 and EHD1 can hetero-dimerize and are potentially both needed for TRE fission and regulation of cargos back to the PM (unpublished data).

3. REGULATION OF MITOCHONDRIAL FUSION/FISSION

3.1. Overview

Mitochondria are known for their role in generating ATP via oxidative phosphorylation but also contribute significantly to many other cellular processes including but not limited to regulation of reactive oxygen species (Hamanaka & Chandel, 2010), calcium signaling, (Duchen, 2000; Nicholls, 2005), apoptosis (C. Wang & Youle, 2009), iron homeostasis (Horowitz & Greenamyre, 2010; Richardson et al., 2010), and cellular aging (Srivastava, 2017; Sun, Youle, & Finkel, 2016). The functions that are performed by the mitochondria are closely associated with the regulation of their

dynamics, which includes continuous rounds of fission and fusion that the mitochondria depends upon to remain healthy (Chan, 2012). Disruption of the regulation of mitochondrial fission and fusion may result in many diseases, including Alzheimer's disease (Cho et al., 2009) and Parkinson's disease (PD) (Tang et al., 2015). While there have been recent advances in the field of mitochondrial homeostasis, many aspects of the mechanisms that control the dynamics of fission and fusion remain undiscovered.

In order for 2 mitochondria to fuse together, two separate fusion events must occur, with the first being fusion of the mitochondrial outer membrane (MOM) and the second being the fusion of the mitochondrial inner membrane (MIM). To date, it is known that 3 GTPases directly regulate mitochondrial fusion. Mitofusin-1 (Mfn1) and Mitofusin-2 (Mfn2) are in charge of fusing the MOM, while the MIM is fused together by optic atrophy 1 (OPA1). The fusion of two mitochondria is critical for maintaining membrane potential and thus ATP production (H. Chen et al., 2003). Fusion events are also critical for the proper transfer of mitochondrial proteins and mitochondria DNA (mtDNA) to newly formed mitochondria (Twig & Shirihai, 2011).

The proteins that are needed for mitochondrial fission are just as crucial as the fusion proteins. Mitochondria are constantly balancing the amount of fission and fusion to maintain optimal size and shape. Mitochondrial fission is regulated by a long-known GTPase fission protein, dynamin-related protein 1 (Drp1) (Smirnova, Griparic, Shurland, & van der Bliek, 2001). However, it wasn't until recently that researchers discovered a role for another GTPase, dynamin-2 (J. E. Lee, Westrate, Wu, Page, & Voeltz, 2016).

While the GTPases are thought to provide the energy needed for a mitochondria to undergo fission, the process of mitochondrial fission is more complicated and requires the use of other organelles, such as the endoplasmic reticulum (ER), which helps initiate the mitochondrial fission before the GTPases are present. Mitochondrial fission events are critical for remodeling and rearrangement of mitochondria within the cell or the need to be transferred to a new cell during mitosis (Pagliuso, Cossart, & Stavru, 2018). Since mitochondrial fission is an important cellular event, subtle changes in the rate of fission are enough to influence disease states such as Alzheimer's disease (Castellani et al., 2002; Moreira, Cardoso, Santos, & Oliveira, 2006) or cardiomyocyte hypertrophy (Ago et al., 2010; Pennanen et al., 2014).

3.2 Effectors of fusion

3.2.1 Mitofusin-1 and Mitofusin-2 (Mfn1 and Mfn2)

Mfn1 and Mfn2 perform similar functions in the fusion of the MOM and can even interchange under certain conditions (H. Chen et al., 2003). While Mfn1 and Mfn2 are interchangeable, mutations in Mfn2 alone can have serious consequences and result in disease states such as Charcot-Marie-Tooth Neuropathy type 2A (H. Chen, Chomyn, & Chan, 2005; H. Chen et al., 2003). This suggests that it only takes a minor disturbance in the balance between fission and fusion to disrupt mitochondrial function and lead to a disease state. Mfn1 and Mfn2 are MOM transmembrane GTPases that contain several conserved domains such as an amino-terminal GTP-binding domain, 2 coiled-coil domains and a carboxyl-terminal with a bipartite transmembrane domain (Chandhok,

Lazarou, & Neumann, 2017). While Mfn1 and Mfn2 do play similar roles and have structural homology, Mfn2 has an N-terminal Ras-binding domain that is lacking in Mfn1, suggesting that Mfn2 might have specificity towards a cellular pathway that Mfn1 does not have (K. H. Chen et al., 2004). The second coiled-coil domain of Mfn1 or Mfn2 is responsible for the tethering of the opposing mitochondria through dimerization of anti-parallel coiled-coiled domains, forming either homotypic or heterotypic dimers (Koshiba et al., 2004). Understanding the precise mechanism of signaling that allows Mfn1 or Mfn2 to join two adjacent mitochondria is under active research. (Figure 1.6).

3.2.2 Optic atrophy protein 1 (OPA1)

OPA1 is the major protein that is responsible for the fusion of the MIM and is also thought to be involved in proper cristae folding as well as potentially playing a role in apoptosis (Griparic, van der Wel, Orozco, Peters, & van der Bliek, 2004; Ni, Williams, & Ding, 2015). Interestingly, OPA1 requires the presence of Mfn1 but not Mfn2 to be functional (Cipolat, Martins de Brito, Dal Zilio, & Scorrano, 2004). The loss of OPA1 function can lead to dominant atrophy, an inherited disease that culminates in the degeneration of the optic nerve, suggesting that OPA1 may be important in mitochondrial fusion and homeostasis (H. Chen & Chan, 2005, 2009). For OPA1 to become fully functional, it must be transported to the mitochondria and undergo proteolytic cleavage into 2 separate isotypes, known as long and short forms (Ishihara, Fujita, Oka, & Mihara, 2006). The concentrations of the 2 isotypes under normal

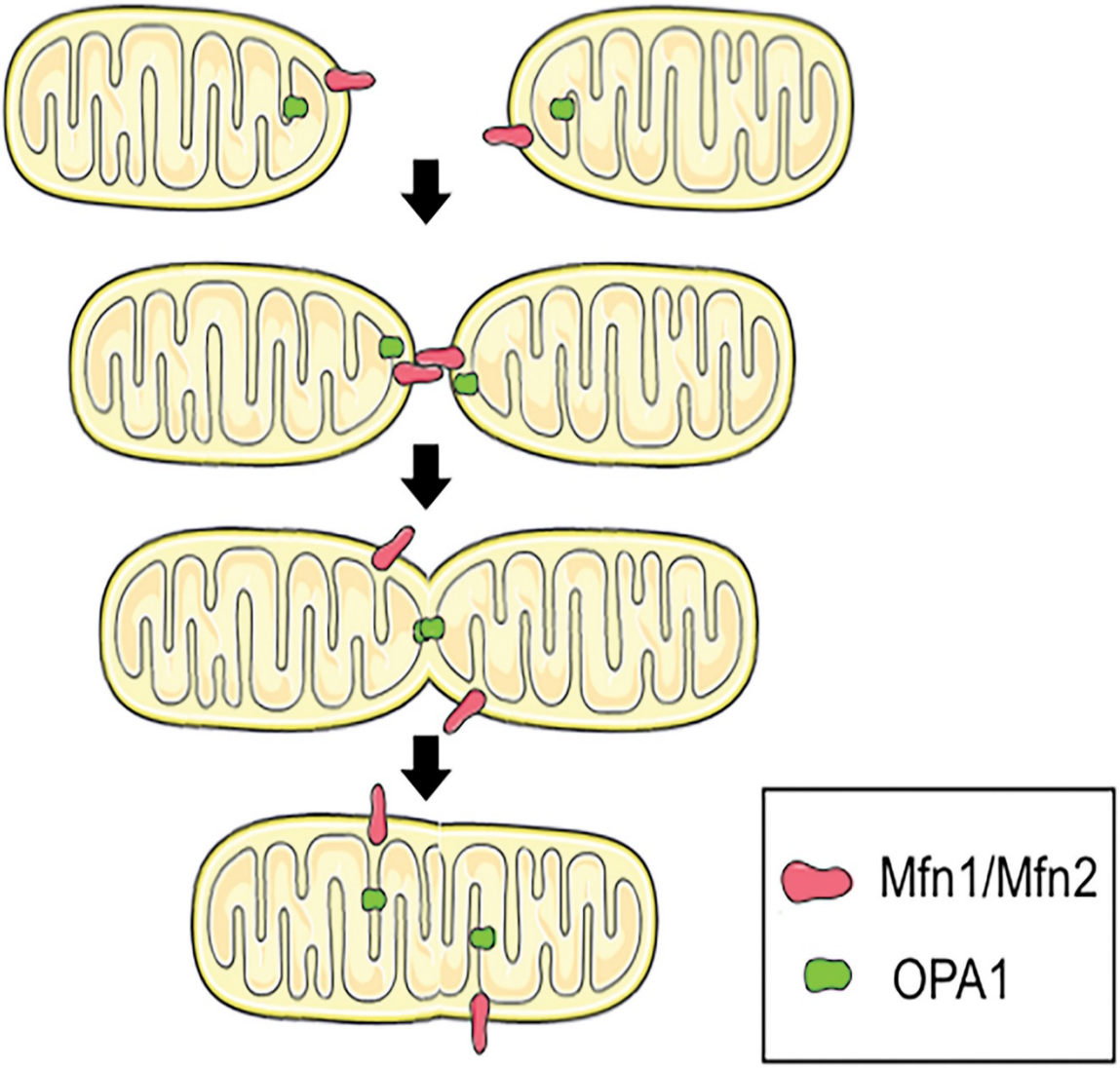

Figure 1.6

Mitochondrial fusion. Mitochondrial fusion via homotypic and heterotypic mitofusin interactions mediates OMM fusion, while OPA1 is responsible for IMM fusion events. Used with permission from Traffic (Farmer et al., 2018).

conditions are nearly equal and must remain that way for fusion of the MIM (Liesa, Palacin, & Zorzano, 2009). The long and short isotypes cannot work separately to complete MIM fusion but must work in tandem to successfully fuse two mitochondria (Song, Chen, Fiket, Alexander, & Chan, 2007) (Figure 1.6).

3.3 Effectors of fission

3.3.1 ER/mitochondria contact sites

Previous studies have shown that the ER and the mitochondria share contact sites that are essential for phospholipid synthesis, calcium signaling, and marking constriction sites on the mitochondria, indicating where fission needs to occur (de Brito & Scorrano, 2010; Friedman et al., 2011). There are several types of connections or bridges that can be made between the ER and the mitochondria. For example, a distinct structure termed the ER mitochondria encounter structure (ERMES) can be found in yeast and is involved in mitochondrial fission, while in mammalian cells, the fusion protein, Mfn2, is potentially responsible for tethering the ER and mitochondria together (de Brito & Scorrano, 2008; Kornmann et al., 2009). More recent studies have been able to identify PDZ domain containing 8 (PDZD8), a homolog of the yeast ERMES protein maintenance of mitochondrial morphology protein (MMM1), as playing a crucial role in tethering mitochondria to the ER in mammalian neurons (Hirabayashi et al., 2017). It is interesting to note that even with mitochondria remaining dynamic under physiological conditions, the ER contact sites seem to be very stable, suggesting their presence is

constantly needed for mitochondrial homeostasis (Friedman, Webster, Mastronarde, Verhey, & Voeltz, 2010).

It is thought that the ER plays a role in the initial constriction of the mitochondria, to promote fission (Friedman et al., 2011; Korobova, Ramabhadran, & Higgs, 2013). Indeed, it has been demonstrated that the ER-localized inverted formin 2 protein is able to induce actin polymerization between the ER and mitochondria, which is the driver for initial mitochondrial fission (Korobova et al., 2013). The initial constriction done by the ER is critical to facilitate a proper fission event as Drp1 oligomers are unable to wrap around a non-constricted mitochondria. Mitochondria typically have a diameter around 200 nm or more and based on their size, Drp1 oligomers can form around structures that have a maximal diameter of 110 to 130 nm (Friedman et al., 2011). Consistent with this data, ER constriction sites have been known to constrict the mitochondria down to around 140 nm in diameter, suggesting that the ER must first constrict the mitochondria to allow Drp1 oligomers to further constrict (Friedman et al., 2011) (Figure 1.7).

3.3.2 Dynamin-related protein 1 (Drp1)

Under normal conditions, Drp1 is mainly a cytosolic protein that is recruited to the mitochondria upon initial constriction by the ER. Drp1 is part of the dynamin family of GTPase proteins but unlike its isoform, dynamin-2, Drp1 lacks a lipid-binding pleckstrin homology domain; therefore it is unable to bind directly to the mitochondrial membrane (Mears et al., 2011; Pagliuso et al., 2018). To make up for the lack of binding,

Drp1 must bind to receptors that are found on the mitochondrial membrane. In mammalian cells, many Drp1 receptors located on the MOM have been identified, such as mitochondrial fission 1 protein (Fis1), mitochondrial fission factor (Mff), or mitochondrial dynamics protein 49 and 51 (MiD49/MiD51) (Loson, Song, Chen, & Chan, 2013; Otera et al., 2010; Palmer et al., 2013; Palmer et al., 2011; Zhao et al., 2011). While all of the receptors can recruit and bind Drp1 to the mitochondrial membrane, studies suggest that Mff is the most prominent receptor for mitochondrial fission (Loson et al., 2013). Once Drp1 is recruited to the MOM, oligomers form around the ER and Drp1 uses GTP hydrolysis to further constrict the mitochondria. However, it is important to note that Drp1 is unable to complete the fission process and therefore needs an additional fission factor (Frohlich et al., 2013). (Figure 1.7).

3.3.3 Dynamin-2 (Dyn2)

As previously mentioned, the role of Dyn2 has been well-established in the fission of clathrin-coated vesicles at the plasma membrane during endocytosis (Gonzalez-Jamett et al., 2013). Similar to Drp1, Dyn2 is able to form oligomers around a membrane and use its GTPase function to complete a fission event (Ferguson & De Camilli, 2012). Until recently, the model for mitochondrial fission proposed that after the initial constriction of the mitochondria by the ER, Drp1 was able to further constrict the mitochondria until a single mitochondria splits into two separate structures. However, new evidence now supports the model that Dyn2 not only acts at the plasma membrane but also plays a key role in the later stages of mitochondrial fission, following

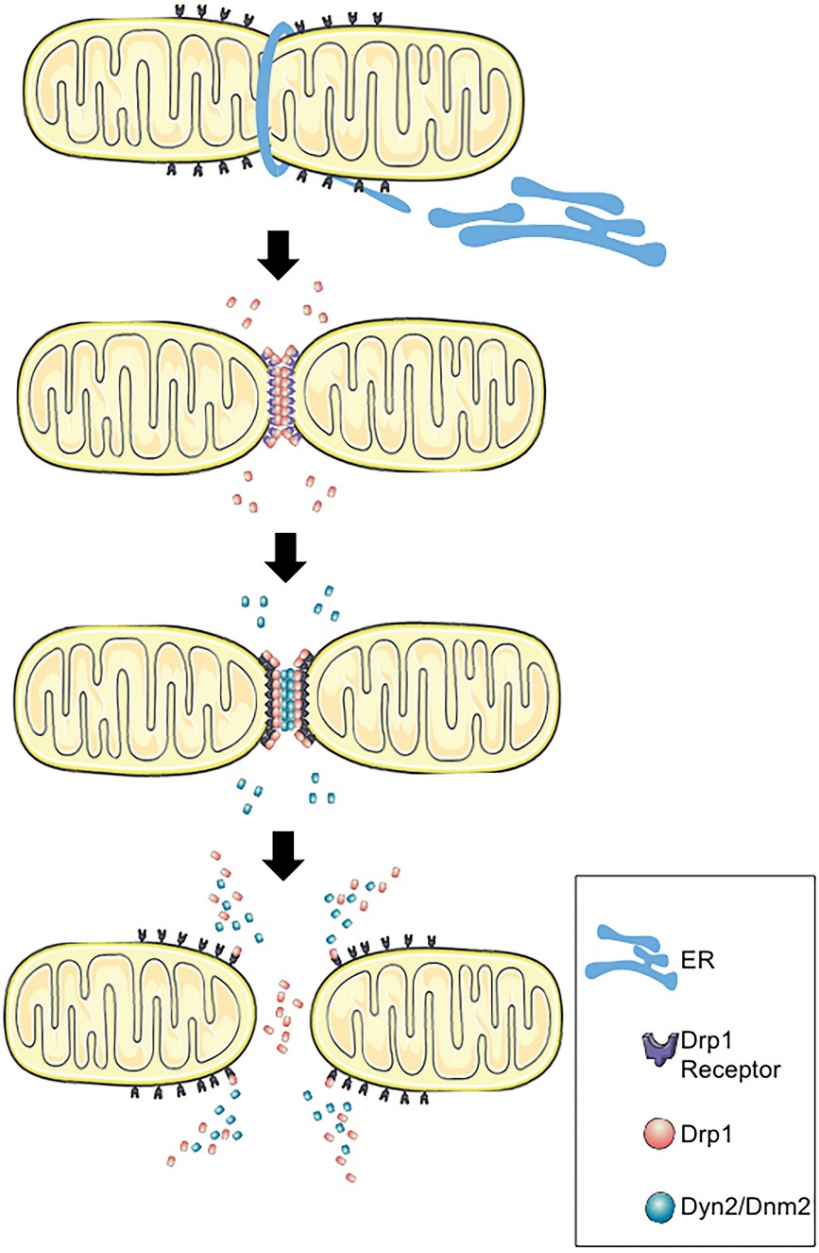

Figure 1.7

Mitochondrial fission. Constriction of the mitochondrial membrane is first initiated by the ER at ER/mitochondria contact sites. After constriction by the ER, the mitochondrial membrane is "marked" for fission, thus resulting in Drp1 recruitment by Drp1 receptors. Drp1 then forms oligomers around the constriction site and further constricts the membrane through GTPase activity, leading to Dyn2/Dnm2 recruitment, additional GTP hydrolysis, and completion of the process of fission resulting in 2 separate mitochondria. Used with permission from Traffic (Farmer et al., 2018).

constriction by the ER and Drp1 (J. E. Lee et al., 2016). It has been shown that Drp1 and Dyn2 must both be present for mitochondrial fission to occur. Loss of either protein leads to elongated mitochondria due to a lack of fission (J. E. Lee et al., 2016). The studies performed by Lee *et al.* highlight the growing appreciation for the role of endocytic regulatory proteins in mitochondrial homeostasis. (Figure 1.7)

3.4 Other modes of regulating mitochondrial fusion and fission

Traditionally, it is thought that mitochondrial homeostasis is regulated by the GTPases, Mfn1, Mfn2, OPA1, Drp1 and its MOM receptors, and more recently, Dyn2. However, recent mitochondrial homeostasis research has demonstrated that the regulation of mitochondria is far more complex than previously thought. Studies are starting to show how important the upstream events that involve the trafficking and regulation of the mitochondria-associated proteins, thus providing additional mechanisms of indirect mitochondrial fission and fusion.

One key protein that indirectly regulates mitochondrial homeostasis through the trafficking of mitochondrial-associate fusion or fission proteins is vacuolar protein sorting 35 (VPS35) (Tang et al., 2015; W. Wang, Ma, Zhou, Liu, & Zhu, 2017; W. Wang et al., 2016). VPS35 is a subunit of a larger complex termed retromer cargo selective complex (CSC). The retromer CSC is comprised of 3 vacuolar protein sorting proteins, VPS26, VPS29, and VPS35, and associates with sorting nexin proteins (SNX) (Seaman, 2004). The original function described for the retromer CSC was retrieval of the mannose-6 phosphate receptor (M6PR) from peripheral endosomes back to the trans-

Golgi network (TGN) (Arighi, Hartnell, Aguilar, Haft, & Bonifacino, 2004). Later on, other cargo was found to be regulated by the retromer, including the iron transporter DMT1-11/Slc11a2 (Tabuchi, Yanatori, Kawai, & Kishi, 2010), the Wnt transport protein Wntless/MIG-14 (Eaton, 2008), and others. Exciting new studies have implicated a role for VPS35 in mitochondrial fusion and fission as they relate to PD (Tang et al., 2015; W. Wang et al., 2017; W. Wang et al., 2016). While VPS35 has been associated with mitochondrial homeostasis and PD, the mechanisms by which VPS35 regulates mitochondrial morphology remains controversial and unclear.

3.4.1. Indirect role of VPS35 in mitochondrial fusion

The proteins associated with regulating the fusion of mitochondria, Mfn1, Mfn2, and OPA1, are regulated by post-translational modifications, with one key type of modification being ubiquitination. The ubiquitination of Mfn2 targets the fusion protein for degradation by the proteasome, thus limiting the amount of fusion that can take place. Recent studies have demonstrated a role for VPS35 in regulating the ubiquitination of Mfn2, most likely by trafficking of the E3 ubiquitin ligase, MUL1, which is responsible for ubiquitinating Mfn2 on the mitochondria membrane (Tang et al., 2015). Tang *et al* showed that VPS35-depletion induces a PD-like condition that causes fragmented mitochondria and cell death in mouse dopamine neurons (Tang et al., 2015). Under these experimental conditions, VPS35 interacts with MUL1 and sequesters it in the cytoplasm but under VPS35-depletion conditions, the MUL1 is free to traffic to the mitochondria where it ubiquitinates Mfn2 and induces the degradation of

Mfn2, leading to reduced mitochondrial fusion and fragmented mitochondria. (Top portion of Figure 1.8)

3.4.2. Indirect role of VPS35 in mitochondrial fission

While the previously mentioned study suggests a role for VPS35 in the regulation of mitochondrial fusion, a recent study provides experimental evidence that supports a role for VPS35 in the regulation of mitochondrial homeostasis. Wang *et al.* demonstrated that VPS35 binds to complexes of inactive mitochondrial fission proteins, Drp1, on the mitochondrial membrane. It is proposed that upon binding of VPS35 and inactive Drp1 on the mitochondrial membrane, mitochondrial-derived vesicles (MDVs) are generated and therefore remove the inactive Drp1 for transport to the lysosome for degradation (W. Wang et al., 2017; W. Wang et al., 2016). As a result, this frees Drp1 receptors at mitochondrial constriction sites to recruit and/or activate Drp1 and promote mitochondrial fission (W. Wang et al., 2017; W. Wang et al., 2016). The MDVs generated in this model consist of structures with diameters of 70 to 150 nm (Cadete et al., 2016) and are considered to be important for quality control mechanisms that deliver mitochondria-related proteins and membranes to the late endosomes or multivesicular bodies (Soubannier, McLelland, et al., 2012). While the exact mechanism of how the cargo for the MDVs is selected at the mitochondria is unknown, studies have shown that both MIM and MOM membranes can be used to generate MDV and contain both membrane bound and mitochondrial matrix proteins (McLelland, Soubannier, Chen, McBride, & Fon, 2014; Neuspiel et al., 2008; Soubannier, McLelland, et al., 2012; Soubannier, Rippstein, Kaufman, Shoubridge, & McBride, 2012). It is important to note

that a mutated form of VPS35 that is commonly found in PD, VPS35^{D620N}, causes extensive mitochondrial fragmentation and loss of function, providing additional evidence that VPS35 plays a critical part in PD related dysfunction. (Bottom portion of Figure 1.8).

4. REGULATION OF MITOCHONDRIA INDUCED APOPTOSIS

4.1 Overview

Apoptosis is an essential cellular event that is required for normal development and maintenance of whole tissue homeostasis, protection from genomic miscues, and to control humoral immune responses (Slomp & Peperzak, 2018). During the process of apoptosis, a cell will begin to shrink, fragment its DNA, and eventually break up into smaller apoptotic bodies that can easily be cleared by phagocytes (Fadeel & Orrenius, 2005). The process of apoptosis results in activation of cysteine proteases termed caspases that cleave cellular proteins that are critical for survival. These caspases are activated through either an extrinsic apoptosis pathway, which becomes active when the death receptor, located on the surface of the target cell, becomes engaged. Caspases can also be activated by the intrinsic pathway that is initiated by internal cellular stresses. Apoptosis is a highly regulated process, making it impossible to expand on every aspect of both the extrinsic and intrinsic pathways. Due to this, I will focus primarily on the intrinsic pathway of apoptosis, in particular, the regulation of the intrinsic pathway by the B-cell lymphoma 2 (Bcl-2) family of proteins. For more detailed information on the extrinsic and intrinsic pathway, refer to the review by Elmore (Elmore, 2007).

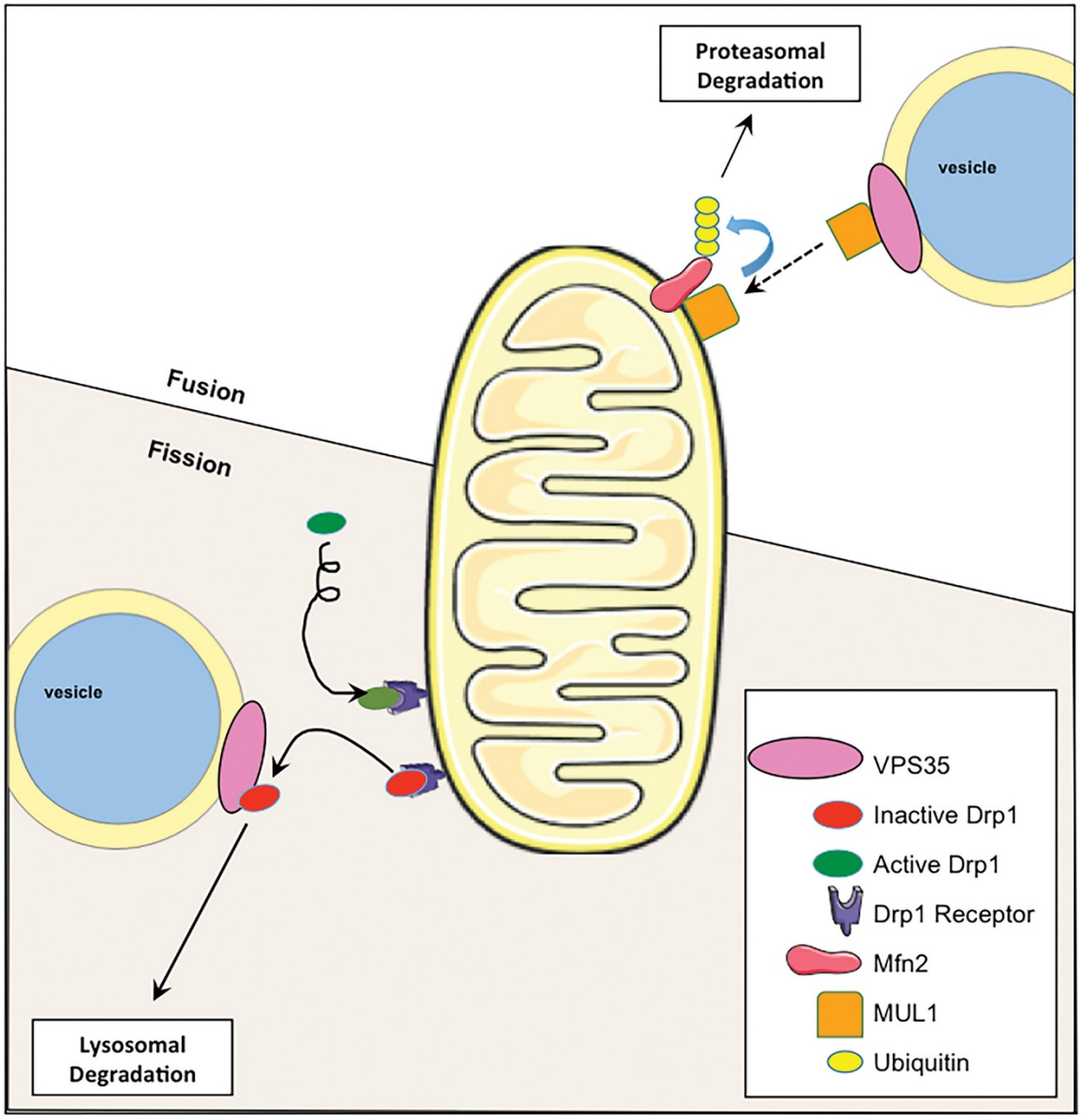

Figure 1.8

Potential roles of VPS35 in mitochondrial fission/fusion. Model representing the role of VPS35 (pink) in mitochondrial fission (bottom left) or mitochondrial fusion (top right). For fission, VPS35 removes inactive Drp1 (red) and traffics it to the lysosome for degradation, to allow active Drp1 (green) to further constrict the OMM. For fusion, VPS35 regulates MUL1 (orange) localization to the OMM, where it binds to Mfn2 (red) and induces its polyubiquitination (yellow) to target it for proteasomal degradation. Used with permission from Traffic (Farmer et al., 2018).

4.2 Bcl-2 protein family regulation

The Bcl-2 family of proteins is a key group of regulators that controls apoptosis by regulating the mitochondrial outer membrane permeabilization MOMP. Once MOMP occurs, cytochrome *c* is released and activates the caspases that carry out the rest of the apoptotic process. The Bcl-2 family can be divided into 3 main groups depending on the function that they serve in either preventing or promoting mitochondria induced apoptosis (1) anti-apoptotic proteins (Bcl-2, Bcl-xL, Bcl-W, Mcl-1, Bfl-1/A1), (2) pro-apoptotic pore-formers (Bax, Bak) and (3) pro-apoptotic BH3-only proteins (BAD, BID, BIK, BIM, BMF, HRK, NOXA, PUMA, etc.) (Kale, Osterlund, & Andrews, 2018). All of the Bcl-2 family members contain a BH3 domain, which is one of the four BH domains that help facilitate the interactions between family members (Lomonosova & Chinnadurai, 2008). Members of the anti-apoptotic and pro-apoptotic groups contain all 4 of the BH domains and therefor have a highly conserved structure that forms a hydrophobic BH3 domain-binding groove (Shamas-Din, Brahmbhatt, Leber, & Andrews, 2011). In addition to the BH domains, most of the Bcl-2 family members have a transmembrane domain (TD) that allows them to localize to various membranes, such as the mitochondria or ER. The Bcl-2 family members who do not have the TD interact with other proteins on the membranes. The ability of different Bcl-2 proteins to interact with each other is critical for regulation of MOMPs. When the interactions favor the pore formation of Bax/Bak on the MOM, cytochrome *c* is released from the mitochondria and the intrinsic pathway is activated (Wei et al., 2001). BH3-only proteins play a role as cell death initiators whose activity is transcriptionally or post-translationally regulated

depending on the upstream cell signaling (Czabotar, Lessene, Strasser, & Adams, 2014; Danial & Korsmeyer, 2004; Youle & Strasser, 2008). (Figure 1.9)

There are various competing models for how the interactions between Bcl-2 family members interact to either prevent or promote apoptosis. However, in all models, the BH3 domain is a necessary component for the primary apoptotic function of Bcl-2 family members and mediates the interactions between them. For example, the BH3 domain of the BH3-only activator proteins can bind to the BH3 domain-binding groove of the Bax or Bak and activate them to induce mitochondria pore formation and apoptosis (Czabotar et al., 2013; Moldoveanu et al., 2013). Upon binding of the BH3-only activator to Bax or Bak, a series of conformational changes occurs that allows for the Bax or Bak to be homo-oligomerized and form the pore in the MOM (Kale et al., 2018). On the other hand, the BH3 domain-binding groove of the anti-apoptotic proteins can bind to the BH3 domains of Bax and Bak, along with the BH3-only activator proteins and thus inhibit their function by sequestering the pro-apoptotic proteins and thus preventing MOM pore formation (Ku, Liang, Jung, & Oh, 2011; Liu et al., 2010). The BH3-only sensitizer proteins can bind also bind to the BH3 domain-binding groove of the anti-apoptotic proteins and inhibit them from sequestering the pro-apoptotic proteins, resulting in an increase in the pore formation in the MOM (Petros et al., 2000). For the most part these interactions occur at or in the MOM and the lipid composition of the membrane plays a key role in facilitating structural changes of the Bcl-2 family of proteins and the structure of the protein dictates the binding affinity between family

members, thus controlling whether pores will be formed or not (Chi, Kale, Leber, & Andrews, 2014; Shamas-Din et al., 2013). (Figure 1.9)

5. SUMMARY AND CONCLUSIONS

Endocytic trafficking is a highly regulated and important process for overall cellular health. There have been major advances in understanding how the proteins that regulate this pathway interact, sort, and traffic internalized cargo from the PM over the last two decades. Along with determining the mechanisms by which they regulate trafficking, there is a growing body of work showing a relationship between endocytic regulatory proteins and other organelles, such as centrosomes, cilia, and mitochondria. For example, the role of the GTPase Dyn2 in both endocytic fission at the PM and in mitochondrial fission has been highlighted recently as well as the novel role for the retromer complex in regulating the trafficking of Drp1. The newly discovered function of the retromer has solidified the links between endocytic pathways and mitochondria. However, it remains unknown whether other proteins that interact with the retromer also play a role in the regulation of mitochondrial fusion or fission. Chapter II will highlight a novel role for the retromer interaction partners, EHD1 and Rabankyrin-5, in indirectly regulating mitochondrial fission through control of the retromer localization.

Mitochondria play many roles within the cell to help maintain overall homeostasis, such as reactive oxygen regulation, calcium signaling, apoptosis, iron homeostasis, and cellular aging. With the growing body of work supporting the idea

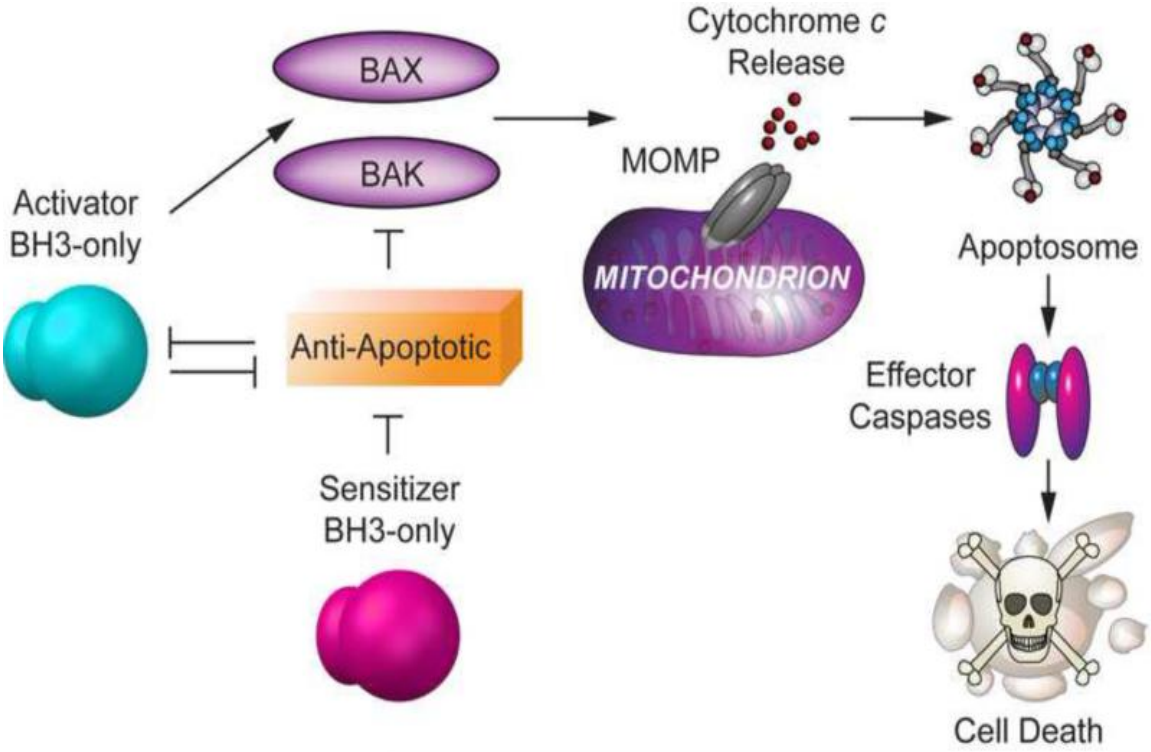

Figure 1.9

BCL-2 family interactions and regulation of BAX/BAK oligomerization. BAX/BAK activation is directly triggered by activator BH3-only proteins (BIM, BID and PUMA) and is inhibited by anti-apoptotic BCL-2 family members. Sensitizer BH3-only proteins do not activate BAX and BAK directly, but lower the threshold for apoptosis by binding anti-apoptotic members and releasing activators to trigger BAX and BAK oligomerization. Anti-apoptotic BCL-2 proteins inhibit activator BH3-only proteins and BAX/BAK oligomerization. Used with permission from Trends in Endocrinology and Metabolism (Gimenez-Cassina & Danial, 2015).

that endocytic regulatory proteins play a key role in regulating the fusion and fission of mitochondria, it raises the question whether they also play a role in other mitochondrial functions. All of these functions are extremely important for cellular health but the role that mitochondria play in apoptosis might be the most important. Apoptosis induced by permeabilization of the mitochondrial membrane is regulated by the Bcl-2 family of proteins. Some of these proteins can be found on the mitochondrial membrane, while others, such as Bax or Bcl-xL, must traffic to the mitochondria to either form pores or prevent pore formation,. Studies have shown that Bax most likely undergoes simple diffusion to reach the mitochondrial membrane. However, to date there is no available data to explain how Bcl-xL traffics to the mitochondria to prevent pore formation. Although Bcl-xL may undergo simple diffusion, given how highly regulated apoptosis is, it is logical to think there is something regulating this translocation from the cytoplasm to the mitochondria. Chapter III will describe, for the first time, a relationship between endocytic regulatory proteins and Bcl-xL. In this chapter I propose a model for how the retromer is able to regulate the translocation of Bcl-xL to the mitochondrial membrane, and I demonstrate that without the retromer, the rate of apoptosis is enhanced.

Chapter II

ROLE OF ENDOCYTIC REGULATORY PROTEINS IN MITOCHONDRIAL HOMEOSTASIS

With permission from Journal of Cell Science, parts of this chapter were derived from: (Farmer et al., 2017)

Farmer, T., J.B. Reinecke, S. Xie, K. Bahl, N. Naslavsky, and S. Caplan. 2017. Control of mitochondrial homeostasis by endocytic regulatory proteins. *J Cell Sci*.

6. ABSTRACT

Mitochondria play crucial roles in producing cellular energy, regulating reactive oxygen species (ROS), and controlling apoptosis. Mitochondrial function is regulated by constant fusion and fission but the mechanisms that maintain mitochondrial homeostasis remain incompletely understood. Recent studies implicate Dyn2 and Drp1 as two GTPases that are required for regulating mitochondrial fission. In Chapter II, we demonstrate that the ATPase and endocytic protein, EHD1, is a novel regulator of mitochondrial fission. Depletion of EHD1 results in static and elongated networks of mitochondria, similar to that observed upon Dyn2- or Drp1-depletion. However, depletion of Dyn2 or Drp1 interferes with the susceptibility of cells to staurosporine-induced mitochondrial fragmentation, whereas EHD1-depleted cells remain sensitive to staurosporine (STS), suggesting that EHD1 functions through a different mechanism than the two GTPases. Recent studies have demonstrated that VPS35 and the retromer complex influence mitochondrial morphology by one of two mechanisms: 1) Decreased fusion by Mul1-mediated ubiquitination and degradation of fusion protein Mfn2, or 2) Increased fission by removing inactive Drp1 from the mitochondrial membrane. Herein, we provide evidence that EHD1 and its interaction partner, Rabankyrin-5, interact with the retromer complex to influence mitochondrial dynamics, likely by inducing VPS35 to remove inactive Drp1 from the mitochondrial membrane. Chapter II sheds light on mitochondrial homeostasis, expanding on novel concepts pertaining to endocytic regulatory proteins and their impact on mitochondrial dynamics.

7. INTRODUCTION

Mitochondria play an essential role in the overall homeostasis of a cell. Among their many functions are the regulation of ATP levels via oxidative phosphorylation, Ca^{2+} signaling (Duchen, 2000; Nicholls, 2005), apoptosis (C. Wang & Youle, 2009), and ROS generation and sequestration (Hamanaka & Chandel, 2010). The function of the mitochondria is closely controlled by their dynamics, and they are continually undergoing rounds of fusion and fission, a process required for mitochondrial health and homeostasis (Chan, 2012). Indeed, small disruptions in the dynamics of mitochondria can result in a wide variety of diseases, such as Alzheimer's disease (Cho et al., 2009) and PD (Tang et al., 2015). The mechanisms by which mitochondrial dynamics influence these neurological disorders remain unclear. However, fusion and fission control mitochondrial size and shape, the total number of mitochondria, and many mitochondrial functions such as respiration and cell survival (Chan, 2012; Flippo & Strack, 2017). Despite the significance of mitochondrial dynamics and the growing number of molecules involved in these events, many of the mechanisms regulating mitochondrial dynamics remain unknown.

For mitochondria to undergo fusion, there need to be two distinct fusion events, between both the outer membranes and inner membranes of apposing mitochondria. Three mammalian GTPases have been implicated in regulating mitochondrial fusion: the mitofusins Mfn1 and Mfn2 control fusion of the MOM (Rojo, Legros, Chateau, & Lombes, 2002; Santel & Fuller, 2001) and OPA1 mediates fusion of the MIM (Alexander et al., 2000; Delettre et al., 2000). The dynamin-related GTPase Drp1 has been identified

as a key protein required for mitochondrial fission (Bleazard et al., 1999; Labrousse, Zappaterra, Rube, & van der Bliek, 1999). Mitochondrial membrane receptors recruit Drp1 to the MOM, where it functions in constriction, and the absence of Drp1 from the cell leads to elongated mitochondrial networks. In addition to Drp1, a recent study demonstrated that Dyn2 coordinates with Drp1 to sequentially mediate the final step of mitochondrial fission (J. E. Lee et al., 2016).

While identification of proteins that play a direct role in mitochondrial homeostasis and the elucidation of their mechanisms of action has expanded rapidly in recent years, less is known about the indirect regulation of mitochondrial fusion and fission. One new enticing area of research relates to recent studies pointing to a novel role for endocytic regulatory proteins in controlling mitochondrial fusion and fission. For example, VPS35, a component of the retromer cargo selection complex that initially was described as being responsible for regulating the trafficking of cargos from endosomes to the Golgi (Arighi et al., 2004), is a key regulator of mitochondrial dynamics and one of only a handful of proteins that cause familial PD (Kumar et al., 2012; Vilarino-Guell et al., 2011; Zimprich et al., 2011). Indeed, suppression of VPS35 in hippocampal neurons results in degeneration, abnormal dendritic spines, and swollen axons (C. L. Wang et al., 2012), and overall VPS35 expression is decreased in PD patients (MacLeod et al., 2013).

The mechanisms by which VPS35 and the retromer control mitochondrial homeostasis are not well understood. A recent study has shown that a reduction in the

protein level of VPS35 in mouse dopamine neurons induces a PD-like phenotype that includes neuronal death, α-synuclein deposition and fragmented mitochondria (Tang et al., 2015). In the same study, it was shown that VPS35 depletion or mutation led to upregulation of Mul1, an ubiquitin ligase that ubiquitinates Mfn2 and inducing the degradation of Mfn2 through the proteasome, and may result in more fission than fusion, and thus fragmented mitochondria (Tang et al., 2015). On the other hand, a second study provides support for a model that suggests VPS35 binds to Drp1 on the mitochondrial membrane and facilitates the removal of inactive Drp1 and transports it to the lysosome for degradation, allowing active Drp1 to bind to free receptors on the mitochondria to promote constriction and eventually fission (W. Wang et al., 2017; W. Wang et al., 2016).

In Chapter II, we demonstrate that the endocytic fission protein and ATPase, EHD1, is a novel player in regulating mitochondrial dynamics and homeostasis. The depletion of EHD1 from cultured cells results in an elongated network of mitochondria that becomes highly static compared to normal mitochondria. While EHD1 has considerable homology to the dynamin family members Drp1 and Dyn2, EHD1 knockdown is unable to prevent STS-induced mitochondrial fragmentation, unlike the knockdown of Drp1 and Dyn2. This suggests that EHD1 does not play a role alongside Drp1 and Dyn2 and more likely functions in a regulatory capacity. Previous work in the lab has shown that EHD1 and its binding partner Rabankyrin-5 both interact with the retromer complex, and we now hypothesize that EHD1 regulates mitochondrial fission through its control of VPS35 localization within the cell. My findings support a

mechanism by which EHD1 and Rabankyrin-5 interact with the retromer and influence mitochondrial homeostasis by controlling VPS35-mediated removal of inactive Drp1 from the mitochondrial membrane.

8. MATERIALS AND METHODS

8.1 Reagents and antibodies

Mitotracker Red was purchased from Thermo Fisher Scientific (M7512). STS was purchased from Sigma-Aldrich (S5921). Antibodies against the following proteins were used: EHD1 (ab109311, 1:1000 dilution for immunoblotting), Vps26 (ab23892, 1:500 dilution for immunoblotting), VPS35 (ab97545, 1:500 dilution for immunoblotting), Mfn2 (ab56889, 1:500 dilution for immunoblotting) and actin (ab14128, 1:4000 dilution for immunoblotting) from Abcam; Tom20 (sc-11415, Santa Cruz Biotechnology, 1:1000 dilution for immunofluorescence); Mul1 (GTX112673, GeneTex, 1:500 dilution for immunoblotting); GST conjugated to horseradish peroxidase (HRP) (NA935, Amersham, 1:5000 dilution for immunoblotting); MICAL-L1 (H00085377-B01P, Abnova, 1:500 dilution for immunoblotting); Rabankyrin-5 (PA5-24640, Thermo Scientific, 1:200 dilution for immunoblotting); Drp1 (8570s, Cell Signaling, 1:500 dilution for immunoblotting); GM130 (610822, BD Biosciences, 1:500 dilution for immunoblotting); donkey anti-mouse IgG light chain conjugated to HRP (715-035-151, 1:10,000 dilution for immunoblotting), mouse anti-rabbit IgG light chain conjugated to HRP (211-032-171, 1:10,000 dilution for immunoblotting), from Jackson; and donkey anti-mouse-IgG conjugated to Alexa Fluor 488 (A21202, 1:700 dilution for immunofluorescence), donkey

anti-mouse-IgG conjugated to Alexa Fluor 568 (21043, 1:700 dilution for immunofluorescence), goat anti-rabbit-IgG Alexa Fluor 488 (A11034, 1:700 dilution for immunofluorescence), and goat anti-rabbit-IgG conjugated to Alexa Fluor 568 (A11036, 1:700 dilution for immunofluorescence) from Molecular Probes.

8.2 Cell Culture

The HeLa cervical cancer cell line was purchased from American type Culture Collection (ATCC) and grown in DMEM with high glucose containing 10% fetal bovine serum (FBS), 1x penicillin-streptomycin (Invitrogen, 10378016), and 2mM glutamine. The immortalized retinal pigment epithelium (RPE) cell line was obtained from ATCC and grown in DMEM/F12 containing 10% FBS, 1× penicillin-streptomycin and 2 mM glutamine. Cell lines were routinely tested for mycoplasma contamination.

8.3 siRNA transfection and rescue experiments

Custom EHD1 siRNA oligonucleotides (described in (Sharma, Giridharan, Rahajeng, Naslavsky, & Caplan, 2009)), and On-Target Rabankyrin-5 siRNA oligonucleotides were purchased from Dharmacon. RPE cells were transfected using Liptofectamine RNAiMax (Invitrogen) with 40nM oligonucleotide. The efficiency of the knockdown was measured by immunoblotting or immunofluorescence at 72 h post transfection for each experiment. For rescue experiments, RPE cells were simultaneously treated for EHD1 siRNA and transfected using Fugene 6 (Roche) with a GFP-myc-EHD1 construct engineered with silent mutations making it resistant to the siRNA oligonucleotides.

8.4 Recombinant gene expression and protein purification

The recombinant DNA constructs (GST-EHD1 and GST-EH1) were expressed in *E. coli* Rosetta (R2) cell strain and purified by affinity chromatography. Briefly, a freshly transformed colony of *E. coli* was inoculated in 50 ml of Luria-Bertani (LB) broth (with 100 μg/ml of ampicillin) and cultured overnight at 37°C with continuous shaking (primary culture). Next, the primary culture was inoculated in 1000 ml of fresh LB broth in a 1:100 dilution and incubated at 37°C with continuous shaking until the OD was within 0.4-0.6 at 600 nm. The culture was then induced with 1 mM IPTG overnight at 18°C. The cells were then centrifuged at 2100 x g for 15 min at 4°C. The bacterial pellet obtained was re-suspended in ice-cold lysis buffer (1 x PBS, pH 7.4) containing 1 tablet/10 ml protease inhibitor cocktail (Roche). Sample lysis was performed by six cycles of sonication on ice (2 min bursts/2 min cooling/200-200 watts in a Branson Sonicator, USA). The lysate was centrifuged at 18000 x g for 30 min at 4°C, which allowed separation of clear supernatant and cellular debris. The supernatant was then mixed and allowed to bind with glutathione sepharose resin for 4 h at 4°C. The beads were then washed two times with 2 x PBS, followed by one time with 1 x PBS. The GST-tagged proteins then underwent elution for 4 h at 4°C in elution buffer containing 300 mM Imidazole, 50 mM Tris and 200 mM NaCl, pH 8.0, and 30 mM glutathione (reduced) in 50mM Tris-HCl, pH 8.0 followed by centrifugation at 2100 x g for 5 min at 4°C. The purified proteins were then dialyzed against dialysis buffer (50 mM Tris pH 8.0, 200 mM NaCl, and 100 mM PMSF) overnight at 4°C.

8.5 Co-immunoprecipitation and GST pulldown

HeLa cells were grown in 100mm dishes until confluent. Cells were lysed using buffer containing 50 mM Tris, pH 7.4, 100 mM NaCl, 0.5% Triton X-100, and 1x protease cocktail inhibitor (Millipore) (lysis buffer) on ice for 30 min. Lysates were incubated with either anti-Mul1 at 4°C overnight. Protein G beads (GE Healthcare) were added to the lysate-antibody mix at 4°C for 4 h. Samples were then washed 3 times with the same buffer used to lyse the cells. Proteins were eluted from the protein G beads by boiling in the presence of 4x loading buffer (250 mM Tris, pH 6.8, 8% SDS, 40% glycerol, 5% β-mercaptoethanol, 0.2% bromophenol blue) for 10 min. Eluted proteins were then identified by immunoblotting (described below).

For GST pulldowns, 50 μg of purified GST fusion proteins, EHD1 and EH1, were incubated with GST beads in lysis buffer and incubated at 4°C for 4 h. The GST beads were then washed three times with the lysis buffer. The GST beads were then added to bovine brain cytosol at 4°C overnight. Samples were then washed three times with lysis buffer. Proteins were eluted from the GST beads by boiling in the presence of 4x loading buffer (250 mM Tris, pH 6.8, 8% SDS, 40% glycerol, 5% β-mercaptoethanol, 0.2% bromophenol blue) for 10 min. Eluted proteins were then identified by immunoblotting (described below).

8.6 Immunoblotting

Cells, HeLa or RPE, were washed twice in ice-cold phosphate-buffered saline (PBS) and then scraped off plates with a rubber policeman into ice-cold lysis buffer (50

mM Tris-HCl pH 7.4, 100 mM NaCl, 0.5% Triton X-100 and 1x protease cocktail inhibitor). Protein levels of post-nuclear lysates were quantified by using the Bradford assay for equal protein level loading. For immunoblotting, 20–30 μg of protein per lysate were separated by 10% SDS-PAGE. Proteins within the gel were transferred onto nitrocellulose membranes and blocked for 30 min at room temperature in PBS with 0.3% Tween 20 (PBST) and 5% non-fat dry milk. The membranes were then incubated with the appropriate primary antibodies diluted in PBST. Membranes were then washed in PBST three times for 5 min and then incubated with the appropriate secondary antibody diluted in PBST for 30 min.

8.7 Quantification of immunoblots

The adjusted relative density of the immunoblots was measured in ImageJ according to the following protocol: http://www1.med.umn.edu/starrlab_deleteme/prod/groups/med/@pub/@med/@starrlab/documents/content/med_content_370494.html.

8.8 Quantification of mitochondrial parameters

The average size, perimeter, and circularity of mitochondria were measured in ImageJ, using a plugin called Mito Morphology Macro (http://imagejdocu.tudor.lu/doku.php?id=plugin:morphology:mitochondrial_morphology_macro_plug-in:start). Images of Tom20-stained cells were imported into ImageJ where the program was able to set a common threshold and calculate the mitochondrial parameters.

8.9 Quantification of VPS35 subcellular distribution

The distribution of VPS35-positive vesicles was assessed using ImageJ. Multi-channel images were split into individual channels. An area was drawn around the Golgi region, marked with a Golgi marker GM130, using the 'free hand' tool. The region of interest was then superimposed on the image of the VPS35 immunostaining and the mean VPS35 fluorescence intensity of that region was measured and calculated.

8.10 Immunofluorescence

RPE cells were treated as described in the chapter and then fixed in 4% paraformaldehyde in PBS for 10 min at room temperature. Cells were then rinsed three times with PBS and then incubated with the appropriate primary antibody diluted in PBS containing 0.5% BSA and 0.2% saponin (staining buffer) for 1 h at room temperature. The cells were then washed three time and incubated with the appropriate secondary antibody diluted in staining buffer for 30 min at room temperature. Upon completion, the cells were washed three times with PBS and mounted on a microscope slide with Fluoromount.

Using a Zeiss LSM800 confocal microscope with a 63×1.4 NA oil objective, z-stack confocal images were collected. The series of images from a z-stack was then processed to yield a maximal projection image using the Zeiss Zen software. For quantification, collected maximal projection images were imported into ImageJ as described above.

8.11 Live imaging

RPE cells were plated on 35mm glass-bottom dishes and transfected with the appropriate siRNA treatment. At 72 h post transfection, the cells were treated with 25 nM Mitotracker Red for 15 min in Opti-mem media lacking antibiotics. The cells were then washed three times with DMEM/F12 containing no Phenol Red. After the last wash, DMEM/F12 with no Phenol Red was added to the dish, along with 10% FBS.

Using the system described above, a four slice z-stack image was taken every 15 s for 5 min for each treatment. Each z-stack was then converted into a maximal projection image as described above and quantification was performed.

8.12 STS assay

RPE cells were treated with 1 μM STS (Sigma Aldrich) for the last 1 h of a 72 h siRNA transfection. The cells then underwent processing for immunofluorescence as described above.

8.13 Statistics

Data from ImageJ was imported in Microsoft Excel where means and standard deviations were calculated from the data obtained from three independent experiments with at least 10 images taken per treatment. Statistical significance was calculated using Student's t-test with the Vassarstats program (http://www.vassarstats.net)

9. RESULTS

9.1 EHD1 is a regulator of mitochondrial homeostasis

To answer the question whether EHD1 plays a role in mitochondrial fission and homeostasis, we depleted EHD1 from retinal pigment epithelial (RPE) cells using siRNA and knocked down approximately 90% of the total EHD1 within the cells (Figure 2.1E). To compare mitochondrial morphology in mock-treated and EHD1-depleted cells, we immunostained RPE cells with Tom20, a mitochondrial membrane marker (Figure 2.1A-D). Cells lacking EHD1 displayed a highly extended mitochondrial network that had numerous elongated structures (Figure 2.1B,D) compared to mock-treated cells (Figure 2.1A,C). To quantitatively measure the differences in the mitochondrial networks of mock-treated and EHD1-depleted cells, we used a plug-in on ImageJ that is specifically designed to measure the morphology of mitochondria, Mito Morphology Macro (http://imagejdocu.tudor.lu/doku.php?id=plugin:morphology:mitochondrial_morphology_macro_plug-in:start). Data from multiple cells imaged in three separate experiments indicated that both the average mitochondrial size (Figure 2.1F) and average mitochondrial perimeter (Figure 2.1G) are significantly larger in EHD1-depleted cells. On the other hand, the average circularity is significantly decreased in EHD1-depleted cells, which indicates that less mitochondrial fission is occurring (Figure 2.1H). In order to demonstrate that the mitochondrial fragmentation was due to the EHD1-depletion rather than off-target effects, we performed rescue experiments by knocking down EHD1 and then reintroducing siRNA-resistant GFP-myc-EHD1 into the knockdown

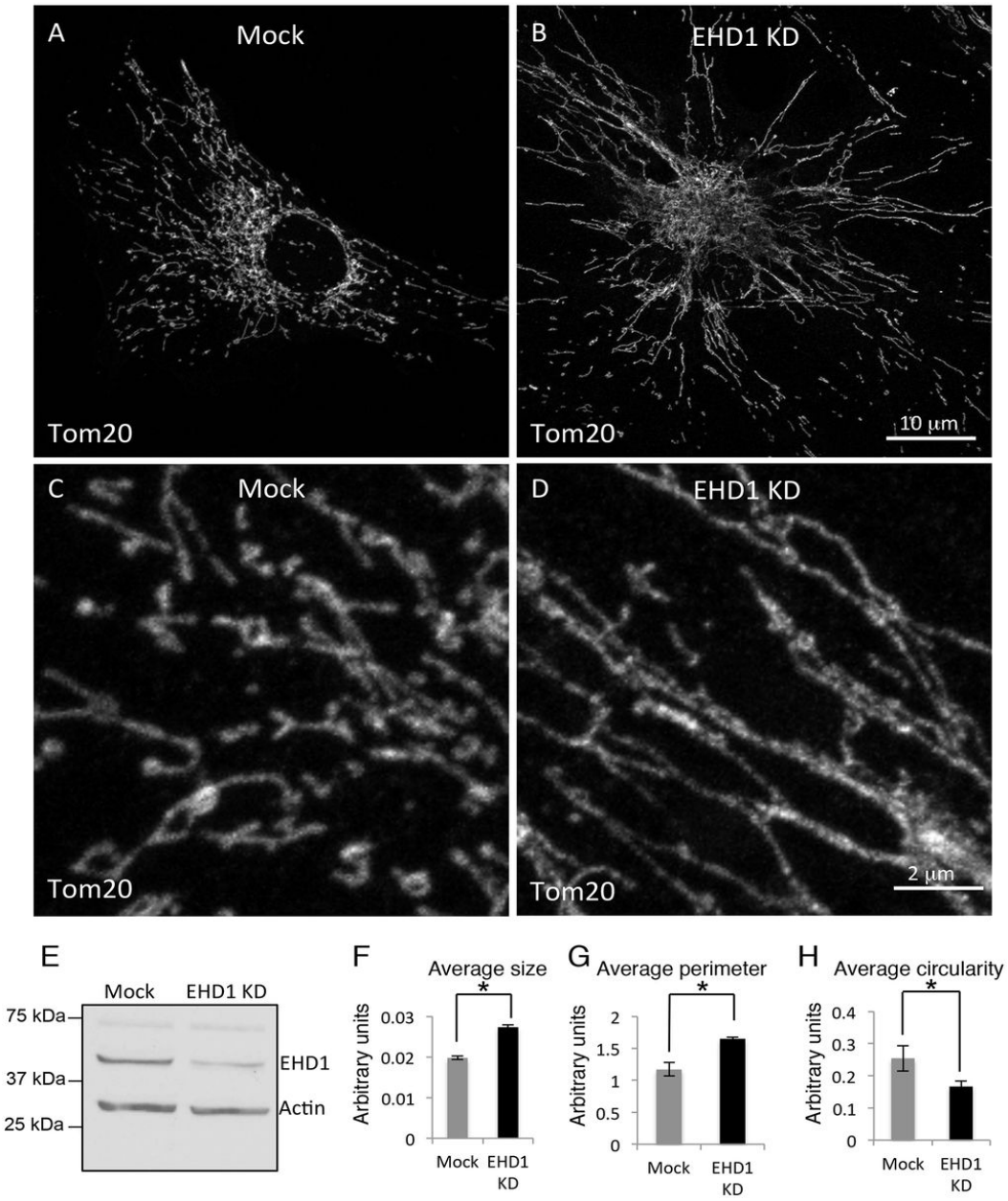

Figure 2. 1

EHD1 is required for mitochondrial homeostasis. (A–D) RPE cells were either mock treated (A,C) or treated with EHD1 siRNA for 72 h (B,D) and immunostained for the mitochondrial membrane marker Tom20. C and D are images of higher magnitude to visualize mitochondrial elongation. (E) The efficacy of the EHD1-depletion for A–D is demonstrated by immunoblotting lysates from mock and EHD1-depleted RPE cells. (F–H) The Mito Morphology Macro plugin in ImageJ was used to quantify mean±s.d. for mitochondrial size, perimeter and circularity, in three independent experiments each using 10 cells per treatment. *P<0.05 (one-tailed Student's t-test). Used with permission from JCS (Farmer et al., 2017).

cells (Figure 2.2). As demonstrated (Figure 2.2A-F) and quantified (Figure 2.2G), EHD1-depleted cells that were transfected with EHD1 were successfully rescued and displayed an average mitochondrial size that was significantly shorter than the knockdown cells and similar to the mock-treated cells. Overall, these data support the notion that EHD1 is needed for mitochondrial homeostasis. Based on the data suggesting an increased mitochondrial length upon EHD1-depletion, we hypothesized that if EHD1 is a mediator of mitochondrial dynamics, then the absence of the protein should result in less dynamic or more static mitochondria compared to mock cells. To test this, we used a mitochondria-specific dye, Mitotracker Red, to follow mitochondria in living cells. As shown, in mock-treated cells, the mitochondria are highly dynamic and constantly undergoing fusion and fission (Figure 2.3A) Images were taken every 15 s for 5 min and the arrows highlight fission events occurring within the cell. In comparison, the EHD1-depleted cells become very static with limited dynamic movement and visible fission events (Figure 2.3B). These live imaging experiments further support the idea that EHD1 is required for normal mitochondrial fission.

9.2 EHD1 likely functions upstream of Dyn2 and Drp1

To date, Drp1 is considered to be the major protein that regulates mitochondrial fission (Pitts, Yoon, Krueger, & McNiven, 1999; Santel & Frank, 2008; Taguchi, Ishihara, Jofuku, Oka, & Mihara, 2007). However, it has recently been determined that the GTPase Dyn2 is also required to complete the mitochondrial fission (J. E. Lee et al., 2016). Due to

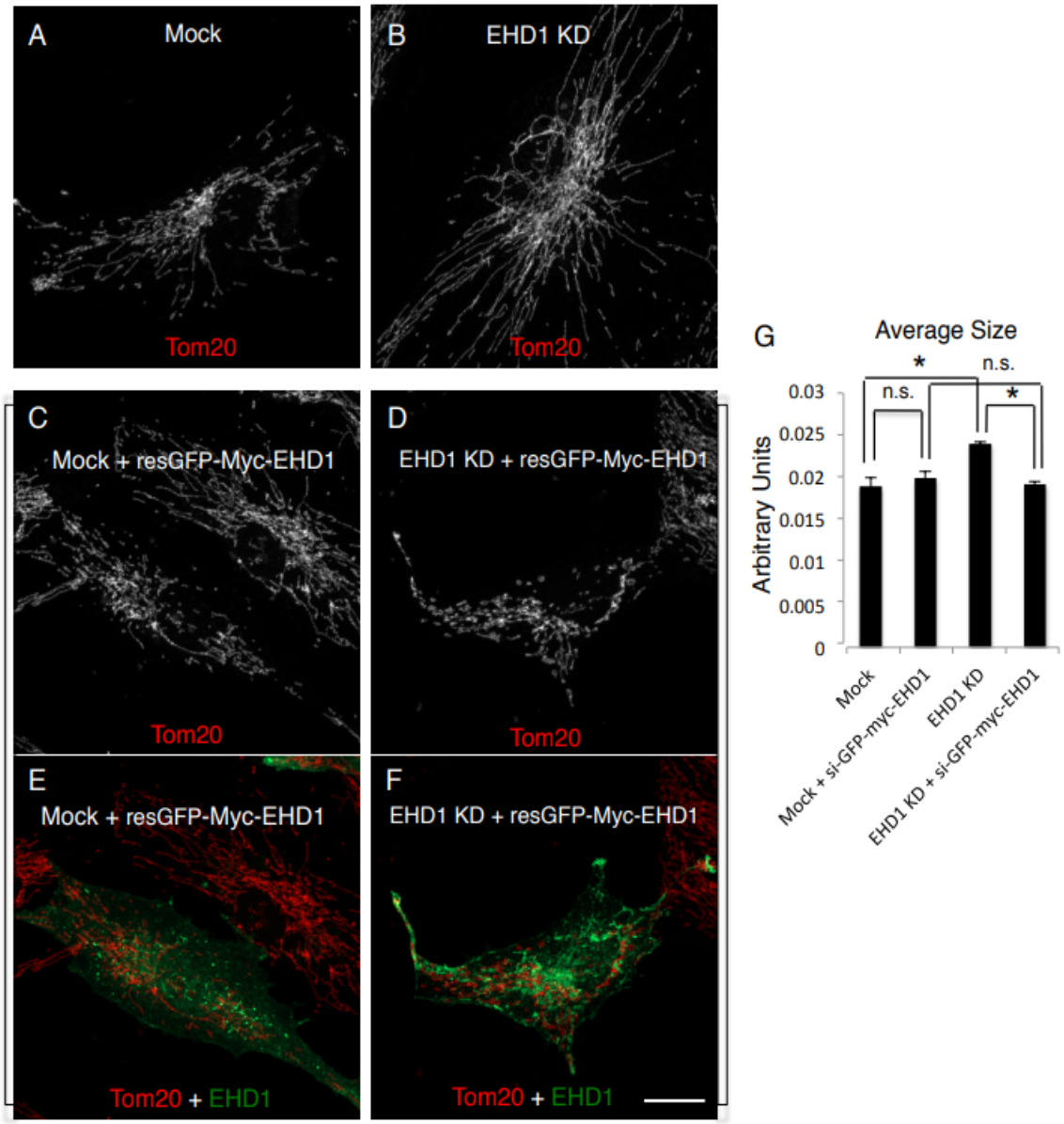

Figure 2. 2

The elongated mitochondrial phenotype is rescued when EHD1 is reintroduced into EHD1 knock-down cells. (A-F) RPE cells were Mock-treated (A, C, E) or treated with EHD1-siRNA (B, D, F) for 72 h. Some of the cover-slips containing Mock or EHD1 knock-down cells were further transfected with a siRNA-resistant GFP-Myc-EHD1 cDNA (si-GFP-myc-EHD1) for the last 24 h (C-F). All cells were fixed and immunostained with antibodies against Tom20 (A-F). GFP-Myc-EHD1 transfected cells are seen in green, Bar, 10 μm. (G) At least 7 cells from each treatment (in 3 independent experiments) in A-F were analyzed by Mito Morphology Macro plugin in ImageJ and the mean+/-s.d. for size of their mitochondria was plotted. * denotes p values of less than 0.05, and n.s. denotes differences that are not statistically significant (p>0.05). Used with permission from JCS (Farmer et al., 2017).

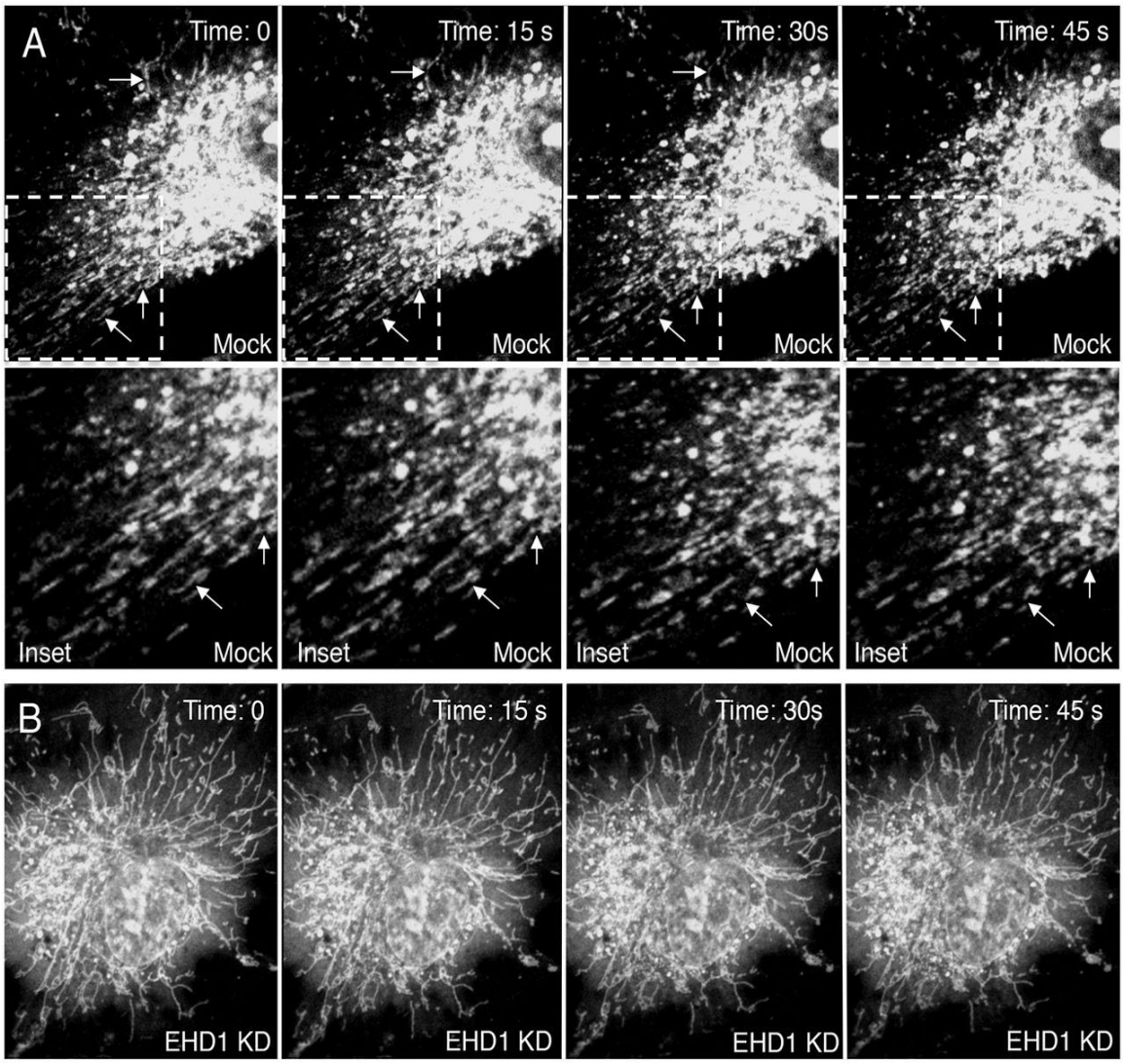

Figure 2. 3

Mitochondrial dynamics are impaired upon EHD1 depletion. Live imaging was performed on RPE cells incubated with Mitotracker Red and either mock treated (A) or treated with EHD1 siRNA for 72 h (B). 4-slice *z*-section images were taken every 15 s for 5 min for each treatment, and compiled to a maximal projection image. The arrows depict examples of fission events in mock-treated cells. Used with permission from JCS (Farmer et al., 2017).

the significant homology between EHD1 and dynamin (Daumke et al., 2007), and the fact that EHD1 is an ATPase involved in endosomal fission (Cai et al., 2013; Cai et al., 2014; Deo et al., 2018; Jakobsson et al., 2011), we hypothesized that EHD1 directly mediates fission at the mitochondrial membrane. To answer this hypothesis, we used a STS assay to induce mitochondria fragmentation in either mock-treated or EHD1-depleted cells. STS is a global kinase inhibitor that induces mitochondrial fission and fragmentation through the activation of Drp1 and Dyn2. If Drp1 or Dyn2 are absent from the cells, fragmentation does not occur when induced by STS (J. E. Lee et al., 2016). We therefore rationalized that if EHD1 plays a similar role to Drp1 and Dyn2 in mitochondrial fission, the absence of EHD1 would protect the cells from STS-induced mitochondrial fragmentation as well. Accordingly, mock-treated and EHD1-depleted cells were either treated with or without STS for 1 h. The cells were then immunostained with antibodies for Tom20 to visualize the mitochondria morphology. EHD1-depleted cells displayed a network of elongated mitochondria compared to mock-treated cells (compare Figure 2.4B to 2.4A). The mitochondria in the EHD1-depleted cells displayed a greater average size (Figure 2.4E) and perimeter (Figure 2.4F) but significantly decreased circularity (Figure 2.4G), consistent with Figure 1 data. As anticipated, mock-treated cells that were subject to STS treatment resulted in mitochondria that underwent fission and fragmentation (compare Figure 2.4B with 2.4A), and the STS-induced cells had significantly decreased average size (Figure 2.4E) and perimeter (Figure 2.4F), but significantly increased circularity (Figure 2.4G). As demonstrated, EHD1-depleted cells

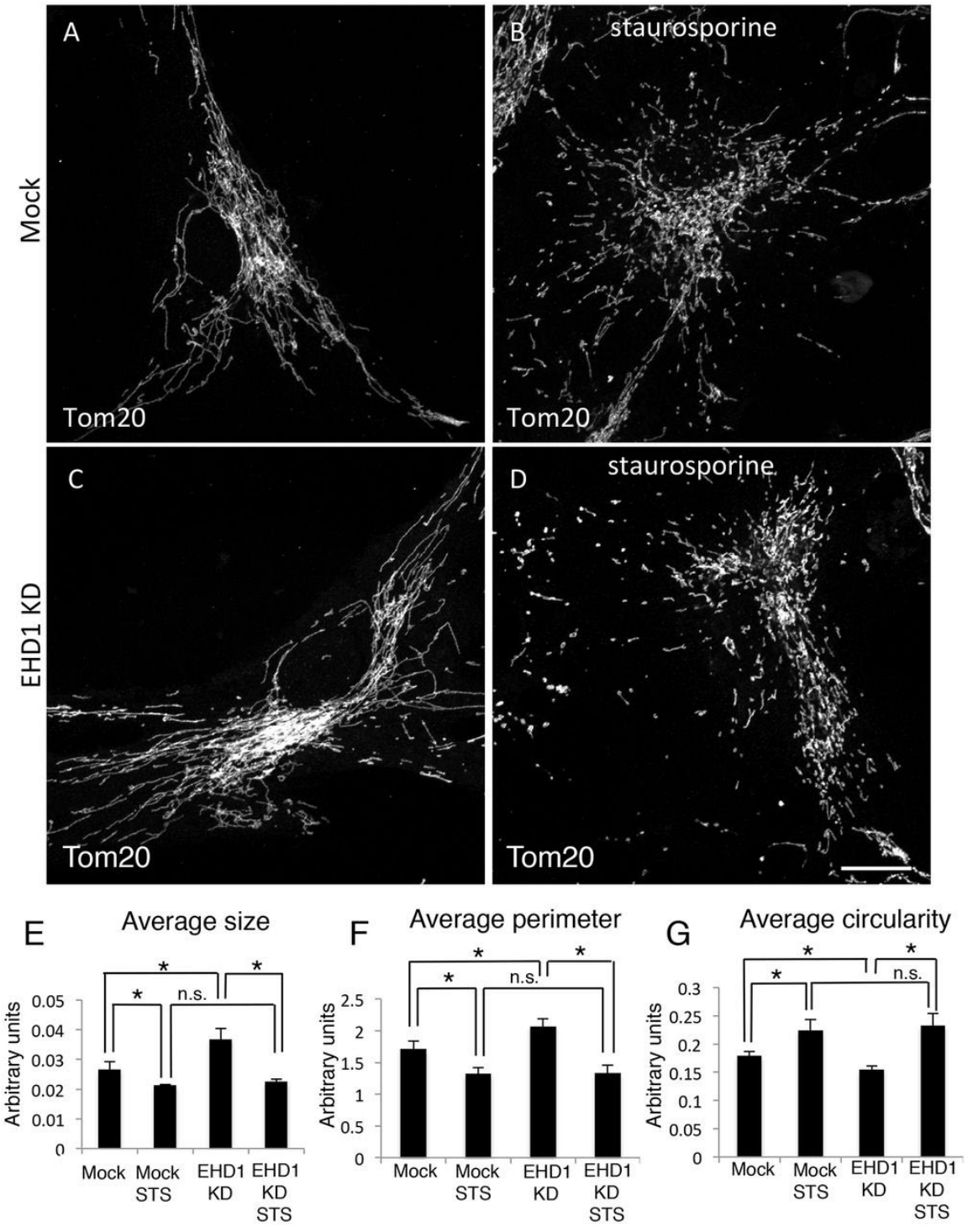
A
B
staurosporine
Mock
Tom20
Tom20
C
D
staurosporine
EHD1 KD
Tom20
Tom20
E
Average size
Arbitrary units
0.05
0.04
0.03
0.02
0.01
0
*
*
n.s.
*
Mock
Mock STS
EHD1 KD
EHD1 KD STS
F
Average perimeter
Arbitrary units
2.5
2
1.5
1
0.5
0
*
*
n.s.
*
Mock
Mock STS
EHD1 KD
EHD1 KD STS
G
Average circularity
Arbitrary units
0.3
0.25
0.2
0.15
0.1
0.05
0
*
*
n.s.
*
Mock
Mock STS
EHD1 KD
EHD1 KD STS

Figure 2. 4

EHD1 plays a regulatory role in mitochondrial fission. (A–D) RPE cells were either mock treated (A,B) or treated with EHD1 siRNA for 72 h (C,D), followed by incubation with STS for the last 1 h of treatment (B,D) or without the drug (A,C). (E–G) The Mito Morphology Macro plugin in ImageJ was used for quantifying mean±s.d. for mitochondrial size, perimeter and circularity in three independent experiments each using 10 cells per treatment. *P<0.05; n.s., not statistically significant (one-tailed Student's t-test). Used with permission from JCS (Farmer et al., 2017).

subject to STS treatment clearly resulted in fission and fragmentation of the mitochondria (Figure 2.4D), and the mitochondria size, perimeter, and circularity were not significantly different than the mock-treated cells subject to STS treatment (Figure 2.4E-G). While we cannot completely rule out the possibility that EHD1 plays a direct role in mitochondrial fission, these data support the idea that EHD1 most likely acts upstream of Drp1 and Dyn2 in the process of mitochondrial fission.

9.3 EHD1 and Rabankyrin-5 regulate the retromer control of mitochondrial homeostasis

Previous studies have identified VPS35, a component of the retromer cargo selection complex, as a key regulator of mitochondria homeostasis and PD (Kumar et al., 2012; Struhal et al., 2014; W. Wang et al., 2017; W. Wang et al., 2016; Zimprich et al., 2011). One recent model suggests that VPS35 is responsible for the transport of the ubiquitin ligase Mul1 to the mitochondrial membrane where Mul1 ubiquitinates the mitochondrial fusion protein, Mfn2, resulting in proteasomal degradation (Tang et al., 2015) (see model, Figure 2.5A). Since our lab has previously described an interaction between EHD1, Rabankyrin-5, and the retromer complex, we hypothesized that EHD1 depletion might interfere with Mul1 trafficking to the mitochondrial membrane. In this scenario, increased levels of Mfn2 on the mitochondrial membrane might skew the fusion-to- fission ratio, resulting in an elongated mitochondria phenotype. To test this hypothesis, we first tested whether or not EHD1 interacted with Mul1. As a positive control, we confirmed that GST-EHD1 and the EH domain of EHD1 (EH1) pulled down

A

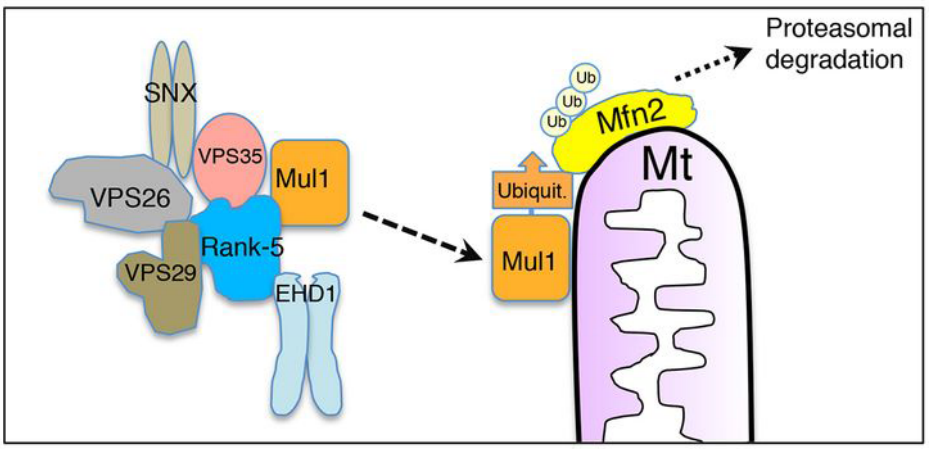
SNX
VPS35
Mul1
VPS26
Rank-5
VPS29
EHD1
Ub
Ub
Ub
Mfn2
Mt
Ubiquit.
Mul1
Proteasomal
degradation

B

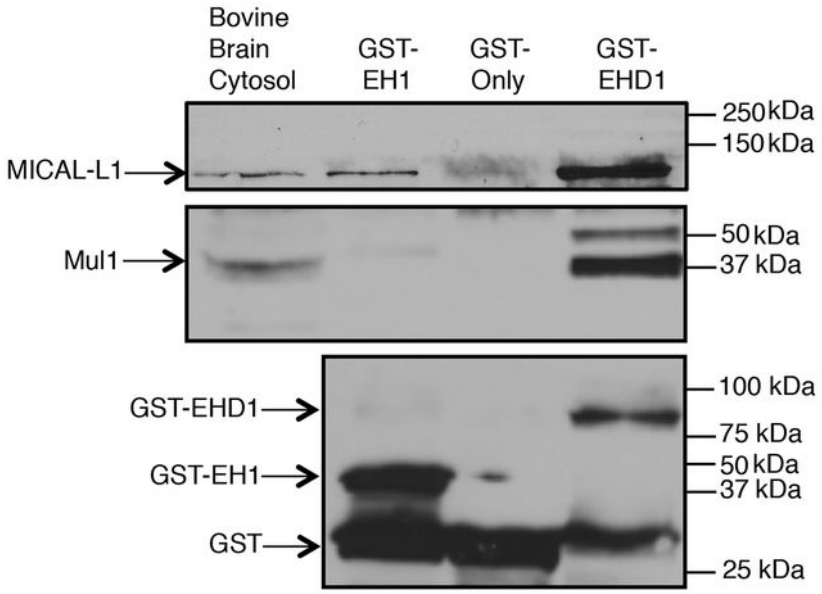
Bovine
Brain
Cytosol
GST-
EH1
GST-
Only
GST-
EHD1
MICAL-L1
250kDa
150kDa
Mul1
50kDa
37 kDa
GST-EHD1
GST-EH1
GST
100 kDa
75 kDa
50kDa
37 kDa
25 kDa

C

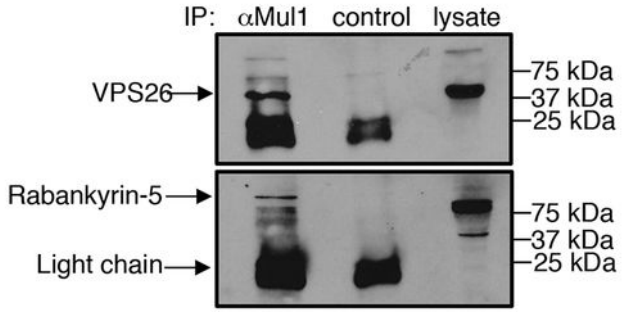
IP: αMul1 control lysate
VPS26
75 kDa
37 kDa
25 kDa
Rabankyrin-5
Light chain
75 kDa
37 kDa
25 kDa

Figure 2. 5

EHD1 interacts with Mul1. (A) Model for the potential role of EHD1 in regulating mitochondrial dynamics via Mul1. Under normal conditions, the ubiquitin ligase Mul1 is released from an interaction with VPS35 and the retromer components (including EHD1), and relocates to the mitochondrial membrane, where it ubiquitinates Mfn2, inducing its proteasomal degradation and promoting normal mitochondrial fission. Upon EHD1 depletion, Mul1 would be retained in association with VPS35 and the retromer, preventing Mfn2 degradation and thus enhancing mitochondrial membrane fusion. (B) GST pulldown from bovine brain cytosol was performed with GST only, a GST-tagged EH domain of EHD1 (GST–EH1) and GST–EHD1. Eluates were immunoblotted with antibodies against MICAL-L1 (top panel), as a positive interactor with EHD1, and Mul1 (middle panel). GST fusion protein samples were immunoblotted with anti-GST (bottom panel). (C) Co-immunoprecipitation (IP) of proteins from a HeLa cell lysate using anti-Mul1 (αMul1), and immunoblotted with anti-Vps26 and anti-rabankyrin-5 antibodies. 25 kDa immunoglobulin light chains detected by the secondary anti-light chain antibody are indicated in the bottom panel. Used with permission from JCS (Farmer et al., 2017).

the known EHD1 interaction partner MICAL-L1 from bovine brain cytosol (Figure 2.5B, top panel), consistent with our previous results (Sharma, Giridharan, et al., 2009). Additionally, the purified GST-EHD1 pulled down Mul1 from the bovine brain cytosol, whereas the GST and GST-EH1 were unable to (Figure 2.5B, middle panel). To further elucidate the relationship between EHD1, Rabankyrin-5, the retromer, and Mul1, we performed co-immunoprecipitation experiments with endogenous levels of proteins (Figure 2.5C). In these biochemical assays, we were able to show that an antibody against Mul1 pulled down a component of the retromer complex, VPS26, as anticipated. However, in the same experiment, we also showed that Mul1 pulled down Rabankyrin-5 (Figure 2.5C), and low levels of EHD1 (data not shown). These experiments suggest that EHD1 and Rabankyrin-5 interact with Mul1 to mediate its transport to mitochondria, where it regulates Mfn2 degradation.

We rationalized that if Rabankyrin-5 and EHD1 are cooperating together with the retromer to transport Mul1 to the mitochondrial membrane, then depletion of Rabankyrin-5 should result in a phenotype similar to EHD1-depletion. To test this, RPE cells were depleted of Rabankyrin-5 and immunostained with Tom20 to analyze the mitochondrial-morphology compared to mock-treated cells. As demonstrated, Rabankyrin-5-depleted cells displayed an elongated network of mitochondria compared to mock-treated cells (compare Figure 2.6B to 2.6A). Quantification of three independent experiments showed that the average size and perimeter of Rabankyrin-5-depleted cells were greater than mock-treated cells, whereas the mitochondrial circularity was

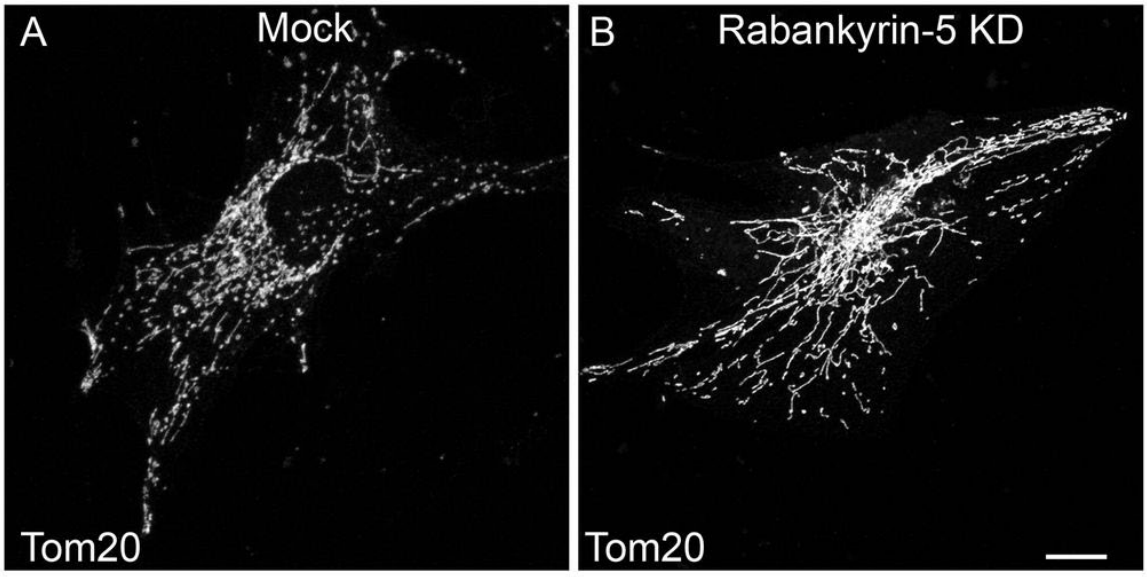
A
Mock
Tom20
B
Rabankyrin-5 KD
Tom20

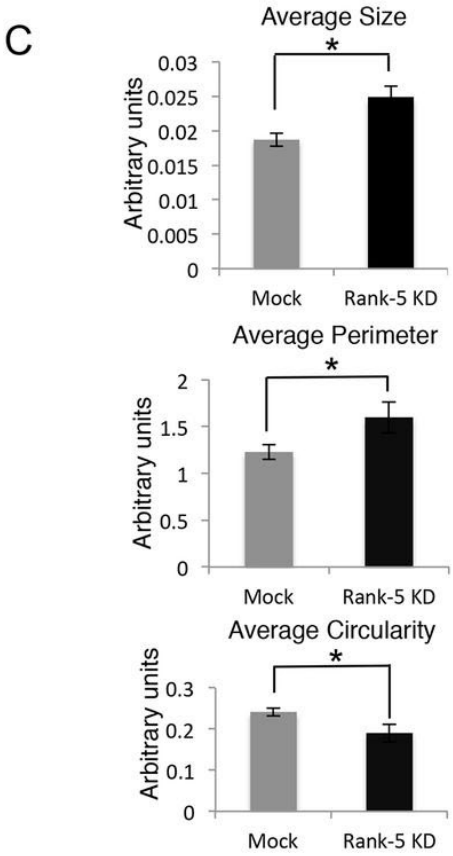
C
Average Size
*
Arbitrary units
0.03
0.025
0.02
0.015
0.01
0.005
0
Mock
Rank-5 KD
Average Perimeter
*
Arbitrary units
2
1.5
1
0.5
0
Mock
Rank-5 KD
Average Circularity
*
Arbitrary units
0.3
0.2
0.1
0
Mock
Rank-5 KD

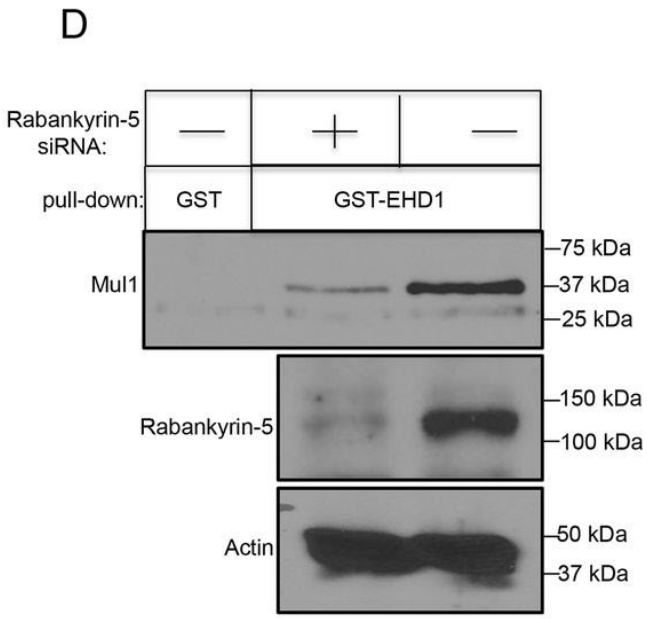
D
Rabankyrin-5 siRNA:
—
+
—
pull-down:
GST
GST-EHD1
Mul1
75 kDa
37 kDa
25 kDa
Rabankyrin-5
150 kDa
100 kDa
Actin
50 kDa
37 kDa

Figure 2. 6

Rabankyrin-5 mediates the interaction between EHD1 and Mul1, and its depletion induces an elongated mitochondrial network similar to that observed upon EHD1 depletion. (A,B) RPE cells were either mock treated (A) or treated with rabankyrin-5 siRNA for 72 h (B) and immunostained for the mitochondrial membrane marker Tom20. (C) The Mito Morphology Macro plugin in ImageJ was used for quantifying mean±s.d. for mitochondrial size, perimeter and circularity in three independent experiments each using 10 cells per treatment. **P*<0.05 (one-tailed Student's *t*-test). (D) HeLa cells were either mock treated or treated with Rabankyrin-5 siRNA, lysed, and subjected to a GST–EHD1 pulldown, and immunoblotted with Mul1 (upper panel). The efficacy of the Rabankyrin-5-depletion is demonstrated by immunoblotting lysates from mock-treated and Rabankyrin-5-depleted cells (bottom two panels). Used with permission from JCS (Farmer et al., 2017).

significantly decreased in Rabankyrin-5-depleted cells (Figure 2.6C).

Since the EHD1 and Mul1 interaction appeared less robust than that of Rabankyrin-5 and Mul1, and because EHD1 is a direct interaction of Rabankyrin-5 (Zhang, Reiling, et al., 2012), we postulated that Rabankyrin-5 might potentially mediate the interaction between EHD1 and Mul1. To test this idea, we used lysates from mock-treated or Rabankyrin-5-depleted cells in pulldowns using GST-EHD1 as bait. Incubation of mock-treated lysate with GST-EHD1 resulted in significant Mul1 being pulled down, whereas the GST alone did not (Figure 2.6D, top panel). However, efficiently depleting Rabankyrin-5 from lysates (Figure 2.6D, middle panel) and incubating it with GST-EHD1 resulted in very little Mul1 being pulled down (Figure 2.6D, top panel), suggesting that Rabankyrin-5 mediates the interaction between EHD1 and Mul1.

If the mitochondrial elongation phenotype observed upon EHD1- or Rabankyrin-5-depletion is due to the stabilization of Mfn2 on the mitochondrial membrane, one would predict that the levels of Mfn2 would increase under these conditions compared to mock-treated cells. To test this idea, we depleted EHD1, Rabankyrin-5, or VPS35 and compared the protein expression of Mfn2, Drp1, and actin (loading control) to mock-treated cells. siRNA treatment of HeLa cells resulted in efficient depletion of all three proteins (Figure 2.7A, top panels, and quantified in Figure 2.7B-G), whereas actin levels remain relatively unchanged in the mock- and siRNA-treated cells (Figure 2.7A, bottom

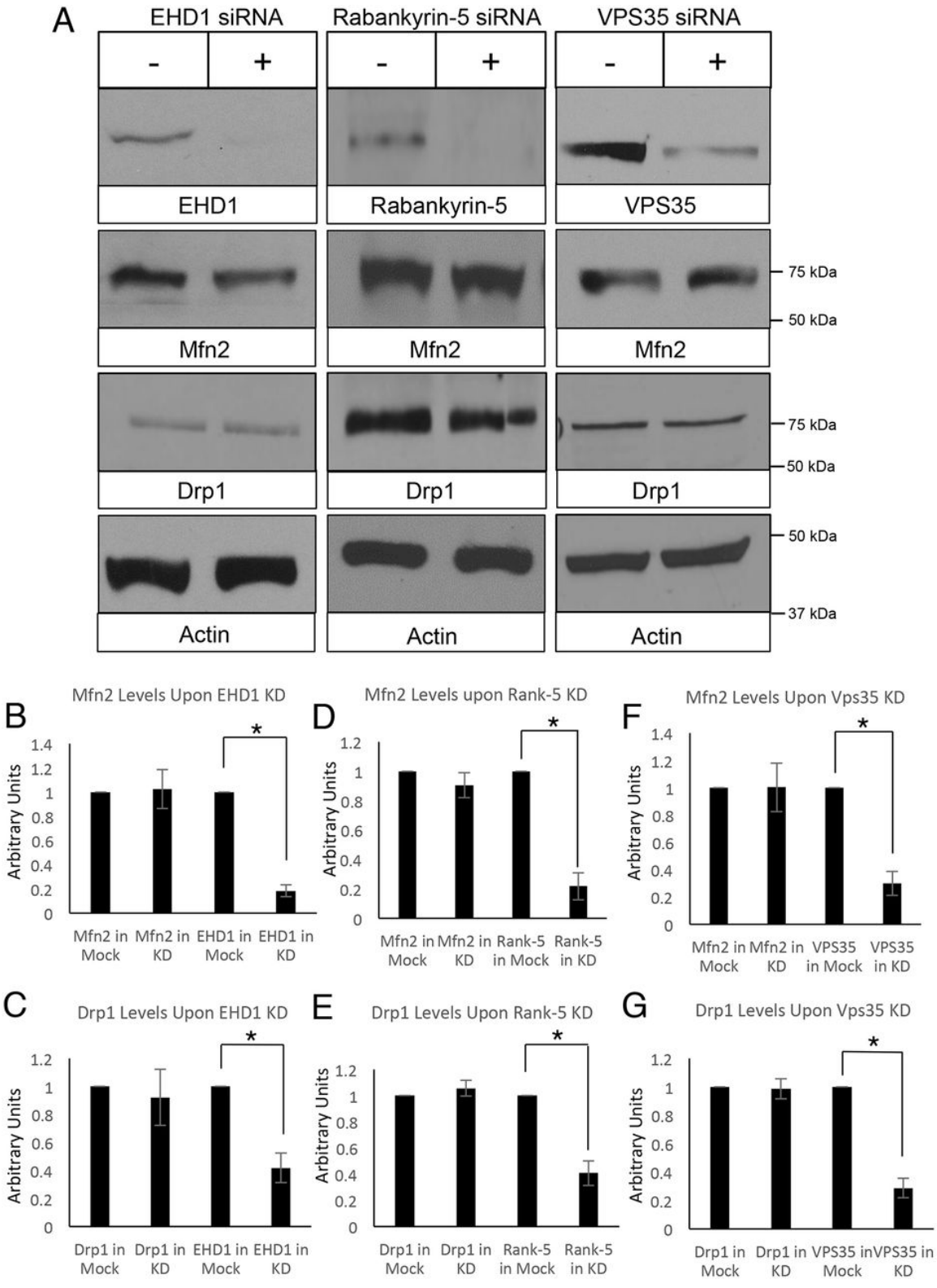
A
EHD1 siRNA
Rabankyrin-5 siRNA
VPS35 siRNA
-
+
EHD1
Rabankyrin-5
VPS35
Mfn2
75 kDa
50 kDa
Drp1
Actin
37 kDa
B
Mfn2 Levels Upon EHD1 KD
Arbitrary Units
Mfn2 in Mock
Mfn2 in KD
EHD1 in Mock
EHD1 in KD
C
Drp1 Levels Upon EHD1 KD
Drp1 in Mock
Drp1 in KD
D
Mfn2 Levels upon Rank-5 KD
Rank-5 in Mock
Rank-5 in KD
E
Drp1 Levels Upon Rank-5 KD
F
Mfn2 Levels Upon Vps35 KD
VPS35 in Mock
VPS35 in KD
G
Drp1 Levels Upon Vps35 KD

Figure 2. 7

Depletion of EHD1, Rabankyrin-5 or VPS35 does not induce Mfn2 accumulation. HeLa cells were either mock treated, or treated with EHD1, Rabankyrin-5 or Vps35 siRNA for 72 h. Depletion efficacy was validated by immunoblotting with antibodies against EHD1, Rabankyrin-5 and VPS35 (A; top three panels), and the effect of the siRNA was assessed with antibodies against Mfn2 (A; second panel from the top), Drp1 (A; third panel from the top) and actin (A; bottom panel). (B–G) Densitometric quantification from three separate experiments. **P*<0.05 (one-tailed Student's *t*-test). Used with permission from JCS (Farmer et al., 2017).

panels). However, no difference was observed in the protein expression level of Mfn2 or Drp1 (Figure 2.7A, middle two panels), and no major changes in the Drp1 association and/or distribution along mitochondria was noted (data not shown). Data from these experiments suggest that despite the ability of EHD1 and Rabankyrin-5 to interact with Mul1, accumulation of Mfn2 and/or Drp1 on the mitochondrial membrane was likely not the mechanism by which EHD1 and Rabankyrin-5-depletion induce elongated mitochondria.

9.4 EHD1 and Rabankyrin-5 differentially regulate VPS35 to control mitochondrial fission

Our previous results were unable to validate the notion that VPS35 is responsible for regulating Mfn2 levels through Mul1. However, a recent study presents an alternative model by which VPS35 and the retromer affect mitochondrial homeostasis by interacting with Drp1. The model suggests that retromer-containing vesicles remove inactive Drp1 from the mitochondrial membrane, enabling active Drp1 to occupy the receptors on the mitochondria to mediate fission (W. Wang et al., 2017) (see model in Figure 2.8L). In this model, depletion or sequestration of VPS35 would impair fission and induce formation of elongated mitochondria. We therefore hypothesized that EHD1 regulates VPS35 expression or localization. To test this, we immunoblotted lysates that were either mock-treated or EHD1-depleted (Figure 2.8A). Upon efficient EHD1-depletion (Figure 2.8A), there was a consistent reduction in VPS35 to approximately 50% of the levels detected in mock-treated cells, suggesting that EHD1's presence stabilizes

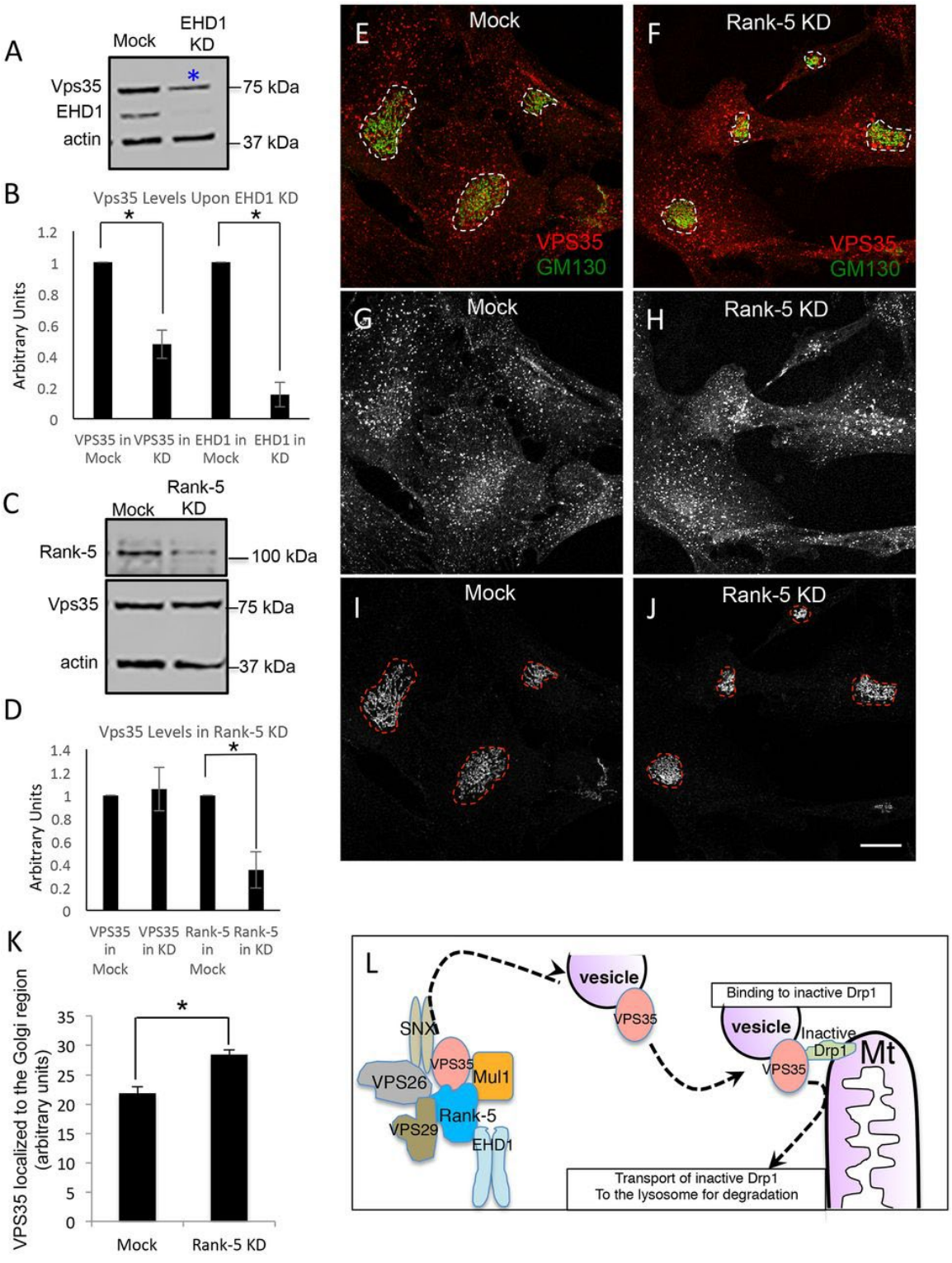
A
Mock
EHD1 KD
Vps35
EHD1
actin
75 kDa
37 kDa
B
Vps35 Levels Upon EHD1 KD
Arbitrary Units
VPS35 in Mock
VPS35 in KD
EHD1 in Mock
EHD1 in KD
C
Rank-5
Mock
KD
Rank-5
Vps35
actin
100 kDa
75 kDa
37 kDa
D
Vps35 Levels in Rank-5 KD
Arbitrary Units
VPS35 in Mock
VPS35 in KD
Rank-5 in Mock
Rank-5 in KD
K
VPS35 localized to the Golgi region (arbitrary units)
Mock
Rank-5 KD
E
Mock
VPS35
GM130
F
Rank-5 KD
VPS35
GM130
G
Mock
H
Rank-5 KD
I
Mock
J
Rank-5 KD
L
vesicle
VPS35
SNX
VPS35
Mul1
VPS26
Rank-5
VPS29
EHD1
Binding to inactive Drp1
vesicle
Inactive
Drp1
VPS35
Mt
Transport of inactive Drp1
To the lysosome for degradation

Figure 2. 8

Depletion of EHD1 and Rabankyrin-5 results in reduced and sequestered VPS35, respectively. (A–D) HeLa cells were either mock treated, treated with EHD1 siRNA (A) or treated with rabankyrin-5 (Rank-5) siRNA (C) for 72 h and immunoblotted for VPS35, EHD1, Rabankyrin-5 and actin. The asterisk (in A) indicates reduced VPS35 protein levels. (B,D) Quantification of protein levels from three independent experiments. **P*<0.05 (one-tailed Student's *t*-test). (E–J) RPE cells were either mock treated (E,G,I) or treated with rabankyrin-5 siRNA for 72 h (F,H,J), and immunostained for VPS35 and the Golgi membrane marker GM130. Regions of interest were drawn with a dashed line around the GM130 Golgi stain (I,J) and superimposed in the merged images (E,F) and in the VPS35-stained images (G,H; note, the region of interest is not shown in G and H so the VPS35 distribution pattern can be observed more clearly). Scale bar: 10 μm. (K) ImageJ was used to quantify the mean±s.d. for fluorescence of VPS35 localized to the central Golgi region marked by the regions of interest in three independent experiments each using 10 cells per treatment. **P*<0.05 (one-tailed Student's *t*-test). (L) Current working model showing the proposed mechanism for EHD1 regulation of mitochondrial dynamics. In this scenario, EHD1 might act in facilitating fission of vesicles that transport VPS35 from endosomes to the mitochondrial membrane. VPS35 might then interact with inactive Drp1, removing it from the mitochondrial membrane and facilitating the function of active Drp1 leading to mitochondrial fission. Thus, the absence of EHD1 might prevent this transport step and lead to elongated mitochondria. Used with permission from JCS (Farmer et al., 2017).

VPS35 (Figure 2.8A, asterisk, and quantified in 2.8B). Additionally, the levels of VPS26 were tested and were similarly decreased when EHD1 was depleted. Moreover, these experiments support the idea that VPS35 and the retromer control mitochondrial fission by removing inactive Drp1, thus allowing fission by active Drp1 (Figure 2.8L).

We went on to test whether Rabankyrin-5 similarly affects VPS35 protein levels. To our surprise, Rabankyrin-5-depleted cells had no impact on VPS35 expression levels (Figure 2.8C, quantified in 2.8D), leading us to hypothesize that Rabankyrin-5 regulates VPS35 in a manner that is distinct from that of EHD1. One potential mechanism is that Rabankyrin-5 is needed for the trafficking of VPS35-positive endosomes to the inactive Drp1 on the mitochondrial membrane. We therefore argued that if Rabankyrin-5 does regulate the trafficking of VPS35, then depletion of Rabankyrin-5 should result in an altered VPS35 localization pattern. To test this, we depleted Rabankyrin-5 and compared the subcellular distribution of VPS35 to mock-treated cells using GM130 to mark the Golgi region as a reference point within the cell (Figure 2.8E-J). As demonstrated, Rabankyrin-5-depleted cells had a significant degree of sequestration of VPS35 in the Golgi region as compared to mock-treated cells (Figure 2.8, compare F and H to E and G; dashed region of interest are the Golgi, as marked by GM130 in I and J). To quantify this, we measured the VPS35 fluorescence localized to the Golgi region and found that it was significantly higher in the Rabankyrin-5-depleted cells compared to mock-treated cells (Figure 2.8K). Overall, these experiments support a model by which depletion of EHD1 and Rabankyrin-5 lead to a reduced level of VPS35 or an altered VPS35 subcellular distribution, respectively. This in turn prevents VPS35 from being able to traffic to the

mitochondrial membrane to remove inactive Drp1, culminating in impaired fission, thus leading to the elongated network of mitochondria observed in these cells.

10. SUMMARY AND CONCLUSIONS

Mitochondrial dynamics have long been correlated with their cellular functions and mitochondrial morphology appears along a continuum from a network of tubular structures to smaller fragmented membranes (Benard et al., 2006). Indeed, early observations of mitochondria found that upon activation of ATP synthesis, mitochondria displayed a smaller and more condensed phenotype (Hackenbrock, 1966). Additionally, mitochondrial fragmentation has been observed in patient fibroblasts that have altered energy production due to defects in respiratory chain subunits (Capaldi, Murray, Byrne, Janes, & Marusich, 2004; Koopman et al., 2005). Since mitochondrial dynamics are highly regulated, researchers have extensively studied mitochondrial fusion and fission and the proteins that regulate these processes. In particular, the role of fission was thought to be controlled by one GTPase, Drp1 (Bleazard et al., 1999; Labrousse et al., 1999). However, a recent study has shed new light on the mechanism of mitochondrial fission and has identified the GTPase Dyn2 in playing a sequential role to Drp1 to mediate cleavage of mitochondrial membranes (J. E. Lee et al., 2016).

In addition to the focus on the proteins carrying out the process of fission and the recent mechanism by which Drp1 and Dyn2 facilitate fission, exciting new studies have implicated a role for VPS35 and the retromer in PD and mitochondrial dynamics, forging a novel connection between endocytic regulatory complex and a non-endocytic

organelle (Follett, Bugarcic, Collins, & Teasdale, 2017; Follett et al., 2014; Kumar et al., 2012; Sharma et al., 2012; Struhal et al., 2014; Tang et al., 2015; Vilarino-Guell et al., 2011; Zimprich et al., 2011). However, while the relationship between VPS35, mitochondrial dynamics, and PD is now irrefutable, the precise mechanism(s) by which VPS35 controls fusion or fission remains somewhat controversial.

In Chapter II, we identify a novel regulatory role for EHD1 as an effector of mitochondrial fission. We demonstrated that upon EHD1-depletion, the mitochondria become more elongated and static, similar to the phenotype upon Drp1-depletion or mutation (Benard et al., 2007). Since EHD1 is an ATPase with homology to the dynamin family of GTPases (Daumke et al., 2007; Melo et al., 2017), it raised the question as to whether EHD1 plays a role in mitochondria fission in a similar manner to Drp1 and Dyn2. However, no significant localization of EHD1 was observed with the mitochondrial membrane, reducing the likelihood that EHD1 plays a direct role in mitochondrial fission. In addition, upon STS treatment of EHD1-depleted cells, the mitochondria nonetheless underwent fragmentation, as opposed to what occurs upon Drp1 or Dyn2 depletion (J. E. Lee et al., 2016). This suggests that the kinase inhibitor likely activates Drp1 and/or Dyn2 directly, bypassing the potential regulatory role carried out by EHD1.

Since it is unlikely that EHD1 directly regulates mitochondrial fission, we asked what could be the potential role of EHD1 upstream of Drp1 and Dyn2. Previous studies in our lab and others have linked EHD1 to the retromer complex (Gokool et al., 2007;

Zhang, Reiling, et al., 2012), suggesting the possibility that EHD1 somehow functions upstream of the mitochondrial fission proteins. One potential model suggests that VPS35 and the retromer regulate the transport of the ubiquitin ligase Mul1 to the mitochondria (Tang et al., 2015; Yun et al., 2014). In this model, if Mul1 and VPS35 lose their interaction, Mul1 traffics to the mitochondria, where it ubiquitinates the fusion-promoting protein Mfn2. Ubiquitination of Mfn2 targets it for proteasomal degradation thus reducing the amount of fusion and leading to a more fragmented phenotype (Tang et al., 2015). While we did demonstrate that Mul1 interacts with EHD1, through the EHD1 interaction partner Rabankyrin-5, which also interacts with the retromer (Zhang, Reiling, et al., 2012), we did not find increased levels of Mfn2 upon depletion of EHD1, Rabankyrin-5, or VPS35 as would be anticipated if less proteasomal degradation occurs. This suggests that the interactions between EHD1, Rabankyrin-5, VPS35, and Mul1 are not the primary mechanism for the control of mitochondrial dynamics.

Another model has been proposed that VPS35 regulates mitochondrial dynamics by a different mechanism where VPS35-containing vesicles interact with inactive Drp1 on the mitochondrial membrane and remove the inactive Drp1. As a result, Drp1 receptors are freed up to bind to active Drp1 and promote fission of the mitochondria (W. Wang et al., 2017). In this model, loss or altered regulation of VPS35 in the absence of EHD1 could lead to impaired fission resulting in an elongated and static mitochondrial network. Indeed, we demonstrated that depleting EHD1 from cells resulted in a decrease in VPS35 protein levels. Surprisingly, Rabankyrin-5-depletion did not result in a decrease in VPS35 proteins levels similar to EHD1. However, when

Rabankyrin-5 was depleted, the subcellular localization of VPS35 was altered, providing a mechanism for the formation of elongated mitochondria that is different from EHD1. While our data suggest that EHD1 and Rabankyrin-5 play a regulatory function upstream of mitochondrial fission through VPS35, we cannot rule out other potential roles that EHD1 and Rabankyrin-5 may play in fission or fusion of mitochondria, including the possibility that EHD1 might serve (at least in part) as a direct mitochondrial membrane fission protein.

In summary, Chapter II highlights a new mechanism of regulation of mitochondrial dynamics and further strengthens the growing crosstalk between endocytic regulatory proteins and non-endocytic organelles. While no mutations or impaired expression of EHD1 or Rabankyrin-5 has been documented thus far in PD, expanding the knowledge of key regulators of mitochondrial dynamics is likely to shed new light on mechanisms that lead or contribute to PD.

Chapter III

The Retromer facilitates the localization of Bcl-xL to the outer mitochondrial membrane

With permission from Molecular Biology of the Cell, parts of this chapter were derived from: (Farmer et al., 2019)

Farmer, T., K.L. O'Neill, N. Naslavsky, X. Luo, and S. Caplan. 2019. Retromer facilitates the localization of Bcl-xL to the mitochondrial outer membrane. *Mol Biol Cell*. 30:1138-1146

11. ABSTRACT

The Bcl-2 family member Bcl-xL is an anti-apoptotic protein that plays a critical role in whether a cell lives or dies by protecting the integrity of the mitochondrial outer membrane (MOM). Bcl-xL works through a mechanism in which it prevents pore formation at the MOM but how Bcl-xL is recruited to the MOM is not fully understood. The retromer is a conserved endosomal scaffold complex involved in membrane trafficking. In Chapter III, we identify two core components of the retromer, VPS35 and VPS26, as novel regulators of the recruitment of Bcl-xL to the MOM. We observed interactions and colocalization between Bcl-xL, VPS35, VPS26, and MICAL-L1, the latter a protein that regulates tubular recycling endosomes and also interacts with the retromer. We also discovered that if VPS35 is depleted from cells, the levels of Bcl-xL that remain unassociated with MOM were significantly increased. Our results from this study suggest that the retromer regulates apoptosis by facilitating Bcl-xL's transport to the MOM. Importantly, this chapter suggests a novel, previously uncharacterized relationship between machinery controlling apoptosis and endosomal trafficking.

12. INTRODUCTION

Apoptosis is an essential cellular event that is required for normal development and the maintenance of tissue homeostasis, protection from genomic instability and mutation, and the control of humoral immune responses (Slomp & Peperzak, 2018). The Bcl-2 family of proteins consists of apoptosis regulators that are either pro-apoptotic (Bax, Bak, Bad, etc.) or anti-apoptotic (Bcl-2, Bcl-xL, Mcl-1, etc.) proteins (Adams & Cory, 1998; Farrow & Brown, 1996; Fuchs & Steller, 2015). On one hand, interference with the

key regulators of apoptosis may lead to uncontrolled cell growth and pathologies that include breast (Placzek et al., 2010; Tawfik, Kimler, Davis, Fan, & Tawfik, 2012) and lung (Han et al., 2002; Viard-Leveugle, Veyrenc, French, Brambilla, & Brambilla, 2003) cancer, as a result of decreased cell death. On the other hand, increased cell death can lead to neurodegenerative disorders such as Alzheimer's (Crews, Patrick, Adame, Rockenstein, & Masliah, 2011; M. H. Lee et al., 2010) and PD (Barcia et al., 2011; Berry, La Vecchia, & Nicotera, 2010). Bcl-xL is a vital anti-apoptotic protein that is up-regulated in a variety of cancers and increases the cell's resistance to undergo apoptosis (Choi et al., 2016; Scherr et al., 2016). While Bcl-xL can function through a number of mechanisms, the main mode of action is sequestering the pro-apoptotic proteins Bax and Bak, thus preventing the formation of pores in the MOM and subsequent release of cytochrome *c* that activates caspases and downstream death signals (Oltvai, Milliman, & Korsmeyer, 1993; Shimizu et al., 1995; Yang et al., 1995). Bcl-xL mainly localizes to the MOM but also is partially localized to the cytoplasm before reaching the MOM (Hausmann et al., 2000; Y. T. Hsu, Wolter, & Youle, 1997; Nijhawan et al., 2003). While the signals that recruit Bcl-xL are unclear, some cellular signals result in the recruitment of Bcl-xL to the mitochondria (Y. T. Hsu et al., 1997), suggesting that Bcl-xL translocation from the cytosol to the mitochondria might be an important regulatory step in the apoptotic cascade. Clues to how Bcl-xL might be translocated to the mitochondria can be found in previous studies that have addressed other Bcl-2 family members. For example, Bax undergoes simple diffusion from the cytoplasm to the mitochondria (Wolter et al., 1997) and given the homology between Bcl-xL and Bax, one possibility is that Bcl-xL also undergoes simple

diffusion to the MOM. However, few studies have addressed the mechanism by which Bcl-xL is translocated and targeted to the mitochondrial membrane to prevent Bax and Bak pore formation.

In addition to diffusion as a potential mechanism for Bcl-2 family member translocation from the cytosol to MOM, other mechanisms of transport might also contribute. One possibility is that endocytic membrane trafficking might account for some of the Bcl-xL translocation to the MOM. While endocytic regulatory proteins are primarily responsible for regulating the internalization, sorting, and recycling of proteins and lipids from the PM (Naslavsky & Caplan, 2018), recent studies suggest that endocytic membrane trafficking proteins are responsible for a variety of non-endocytic cellular events, such as mitochondrial fission (Farmer et al., 2017; J. E. Lee et al., 2016) and centriole disengagement/duplication (Xie et al., 2018). For example, EHD1 is a key regulator of receptor recycling to the plasma membrane (Caplan et al., 2002; Guilherme et al., 2004) and also regulates both mitochondrial fission (Farmer et al., 2017) and centriole disengagement (Xie et al., 2018). Furthermore, the endocytic scaffolding complex known as the retromer, consisting of VPS26, VPS29, and VPS35, and two sorting nexin proteins, has also been implicated in mitochondrial fission (Farmer et al., 2017; Naslavsky & Caplan, 2018; Tang et al., 2015; W. Wang et al., 2017) and centriole disengagement (Xie et al., 2018). The retromer subunit, VPS35, also directly interacts with and regulates multiple mitochondrial fission and fusion factors including the E3 ligase Mul1 (Braschi et al., 2010; Tang et al., 2015) and the fission factor, Drp1 (Farmer et al., 2017; Tang et al., 2015; W. Wang et al., 2017). Interestingly, Bcl-xL and Drp1 interact

and colocalize on clathrin-associated vesicles (Li et al., 2013), suggesting a potential control mechanism for Bcl-xL by endocytic regulatory proteins. Accordingly, we hypothesized that VPS35 and the retromer interact with Bcl-xL and control the translocation of Bcl-xL from the cytosol to the MOM, thus influencing apoptosis.

In Chapter III, we address whether the retromer and endocytic trafficking directs Bcl-xL translocation from the cytoplasm to the MOM. We demonstrate for the first time that Bcl-xL physically interacts with the retromer components VPS35 and VPS26 in a Drp1-independent manner. Furthermore, the retromer and Bcl-xL colocalize on vesicles that are distinct from mitochondria. Significantly, the depletion of VPS35, which disrupts retromer function, results in reduced Bcl-xL on mitochondria and increases the rate of STS-induced apoptosis. While only a portion of the Bcl-xL seems to rely on the retromer to translocate to the MOM, our studies suggest a previously uncharacterized pathway for delivering Bcl-xL to the MOM that potentially has a significant consequence if disrupted.

13. MATERIALS AND METHODS

13.1 Reagents and antibodies

Staurosporine was purchased from Sigma Aldrich (S5921). Z-valine-alanine-aspartic acid-(OMe)-fluromethylketone (Z-VAD) was purchased from Fisher Scientific (MP Biomedical; MP3FK00901). Commercial antibodies with their specific use (IB, immunoblotting; IF, immunofluorescence; and IP, immunoprecipitation) and catalogue numbers are indicated. Anti-VPS26 (IB, IF, IP, ab23892), anti-VPS35 (IB, ab157220), anti-

Bcl-xL (IB, IP, ab32370), anti-Bcl-xL (IF, ab26035), anti-Parp1 (IB, ab137653), and anti-Rab5 (IF, ab18211) were from Abcam; anti-DRP1 (IB, 611112) was from BD Cell Analysis; anti- MICAL-L1 (IB, IF, MBS9215151) was from MyBioSource; anti-Tom20 (IF, sc-11415) was from Santa Cruz Biotechnology; anti-EEA1 (IF, #3288) was from Cell Signaling; and anti-GAPDH-HRP (IB, HRP-60004) was from Protein Tech; donkey anti-mouse immunoglobulin (IgG) light chain–HRP (IB, 715-035-151) and mouse anti-rabbit IgG light chain–HRP (IB, 211-032-171) were from Jackson; mouse anti-rabbit IgG heavy chain–HRP (IB, ab99702) was from Abcam; donkey anti-mouse 488 (IF,A21202), donkey anti-mouse 568 (IF, 21043), goat anti-rabbit 488 (IF, A11034), goat anti-rabbit 568 (IF, A11036), and goat anti-rabbit 633 (IF, A21070) were from Molecular Probes.

13.2 Cell Culture

The HeLa cervical cancer cell line was obtained from ATCC and grown in high glucose DMEM containing 10% FBS, 1x penicillin-streptomycin (Invitrogen), and 2 mM glutamine. The immortalized retinal pigment epithelium (RPE) cell line from ATCC was gown in high glucose DMEM containing 10% FBS, 1x penicillin-streptomycin (Invitrogen), 2 mM glutamine, and 2 mM non-essential amino acids. The CRISPR/Cas9 HCT 116 cells lacking endogenous Bak and Bax, with GFP-tagged Bax knocked in (GFP-Bax HCT 116) have been previously described (K. L. O'Neill, Huang, Zhang, Chen, & Luo, 2016)) and were grown in McCoy's medium containing 10% FBS, 1× penicillin-streptomycin (Invitrogen), and 2 mM glutamine.

13.3 Transfection and siRNA treatment

Transfection of RPE cells for 24 h at 37°C was performed using Fugene6 (Promega) according to the manufacturer's protocol. Smart-pool ON-Target Drp1, VPS35, and MICAL-L1 oligonucleotides were obtained from Dharmacon. RPE, HeLa, or GFP-Bax HCT 116 cells were transfected using Dharmafect 1 transfection reagent (Dharmacon) with 40 nM oligonucleotide. The knockdown efficiency of the protein was measured at 72 h post-transfection by immunoblotting for each experiment.

13.4 Plasmids

mCherry-TOMM20 was a gift from Michael Davidson (Addgene; plasmid #55146).

13.4 Co-immunoprecipitation

HeLa cells were grown in 100-mm dishes until confluent. Cells were lysed with lysis buffer containing 50 mM Tris, pH 7.4, 100 mM NaCl, 0.5% Triton X-100, and 1× protease cocktail inhibitor (Millipore) on ice for 30 min. Lysates were incubated with anti–Bcl-xL, anti-VPS26, or anti–MICAL-L1 antibody at 4°C overnight. Protein G beads (GE Healthcare) were added to the lysate-antibody mix at 4°C for 4 h. Samples were then washed three times with the same lysis buffer. Proteins were eluted from the protein G beads by boiling in the presence of 4× loading buffer (250 mM Tris, pH 6.8, 8% SDS, 40% glycerol, 5% β-mercaptoethanol, 0.2% bromophenol blue) for 10 min. Eluted proteins were then identified by immunoblotting.

13.5 Immunoblotting

Cells were washed twice in ice-cold 1x PBS and then scraped off plates with a rubber policeman into ice-cold lysis buffer (50 mM Tris, pH 7.4, 100 mM NaCl, 0.5% TX-100, 1× protease cocktail inhibitor [Millipore]). Protein levels of post-nuclear lysates were quantified using the Bradford assay (BioRad) for equal protein level loading. For immunoblotting, 20–30 μg of protein per lysate (from either HeLa, RPE1, or GFP-Bax HCT 116 cells) was separated by SDS–PAGE. Proteins were transferred onto nitrocellulose membranes, and blocked for 30 min at room temperature in 1x PBST plus 5% nonfat dry milk. The membranes were then incubated overnight at 4°C or for 1 h at room temperature with primary antibodies diluted in 1x PBST. Membranes were then washed three times with 1x PBST and incubated at room temperature with appropriate secondary antibodies diluted in 1x PBST for 30 min. The membranes were then washed again three times with 1x PBST, before enhanced chemiluminescence was used to detect the proteins.

13.6 Mitochondrial enrichment

HeLa cells were grown in 100-mm dishes and subject to either Mock- or VPS35-siRNA treatment for 72 h. Cells were homogenized in buffer containing 150 mM NaCl, 10 mM Tris, pH 6.8, 10 mM KCl, and 1 M sucrose. Homogenates were incubated with anti-Tom20 and rotated at room temperature for 10 min. Homogenates plus anti-Tom20 were added to Dynabeads Protein G (Invitrogen) and rotated for 10 min at room temperature. The samples were placed on the magnet and the supernatant was collected for the non-mitochondrial fraction. The Dynabeads or mitochondrial fraction was

washed three times with the cell homogenization buffer. The beads and supernatant were subject to lysis in equal volumes with lysis buffer containing 50 mM Tris, pH 7.4, 100 mM NaCl, 0.5% Triton X-100, and 1× protease cocktail inhibitor (Millipore) on ice for 30 min. Loading buffer (4×) was added to each fraction and boiled for 10 min. Equal volumes were separated by SDS–PAGE and proteins were detected by immunoblotting with anti–Bcl-xL and anti-Tom20 antibodies.

13.7 Quantification of immunoblots

The adjusted relative density of the immunoblots was measured in Fiji ImageJ according to the following protocol: www1.med.umn.edu/starrlab_deleteme/prod/groups/med/@pub/@med/@starrlab/documents/content/med_content_370494.html.

13.8 Immunofluorescence.

RPE or GFP-Bax HCT 116 cells were treated as indicated in the text and then fixed in 4% paraformaldehyde in 1x PBS for 10 min at room temperature. Cells were then washed three times in 1x PBS. The cells were then incubated with primary antibody in staining buffer (1x PBS containing 0.5% bovine serum albumin (BSA) and 0.2% saponin) for 1 h at room temperature, washed three times in 1x PBS and then incubated with the appropriate fluorochrome-conjugated secondary antibodies diluted in staining buffer for 30 min. Cells were washed three times in 1x PBS and mounted on microscope slides with Fluoromount.

Using a Zeiss LSM800 confocal microscope with a 63×/1.4 NA oil objective, z-stack confocal images were collected. The series of images from a z-stack was then processed into a 3D projection, and a 3D snapshot was obtained using the Zeiss Zen Software. Similarly, 3D rotational videos were generated from the same 3D projections using the Zeiss Zen Software. For quantification, collected 3D snapshots were imported into Fiji ImageJ as described below.

13.9 Colocalization quantification

Colocalization between mCh-TOMM20 and Bcl-xL, VPS26 and Bcl-xL, VPS26 and mCh-TOMM20, Bcl-xL and Rab5, or Bcl-xL and EEA1 were assessed in Fiji ImageJ. Multichannel 3D snapshots were split into separate channels. A region of interest was drawn around individual cells in one of the two channels, using the "freehand" tool. This region was then subject to the colocalization threshold plugin, and colocalization was measured and calculated.

13.10 Bax activation assay

GFP-Bax HCT 116 cells were subject to either Mock- or VPS35-siRNA treatment. In the last 60 min of the siRNA treatment, the cells were treated with 1 μM staurosporine (Sigma Aldrich). Cells were immunostained with anti-Tom20 as previously described. 250 cells per treatment were designated as either having inactive (cytoplasmic) Bax or active (punctate) Bax.

13.11 Parp1 cleavage assay

GFP-Bax HCT 116 cells were subject to Mock- or VPS35-siRNA treatment. The cells were detached using trypsin and treated with 1 μM staurosporine for 0, 30, or 60 min while continuously being rotated at 37°C. Immunoblotting was performed on the samples with anti-Parp1. The amount of full-length Parp1 was quantified by the method described above.

13.12 Statistics

Data from Fiji ImageJ were imported into Microsoft Excel. The mean and the standard deviation of the mean were calculated from data obtained from three independent experiments with at least 10 images taken per treatment. Statistical significance was calculated using a Student's *t* test with the Vassarstats program (http://www.vassarstats.net).

14. RESULTS

14.1 Bcl-xL resides in a protein complex with endocytic proteins and DRP1

Bcl-xL localizes to the MOM where it regulates apoptosis, but a pool of the protein can been observed in the cytoplasm (Hausmann et al., 2000; Y. T. Hsu et al., 1997; Nijhawan et al., 2003). Previous studies suggest a diffusion mechanism for some Bcl-2 family members from the cytosol to the MOM, where the proteins become immobilized (Wolter et al., 1997). For example, conformational changes and homo-oligomerization of the pro-apoptotic protein, Bax, lead to the exposure of mitochondrial targeting sequences within four of the protein's nine helices (N. M. George, Targy,

Evans, Zhang, & Luo, 2010). However, despite the importance of Bcl-xL in preventing apoptosis, the specific mechanism of how it is translocated from the cytoplasm to the MOM remains poorly understood. Recent studies demonstrate the role of membrane trafficking in protein delivery to the MOM (Farmer et al., 2018; Farmer et al., 2017; Tang et al., 2015; W. Wang et al., 2017); accordingly, we hypothesized that a population of Bcl-xL might also be regulated by endocytic membrane trafficking proteins.

We first tested whether Bcl-xL could be found in a complex with other endocytic regulatory proteins. Given the established interaction between Bcl-xL and Drp1 (Li et al., 2013), and between Drp1 and the retromer complex, (W. Wang et al., 2017; W. Wang et al., 2016) and the growing number of trafficking pathways regulated by the retromer (Farmer et al., 2018; Farmer et al., 2017; Tang et al., 2015; W. Wang et al., 2017), we tested if Bcl-xL interacted with the retromer complex. As demonstrated, antibodies to VPS26 immunoprecipitated detectable levels of endogenous VPS26 protein (Figure 3.1A; low and medium exposures), as well as endogenous Drp1 (Figure 3.1A; high exposure) and endogenous Bcl-xL (Figure 3.1A; low and medium exposures). Antibodies to Bcl-xL pulled down endogenous Bcl-xL (Figure 3.1A; low and medium exposures), as well as VPS26 (Figure 3.1A; low and medium exposures) and Drp1 (Figure 3.1A; high exposure), whereas control immunoglobulins (Ctl) did not pull down any detectable VPS26, Bcl-xL, or Drp1. Furthermore, immunoprecipitation with antibodies against MICAL-L1, an endocytic regulatory protein that interacts with the retromer (Zhang, Reiling, et al., 2012), also pulled down Bcl-xL in addition to the retromer

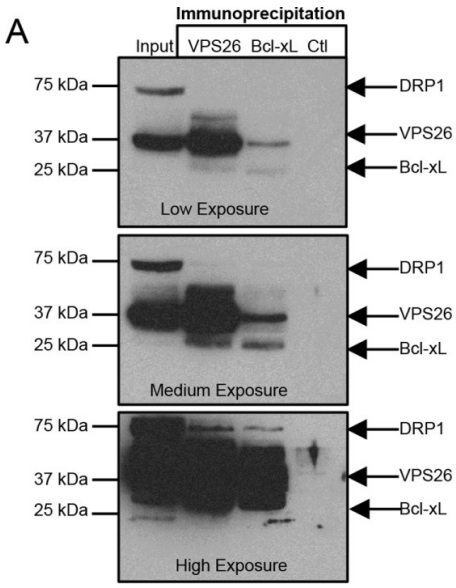
A
Immunoprecipitation
Input
VPS26
Bcl-xL
Ctl
75 kDa
37 kDa
25 kDa
DRP1
VPS26
Bcl-xL
Low Exposure
Medium Exposure
High Exposure

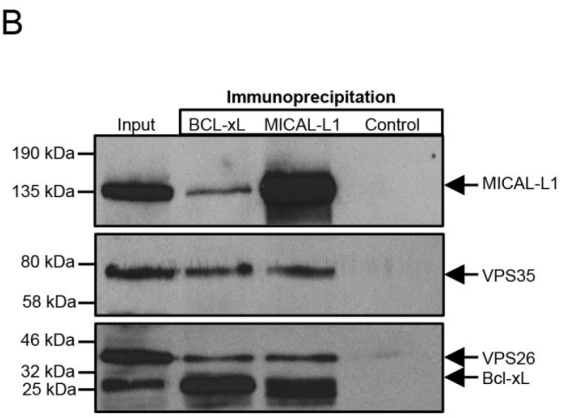
B
Immunoprecipitation
Input
BCL-xL
MICAL-L1
Control
190 kDa
135 kDa
80 kDa
58 kDa
46 kDa
32 kDa
25 kDa
MICAL-L1
VPS35
VPS26
Bcl-xL

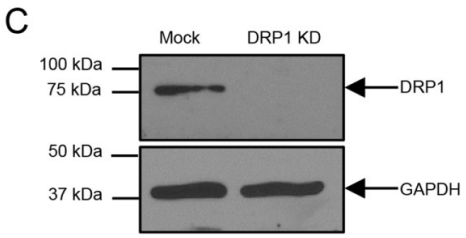
C
Mock
DRP1 KD
100 kDa
75 kDa
50 kDa
37 kDa
DRP1
GAPDH

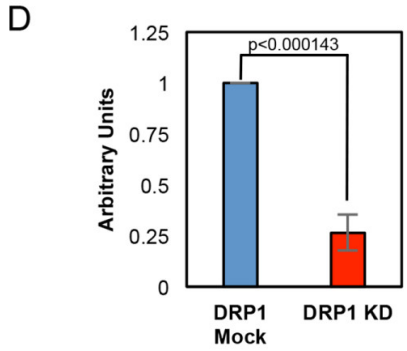
D
p<0.000143
Arbitrary Units
1.25
1
0.75
0.5
0.25
0
DRP1 Mock
DRP1 KD

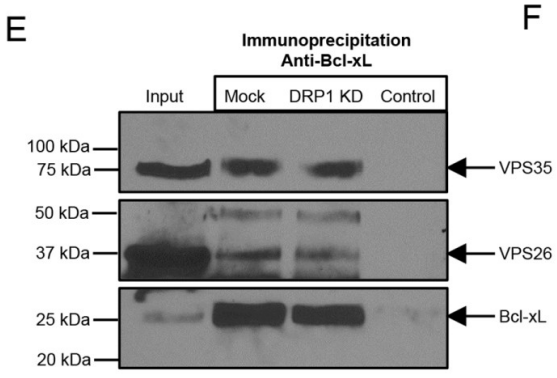
E
Immunoprecipitation
Anti-Bcl-xL
Input
Mock
DRP1 KD
Control
100 kDa
75 kDa
50 kDa
37 kDa
25 kDa
20 kDa
VPS35
VPS26
Bcl-xL

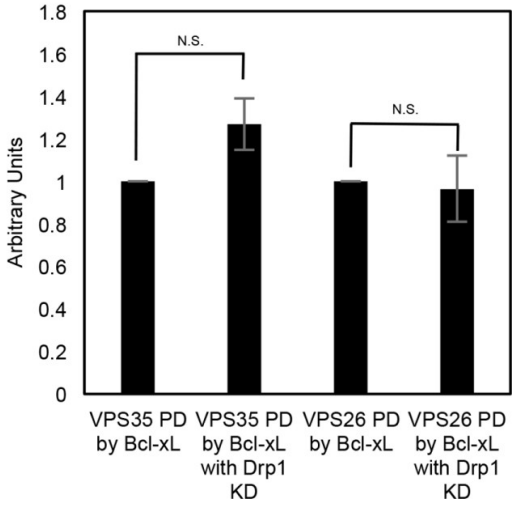
F
N.S.
N.S.
Arbitrary Units
1.8
1.6
1.4
1.2
1
0.8
0.6
0.4
0.2
0
VPS35 PD by Bcl-xL
VPS35 PD by Bcl-xL with Drp1 KD
VPS26 PD by Bcl-xL
VPS26 PD by Bcl-xL with Drp1 KD

Figure 3. 1

Bcl-xL resides in a protein complex with members of the retromer and DRP1. (A) HeLa cell lysates were subjected to immunoprecipitations with anti-VPS26, anti–Bcl-xL, or control IgG, and immunoblotted with antibodies against Drp1, VPS26, and Bcl-xL. Three different exposures of the same immunoblot are depicted: low, medium, or high exposure. Gels depicted are representative of three independent experiments showing similar results. Densitometric analysis from these experiments shows that 1) compared with the level of VPS26 precipitated with anti-VPS26 (defined as 100%), 41–66% of VPS26 precipitates with anti–Bcl-xL, and 2) the level of DRP1 precipitated by anti–Bcl-xL ranges from ~50 to 90% of that precipitated by anti-VPS26. (B) HeLa cell lysates were subjected to immunoprecipitations with anti–Bcl-xL, anti–MICAL-L1, or control IgG, and immunoblotted with antibodies against MICAL-L1, VPS35, VPS26, and Bcl-xL. Gel depicted is representative of three individual experiments showing similar results. Densitometric analysis from these experiments shows that 1) the ratio of VPS26:Bcl-xL precipitated with anti–Bcl-xL is 0.660+/− 0.110, which is very similar to the ratio of VPS35:Bcl-xL precipitated with anti–Bcl-xL (0.6866+/− 0.169), and 2) the ratio of VPS26:MICAL-L1 precipitated with anti–MICAL-L1 (0.589+/− 0.215) is similar to the ratio of VPS35:MICAL-L1 precipitated with anti–MICAL-L1 (0.607+/− 0.129). (C) Efficacy of DRP1 depletion is demonstrated by immunoblotting lysates from Mock- or DRP1-depleted HeLa cells with anti-DRP1, and using GAPDH as a loading control. (D) Densitometric quantification of DRP1 protein levels in either Mock- or DRP1-siRNA treatment. Error bars denote SD. *p* values were determined by the Student's one-tailed *t* test. $n = 3$. (E) HeLa cells were treated with either Mock- or DRP1-siRNA, immunoprecipitated with antibodies against Bcl-xL, and immunoblotted with antibodies against VPS35, VPS26, and Bcl-xL. Gel depicted is representative of three individual experiments showing similar results. (F) Densitometric quantification of VPS35 or VPS26 protein levels immunoprecipitated by anti–Bcl-xL in the presence or absence of DRP1. Error bars denote SD. *p* values were determined by the Student's one-tailed *t* test. $n = 3$. Used with permission from MBoC (Farmer et al., 2019).

proteins (Figure 3.1B). These experiments support the idea that Bcl-xL partially resides in a protein complex containing the retromer complex and MICAL-L1.

Since Drp1 interacts with both Bcl-xL and the retromer complex, we next asked whether Drp1 mediates the interaction between Bcl-xL and the retromer. To answer this question, HeLa cells were depleted of Drp1 by siRNA transfection (Figure 3.1C, quantified in 3.1D), and the Drp1 lysate was used to perform a pull down with antibodies against Bcl-xL. As anticipated, anti-Bcl-xL was able to pull down endogenous Bcl-xL in the mock- and Drp1-depleted lysates (Figure 3.1E, quantified in 3.1F). However, upon depletion of Drp1, anti-Bcl-xL still pulled down VPS26 and VPS35 subunits (Figure 1E, top and middle panels, quantified in F). Similar to the anti-Bcl-xL pull down, depletion of VPS26, which led to a concomitant reduction of VPS35, did not prevent the pull down of Drp1 by Bcl-xL (data not shown). Overall, these experiments support the notion that Bcl-xL interacts with the retromer complex and MICAL-L1 in a Drp1-independent manner.

14.2 Bcl-xL localizes to endocytic vesicles positive for the retromer

Since Bcl-xL interacts with several subunits of the retromer complex and interaction partners of the retromer, we hypothesized that the retromer serves as a regulator of Bcl-xL translocation from the cytosol to the MOM. Given that the ratio of Bcl-xL in the cytoplasm versus the MOM-bound Bcl-xL does not change under apoptotic conditions (Wolter et al., 1997), any slight change in the balance of the cytosolic-to-mitochondrial Bcl-xL might be physiologically important. Accordingly, we postulated

that if a pool of Bcl-xL was translocated to the MOM by the retromer complex, we would visualize Bcl-xL associated with retromer-positive vesicles. To test this, we transfected RPE cells with mCherry-tagged Tom20 N-terminal 10 residues as a mitochondrial membrane marker and then sequentially immunostained the cells with antibodies against endogenous Bcl-xL and VPS26 (Figure 3.2 and 3D images in Figure 3.3). As demonstrated, populations of Bcl-xL were observed on VPS26-positive vesicles (Figure 3.2A, inset in B, E, and H), and interestingly, these vesicles are almost completely devoid of the Tom20 MOM marker. However, most of the Bcl-xL was seen colocalized with the Tom20 and devoid of the VPS26 staining (Figure 3.2A, inset C, E, and F). When quantified, approximately 65% of the Bcl-xL was localized with mitochondria while less than 30% was on VPS26-positive vesicles (Figure 3.2D). Furthermore, endogenous VPS35 displayed approximately 85% overlap with VPS26 as expected, as well as ~25% colocalization with Bcl-xL (Figure 3.4). To further characterize what type of endosomes these were, we also stained the cells for Rab5 and EEA1, two early endosome markers, and observed nearly 20% of the Bcl-xL with Rab5, but little or no colocalization was seen with EEA1 (Figure 3.5). These data illustrate for the first time a population of Bcl-xL that localizes with a subset of endosomal vesicles that contain the retromer and Rab5, further suggesting the possibility that retromer plays a role in translocation of Bcl-xL to the MOM.

14.3 Depletion of VPS35 or MICAL-L1 results in decreased-mitochondrial Bcl-xL

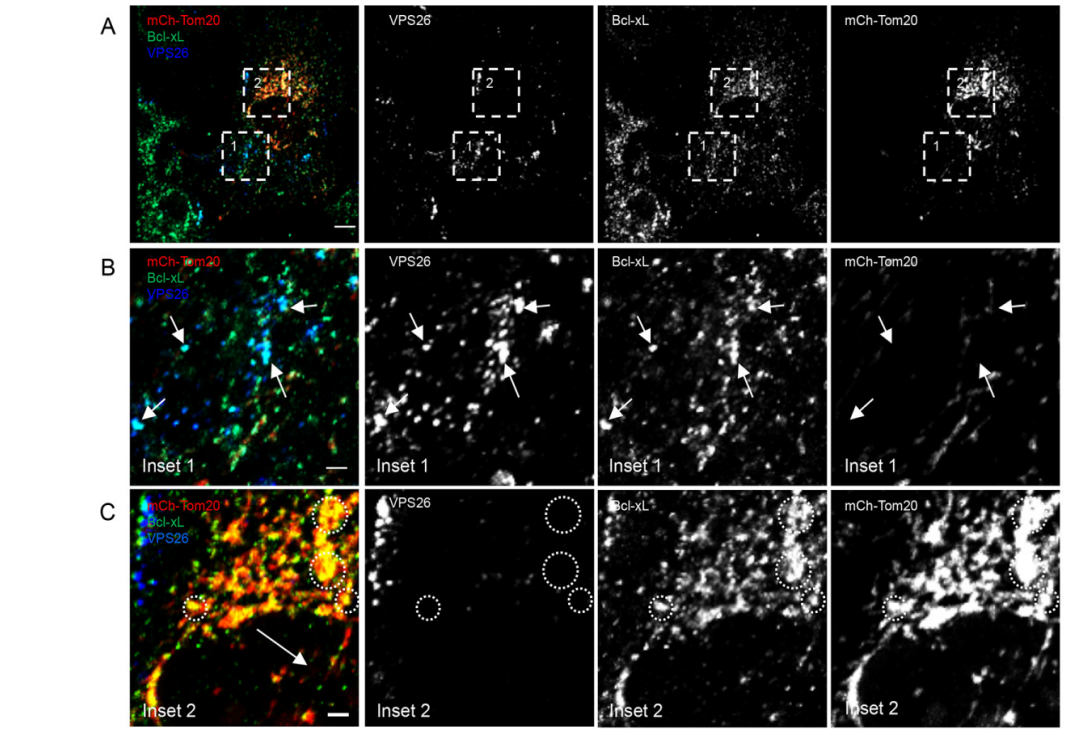
A
mCh-Tom20
Bcl-xL
VPS26
VPS26
Bcl-xL
mCh-Tom20
B
Inset 1
C
Inset 2

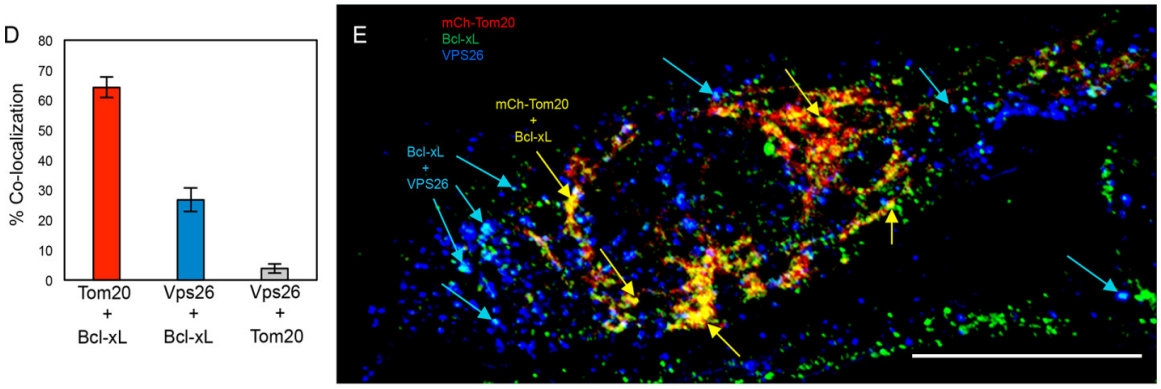
D
% Co-localization
80
70
60
50
40
30
20
10
0
Tom20 + Bcl-xL
Vps26 + Bcl-xL
Vps26 + Tom20
E
mCh-Tom20
Bcl-xL
VPS26
mCh-Tom20 + Bcl-xL
Bcl-xL + VPS26

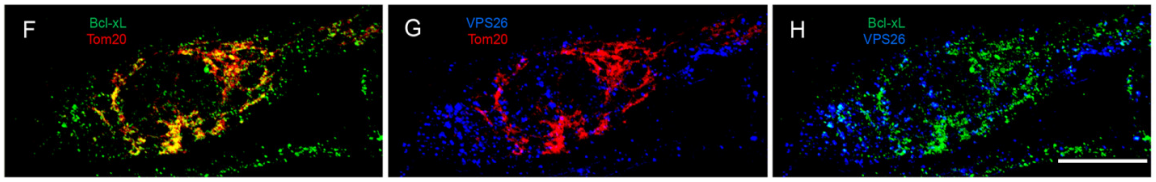
F
Bcl-xL
Tom20
G
VPS26
Tom20
H
Bcl-xL
VPS26

Figure 3. 2

Bcl-xL localizes to endocytic vesicles containing the retromer. (A) RPE1 cells were transfected with the N-terminal 10 residues of the mitochondrial outer membrane protein (Tom20) tagged with mCherry (mCh-Tom20; red), and immunostained with VPS26 (blue) and Bcl-xL (green). Images shown are 3D snapshots of serial z-sections. Channels were split, showing the individual protein localization patterns (right panels). Regions of interest are highlighted with dashed boxes labeled as 1 or 2, and they correspond to the inset images depicted in B and C. Scale bar = 10 μm. (B) Inset area 1 from A. Arrows denote vesicles containing VPS26 (blue) and Bcl-xL (green) but lack mCh-Tom20 (red). Channels were split, showing the individual protein localizations. Scale bar = 2 μm. (C) Inset area 2 from A. Dashed circles show areas where Bcl-xL (green) is colocalized with mCh-Tom20 (red), but not VPS26 (blue). Channels were split, showing the individual protein localizations. Scale bar = 2 μm. Images portrayed are representative of three independent experiments (quantified in D). (D) The colocalization threshold analysis tool in Fiji ImageJ was used to quantify the colocalization between Bcl-xL and mCh-Tom20, Bcl-xL and VPS26, or mCh-Tom20 and VPS26. Data are presented as a mean, and error bars indicate SD. $n = 3$. (E) A single representative RPE1 cell transfected with mCh-Tom20 (red), and immunostained with VPS26 (blue) and Bcl-xL (green). The image shown is a 3D snapshot of serial z-sections. Blue arrows depict VPS26 and Bcl-xL colocalization, whereas yellow arrows depict Bcl-xL and Tom20 colocalization. Scale bar = 10 μm. (F–H) Individual two-channel images from E are shown depicting the colocalization between Tom20 and Bcl-xL (F), VPS26 and Tom20 (G), and between Bcl-xL and VPS26 (H). Used with permission from MBoC (Farmer et al., 2019).

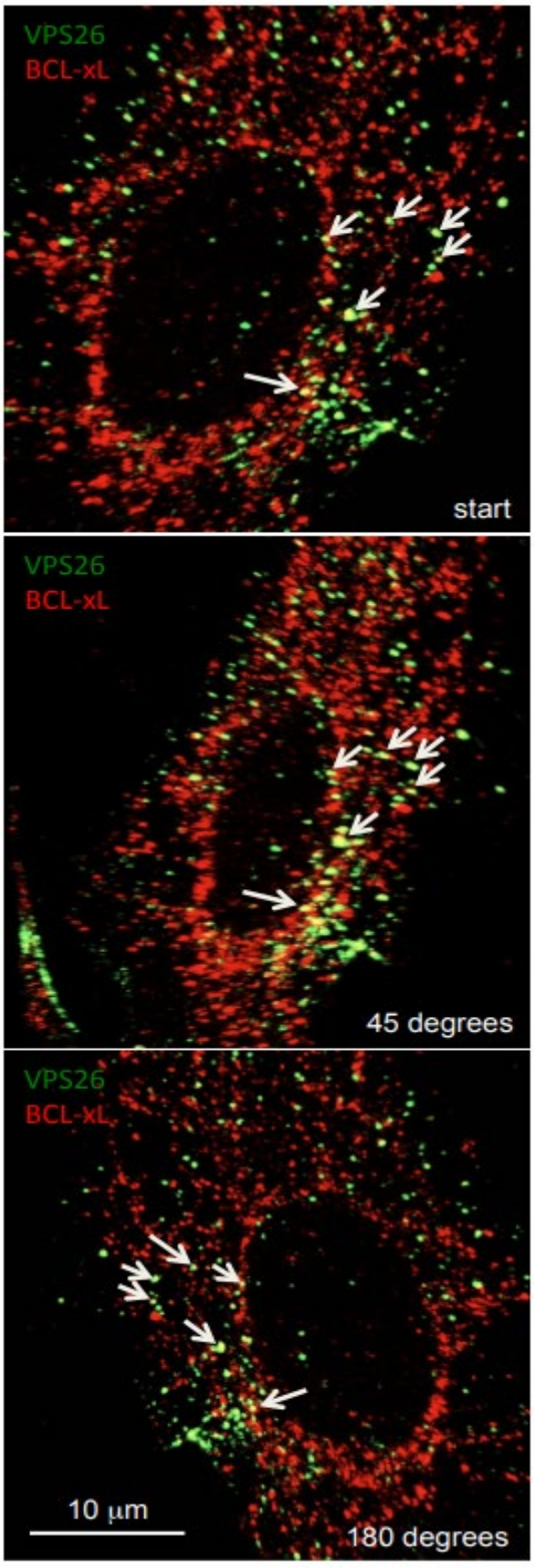
VPS26
BCL-xL
start
VPS26
BCL-xL
45 degrees
VPS26
BCL-xL
10 μm
180 degrees

Figure 3. 3

Bcl-xL and VPS26 localize to common vesicles. RPE1 cells were fixed, permeabilized and immunostained with antibodies to detect endogenous VPS26 (green) and endogenous Bcl-xL (red). Serial z-sections were obtained every 0.4 μm and a 3D rotation was made from the 8 micrographs (see Video 1). The top image represents the initial micrograph prior top rotation, with arrows marking several Bcl-xL and VPS26-containing vesicles. The middle and bottom images denote rotations of 45 and 180 degrees, respectively, and arrows mark the same vesicles seen in the initial image. Used with permission from MBoC (Farmer, O'Neill, Naslavsky, Luo, & Caplan, 2019).

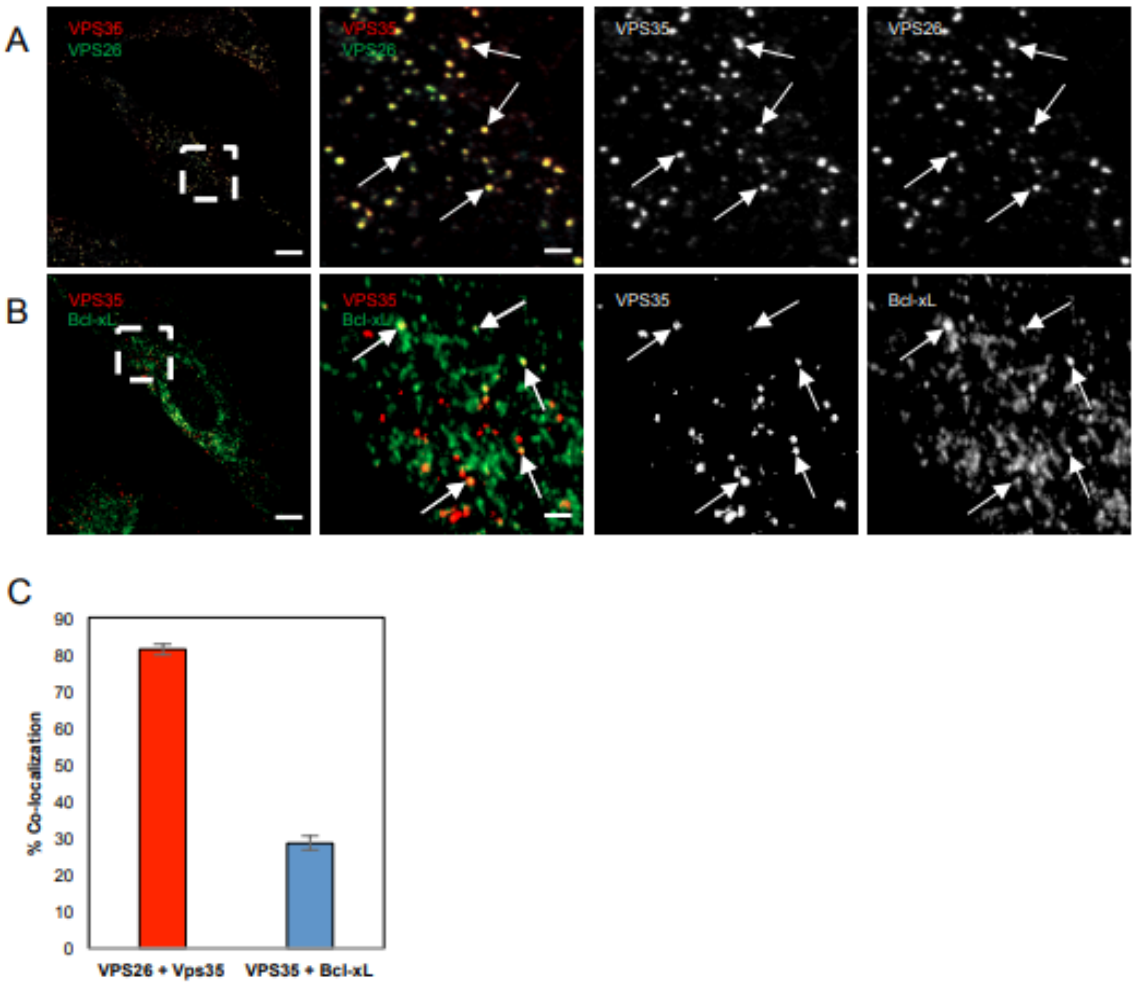

Figure 3. 4

Bcl-xL localizes to endocytic vesicles containing VPS35. (A) RPE1 cells were immunostained with antibodies against VPS26 (green) and VPS35 (red) and serial z-sections were obtained. The images depicted are 3D snapshots. Dashed regions of interest correspond to the insets on the 3 right-hand panels. Inset channels were split, showing the individual protein localization patterns with white arrows depicting vesicles containing VPS26 and VPS35 containing vesicles. Scale Bar= 10 μm, (2 μm; inset). (B) RPE1 cells were immunostained with antibodies against Bcl-xL (green) and VPS35 (red) and serial z-sections were obtained. The images depicted are 3D snapshots. Dashed regions of interest correspond to the insets on the 3 right-hand panels. Inset channels were split, showing the individual protein localization patterns with white arrows depicting vesicles containing Bcl-xL and VPS35 containing vesicles. Scale Bar= 10 μm, (2 μm; inset). (C) The co-localization threshold analysis tool in FIJI ImageJ was used. Data is presented as a mean, and error bars indicate standard deviation. n=3. Used with permission from MBoC (Farmer et al., 2019).

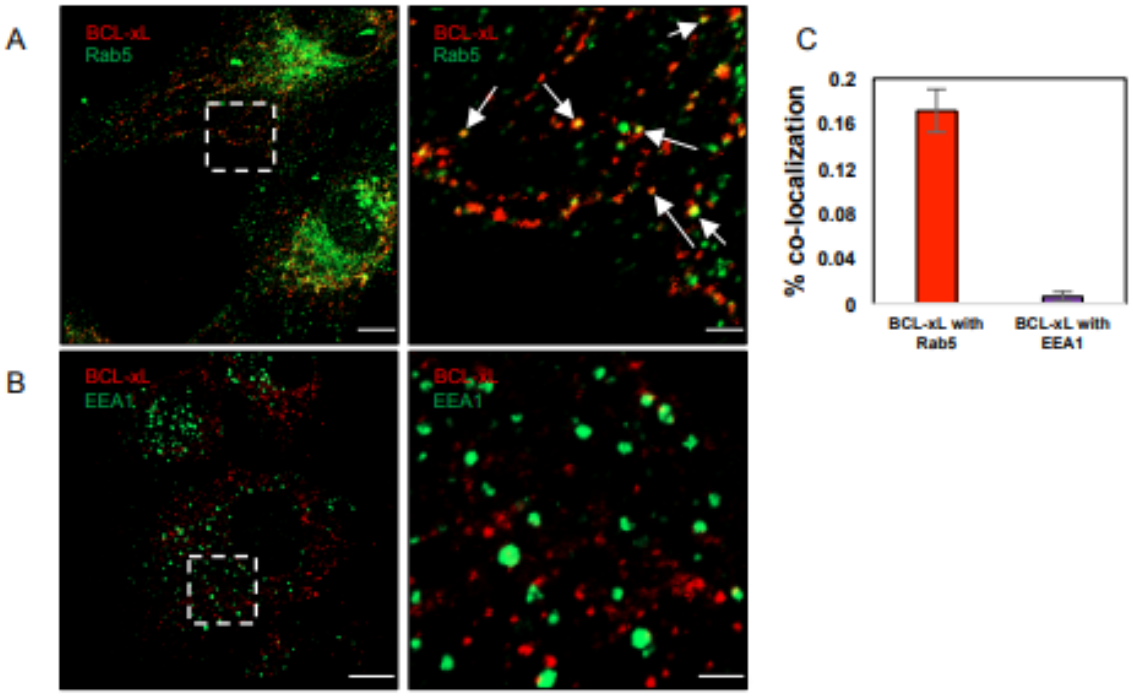

Figure 3. 5

Bcl-xL localizes to Rab5-containing vesicles. (A) 3D snapshot of RPE1 cells immunostained with antibodies against Bcl-xL (red) and Rab5 (green). The dashed region of interest corresponds to the inset to the right. Arrows in the inset depict vesicles containing Bcl-xL (red) and Rab5 (green). Scale Bar= 10 μm, (2 μm; inset). (B) 3D snapshot of RPE1 cells immunostained with antibodies against Bcl-xL (red) and EEA1 (green). The dashed region of interest corresponds to the inset to the right. Scale Bar= 10 μm, (2 μm; inset). (C) The co-localization threshold analysis tool in FIJI ImageJ was used to quantify the co-localization between Bcl-xL and Rab5 and between Bcl-xL and EEA1. Data is presented as a mean, and error bars indicate standard deviation. n=3.

The retromer is a scaffold and endocytic membrane complex responsible for the trafficking of a variety of proteins including the mannose 6-phosphate receptor, iron transporter DMT1-11/Slc11a2, and the Wnt transport protein Wntless/MIG-14 (Arighi et al., 2004; Eaton, 2008; Tabuchi et al., 2010). In each case, interference with retromer function leads to mislocalization (Eaton, 2008; Tabuchi et al., 2010) or occasionally to reduced expression levels of its cargo, possibly due to degradation (Arighi et al., 2004). Given that the these cargos are mislocalized or degraded when the retromer is dysfunctional, we hypothesized that if the retromer is responsible for trafficking Bcl-xL, we should see an impact on Bcl-xL localization or levels when the retromer is disrupted. In order to test this, we treated RPE cells with siRNA specific for VPS35 or the retromer interaction partner, MICAL-L1, and compared the Bcl-xL to cells that were mock-treated. Depletion of VPS35 did not have an impact on the total Bcl-xL protein levels (data not shown). However, mock-treated cells displayed the majority of Bcl-xL on mitochondria (Figure 3.6, top panel, quantified in B), while VPS35- or MICAL-L1-depleted cells (Figure 3.6C and D) had significantly more observable non-mitochondria associated Bcl-xL (Figure 3.6, middle and bottom panels [Bcl-xL in red]). Moreover, depletion of VPS35 led to an increased ratio of non-mitochondria associated Bcl-xL as determined by immunoblotting mitochondrial enriched fragments (Figure 3.6E, quantified in Figure 3.6F). Further testing did not suggest that the non-mitochondrial Bcl-xL observed when depleting VPS35 or MICAL-L1 was interacting with any endocytic or membrane markers (data not shown). Given the ability of Bcl-xL to

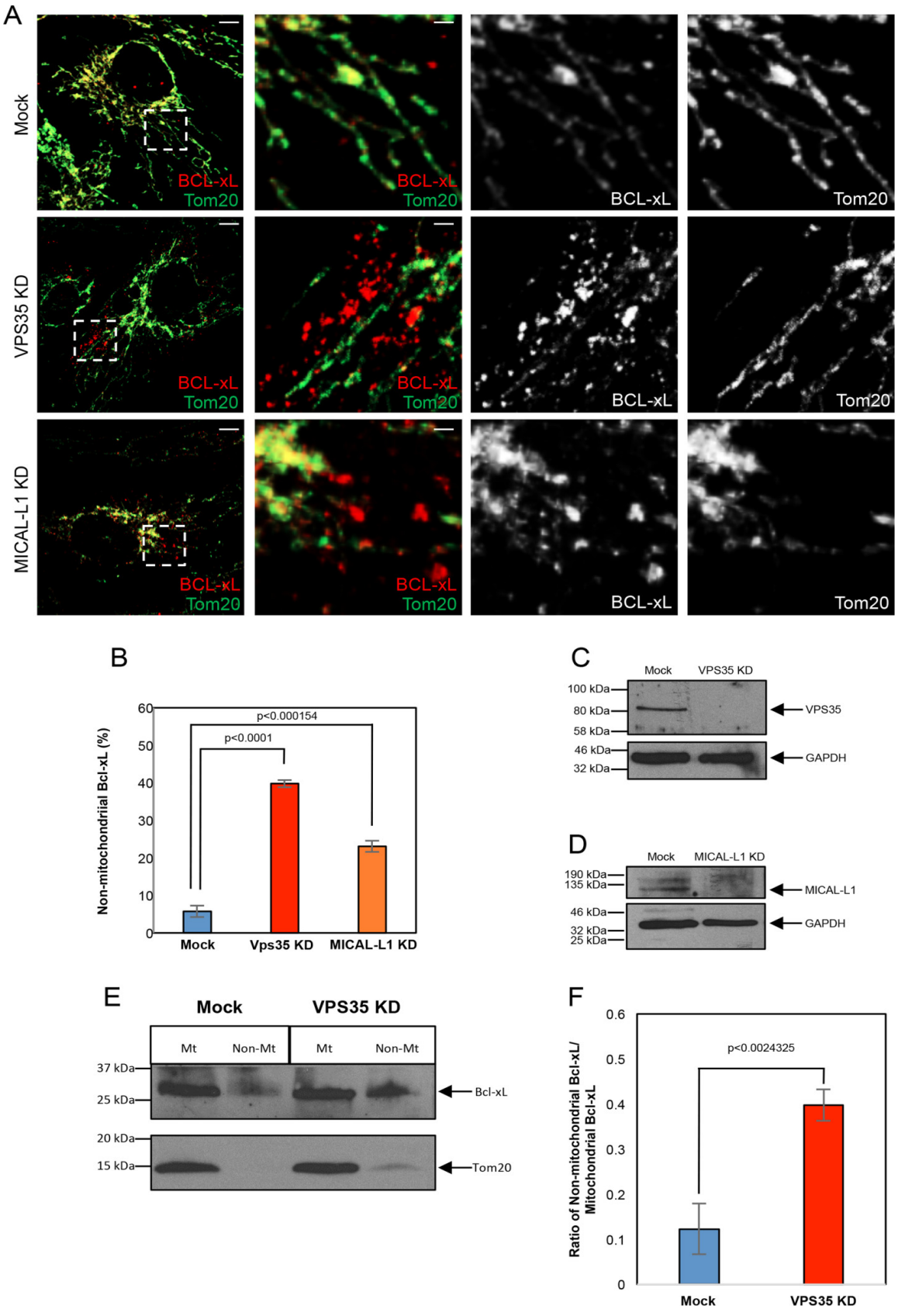
A
Mock
VPS35 KD
MICAL-L1 KD
BCL-xL
Tom20
B
Non-mitochondriial Bcl-xL (%)
p<0.000154
p<0.0001
Mock
Vps35 KD
MICAL-L1 KD
C
Mock
VPS35 KD
100 kDa
80 kDa
58 kDa
46 kDa
32 kDa
VPS35
GAPDH
D
Mock
MICAL-L1 KD
190 kDa
135 kDa
46 kDa
32 kDa
25 kDa
MICAL-L1
GAPDH
E
Mock
VPS35 KD
Mt
Non-Mt
37 kDa
25 kDa
20 kDa
15 kDa
Bcl-xL
Tom20
F
Ratio of Non-mitochondrial Bcl-xL/ Mitochondrial Bcl-xL
p<0.0024325
Mock
VPS35 KD

Figure 3. 6

Loss of VPS35 or MICAL-L1 leads to increased non-mitochondrial Bcl-xL. (A) RPE1 cells were subjected to Mock-, VPS35-, or MICAL-siRNA, immunostained with antibodies against Tom20 (green) and Bcl-xL (red), and serial z-sections were obtained. The images depicted are 3D snapshots. Dashed regions of interest correspond to the insets in the three right-hand panels. Inset channels were split, showing the individual protein localization patterns. Scale bar = 10 μm, (2 μm; inset). (B) Quantification of the mean number of non-mitochondrial-associated Bcl-xL structures upon Mock-, VPS35-, and MICAL-L1-siRNA treatment. Error bars denote SD. *p* values were determined by the Student's one-tailed *t* test. *n* = 3. (C) Efficacy of the VPS35-depletion is demonstrated by immunoblotting lysates from Mock- or VPS35-depleted RPE1 cells, with GAPDH as a loading control. (D) Efficacy of MICAL-L1-depletion is demonstrated by immunoblotting lysates from Mock- or MICAL-L1–depleted RPE1 cells using GAPDH as a loading control. (E) HeLa cells were treated with either Mock- or VPS35-siRNA, homogenized, and subject to immunofractionation with anti-Tom20 to generate an enriched mitochondrial fraction (Mt) and a non-mitochondrial fraction (Non-Mt). The fractions were separated by SDS–PAGE and immunoblotted with anti–Bcl-xL and anti-Tom20. (F) Densitometric quantification of the ratio of non-mitochondrial Bcl-xL vs. mitochondrial Bcl-xL in either Mock- or VPS35- siRNA treatment. Error bars denote SD. *p* values were determined by the Student's one-tailed *t* test. *n* = 3. Used with permission from MBoC (Farmer et al., 2019).

oligomerize (Basanez et al., 2001; J. W. O'Neill, Manion, Maguire, & Hockenbery, 2006), it is possible that Bcl-xL remains in cytoplasmic aggregates as previously observed (Jeong et al., 2004) but further testing would need to be done to confirm this notion. Overall, these experiments support the idea that VPS35 and the retromer must be functional and is at least partially responsible for the translocation of Bcl-xL from the cytoplasm to the MOM and loss of the retromer leads to increased non-mitochondria associated Bcl-xL.

14.4 VPS35-depleted cells display an enhanced rate of apoptosis

Under normal physiological conditions, the pro-apoptotic Bcl-2-family protein Bax is primarily localized to the cytoplasm and there is only a small percentage found on the MOM (Griffiths et al., 1999; Y. T. Hsu et al., 1997; Wolter et al., 1997). A key regulatory role of Bcl-xL is to sequester Bax in the cytoplasm and prevent its translocation to the mitochondrial membrane and/or bind to Bax associated with the MOM and prevent it from forming pores to release cytochrome *c* (Manon, Chaudhuri, & Guerin, 1997; Wolter et al., 1997; Yang et al., 1995). Another pro-apoptotic Bcl-2-family protein, Bad, is responsible for binding to Bcl-xL (Howells, Baumann, Samuels, & Finkielstein, 2011) and allowing Bax to freely translocate to the MOM where Bax can form pores and eventually lead to cell death (Bleicken et al., 2010; Gilmore, Metcalfe, Romer, & Streuli, 2000; Goping et al., 1998). Additionally, because Bcl-xL localized to the MOM has the ability to inhibit the formation of pores by dissociating oligomers or by preventing the insertion of Bax into the membrane (Subburaj et al., 2015; Xu et al., 2013), even a small decrease of Bcl-xL levels on the MOM could have a significant impact on

the regulation and rate of cell death. Based on our previous experiments, we hypothesized that VPS35 depletion decreases the amount of Bcl-xL on the MOM, thus increasing the rate of apoptosis.

To test this, we examined the recruitment of Bax to the MOM (punctate structures that form on the MOM and form pores) in VPS35 depleted cells as compared to mock-treated cells in the presence of the kinase inhibitor and apoptosis inducer (Belmokhtar, Hillion, & Segal-Bendirdjian, 2001), STS (Figure 3.7). In order to perform these experiments, we used CRISPR/Cas9 gene-edited HCT 116 cells that were depleted of endogenous Bax and Bak, but were stably transfected with GFP-tagged Bax (GFP-Bax) (K. L. O'Neill et al., 2016). GFP-Bax cells were treated mock- or VPS35-siRNA and were either given no treatment or treated with STS (Figure 3.7A-B). Efficacy of the siRNA treatment was verified in Figure 3.7C. Additionally, all cells were treated with Z-VAD to prevent the cells from undergoing complete apoptosis and detachment before we could image them. As anticipated, the GFP-Bax in the cells with no STS treatment displayed cytosolic GFP-Bax primarily, suggesting that the cells were not undergoing apoptosis and that Bax was not being recruited to the MOM (Figure 3.7A, left panels). However, upon STS treatment, although both the mock- and VPS35-siRNA treated cells showed recruitment of the GFP-Bax to the MOM from the cytoplasm (indicative of a cell undergoing apoptosis), VPS35 depleted cells showed a significantly higher rate of GFP-Bax recruitment at the 60-min time point as compared to mock cells (Figure. 3.7A, right panels, quantified in B). To further address the rate of apoptosis in the presence or

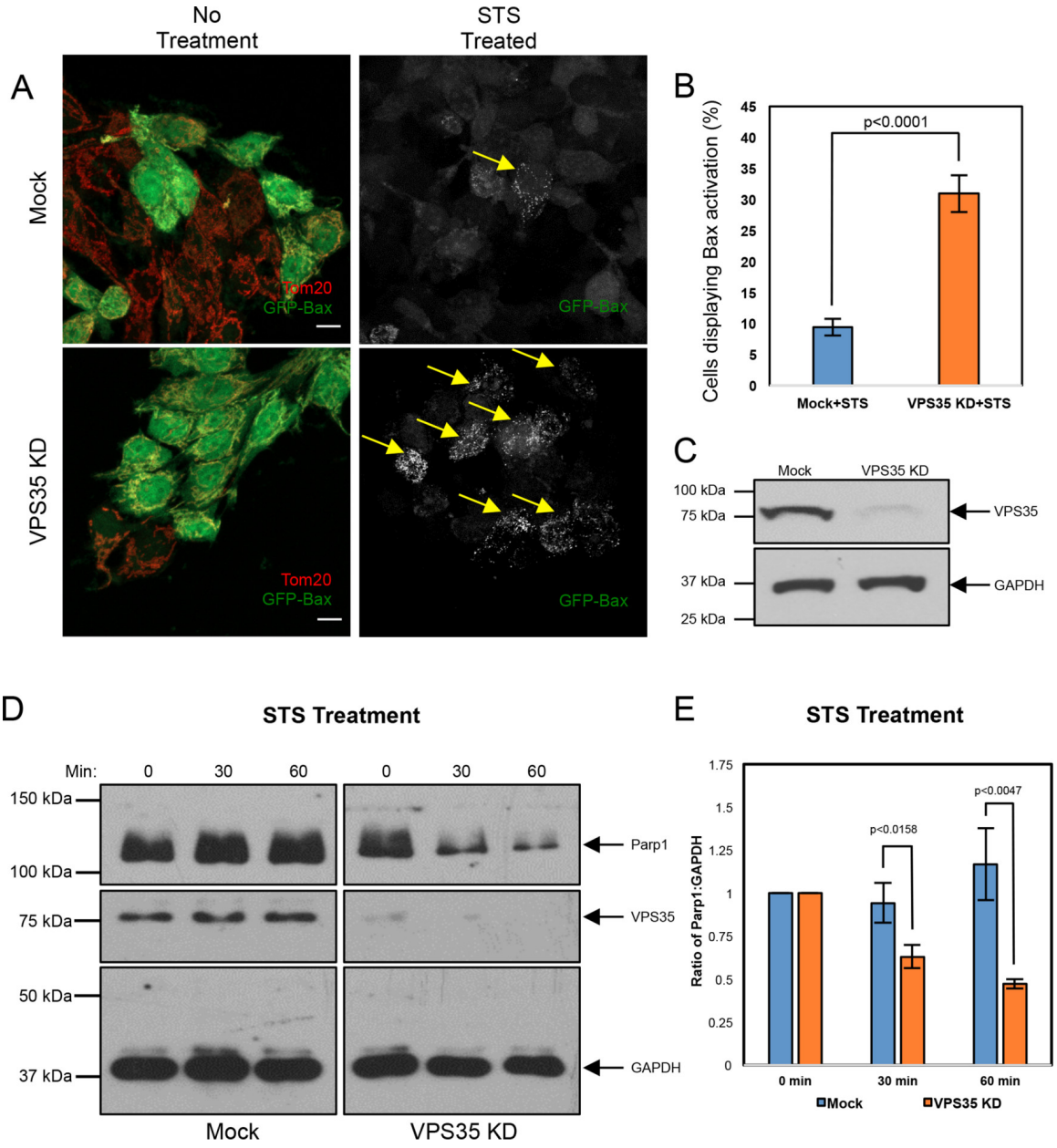
A
No Treatment
STS Treated
Mock
VPS35 KD
Tom20
GFP-Bax
GFP-Bax
B
Cells displaying Bax activation (%)
p<0.0001
Mock+STS
VPS35 KD+STS
C
Mock
VPS35 KD
100 kDa
75 kDa
37 kDa
25 kDa
VPS35
GAPDH
D
STS Treatment
Min: 0 30 60 0 30 60
150 kDa
100 kDa
75 kDa
50 kDa
37 kDa
Parp1
VPS35
GAPDH
Mock
VPS35 KD
E
STS Treatment
Ratio of Parp1:GAPDH
p<0.0158
p<0.0047
0 min
30 min
60 min
Mock
VPS35 KD

Figure 3. 7

The rate of Bax activation at the mitochondrial membrane is enhanced in cells lacking VPS35. (A) CRISPR/Cas9 HCT 116 cells lacking endogenous Bak and Bax, but expressing stably transfected GFP-Bax, were subject to Mock- or VPS35-siRNA knockdown, with or without staurosporine (STS) treatment for 60 min. Cells were fixed and immunostained with anti-Tom20 (red). For micrographs representing the STS treatment, only GFP-Bax is shown. Scale bar = 10 μm. (B) Quantification of the mean percentage of Mock- or VPS35-siRNA–treated cells displaying GFP-Bax activation upon STS treatment. Error bars represent SD. *p* value was determined by the Student's one-tailed *t* test. *n* = 3. (C) Efficacy of the VPS35-siRNA treatment is demonstrated by immunoblotting lysates from Mock- or VPS35-depleted CRISPR/Cas9 HCT 116 cells with anti-VPS35. GAPDH was used as a loading control. (D) CRISPR/Cas9 HCT 116 cells lacking endogenous Bak and Bax, but expressing stably transfected GFP-Bax, were subject to either Mock- or VPS35-siRNA treatment for 48 h, and treated acutely with STS for 0, 30, or 60 min. Lysates from each treatment were analyzed by immunoblotting for Parp1 to assess cleavage over time, and immunoblotting with anti-VPS35 was used to verify the siRNA treatment efficacy. GAPDH was used as a loading control. (E) Densitometric representation of the data from D was done using ImageJ to calculate the ratio of Parp1:GAPDH between Mock- and VPS35-siRNA–treated cells. Data are presented as a mean, and error bars indicate SD. *p* values were determined by the Student's one-tailed *t* test. *n* = 3. Used with permission from MBoC (Farmer et al., 2019).

absence of VPS35, we performed biochemical assays to look at Parp1 cleavage (S. H. Kaufmann, Desnoyers, Ottaviano, Davidson, & Poirier, 1993; Tewari et al., 1995) at three different time points (Figure. 3.7D-E). Based on our previous experiment, as anticipated, we observed a significant increase in the rate of full-length Parp1 over 30-60 min of STS treatment compared to the mock-treated cells induced with STS (Figure. 3.7D-E). We verified the loss of full-length Parp1 by measuring the ratio of Parp1:GAPDH (loading control) and found a significant decrease in the full-length Parp1 in VPS35 depleted cells after 30 and 60 min of STS treatment compared to the mock-treated cells (Figure. 3.7E). These data are consistent with the idea that the retromer is at least partially responsible for translocating Bcl-xL to the MOM from the cytosol, and when VPS35 is depleted, the rate of apoptosis is enhanced due to Bcl-xL not being able to inhibit Bax appropriately.

15. SUMMARY AND CONCLUSIONS

The tight control that Bcl-xL exerts over Bax-driven pore formation at the MOM and apoptosis hints at the significance of regulating its localization. Despite the crucial role of Bcl-xL in preventing apoptosis, although studies have addressed other Bcl-2-family protein recruitment to the MOM (Desagher et al., 1999; Eskes, Desagher, Antonsson, & Martinou, 2000; Wolter et al., 1997) or Bcl-xL insertion into membranes (Adams & Cory, 1998; Y. T. Hsu et al., 1997; T. Kaufmann et al., 2003; Schinzel, Kaufmann, & Borner, 2004), to date few studies have addressed the mechanisms by which Bcl-xL is translocated to the MOM from the cytosol.

In Chapter III, we identified a novel function for the retromer in partially controlling the translocation of Bcl-xL from the cytosol to the MOM where Bcl-xL then can prevent Bax pore formation. We demonstrated that Bcl-xL resides in a complex containing components of the retromer and MICAL-L1 in a Drp1-independent mechanism, along with observing vesicles that contained both Bcl-xL and the retromer or Rab5. Since Bcl-xL interacts and colocalizes with retromer-positive endosomes, it raises the question whether the retromer plays a role in regulating the localization of Bcl-xL in the cell. To answer this, we depleted VPS35 from cells and demonstrated that cytosolic Bcl-xL was increased compared to the mock-treated cells, suggesting that less Bcl-xL was on the MOM to prevent apoptosis. To determine if the change in localization of Bcl-xL impacts its overall ability to prevent apoptosis, we induced apoptosis with STS in the presence or absence of VPS35. These data showed that when VPS35 is depleted, the rate of Bax recruited to the MOM is significantly faster and full-length Parp1 cleavage occurs at a quicker rate, suggesting that VPS35 is at least partially responsible for controlling apoptosis through regulation of Bcl-xL translocation.

In summary, Chapter III describes a model in which disruption of the retromer complex by depleting VPS35 leads to reduced Bcl-xL at the MOM, causing enhanced Bax-mediated pore formation, cytochrome *c* release, and downstream apoptotic events upon STS treatment, and an enhanced rate of apoptosis (Figure. 3.8). Overall, this study highlights a novel role for the retromer, an endosomal protein complex, in the localization of Bcl-xL to the MOM, thus forging a link between endocytic regulation and apoptosis.

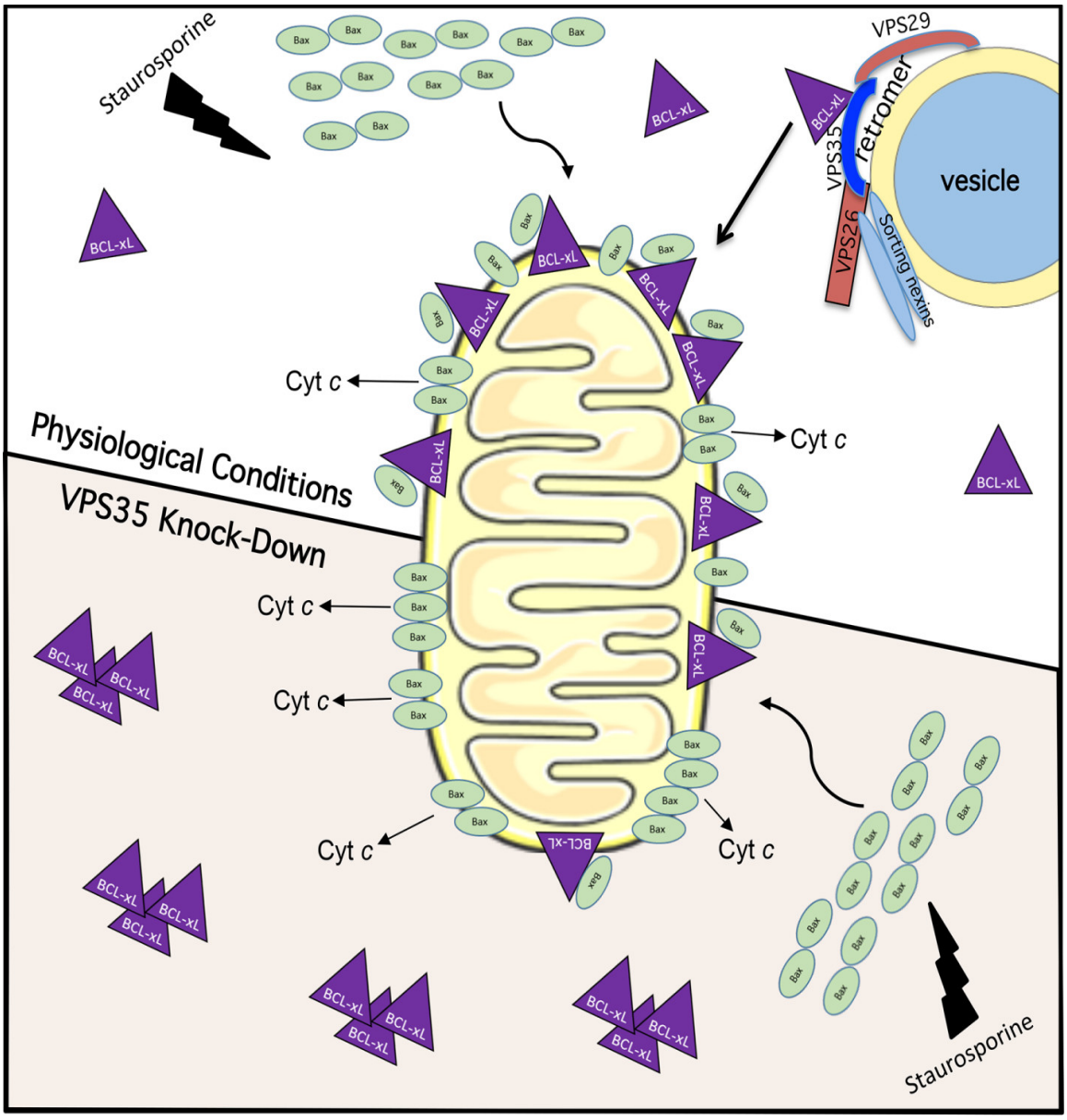
Staurosporine
Bax
BCL-xL
VPS29
retromer
VPS35
vesicle
VPS26
Sorting nexins
Cyt c
Physiological Conditions
VPS35 Knock-Down
Staurosporine

Figure 3. 8

Model for the role of retromer in regulating Bcl-xL's translocation to the mitochondrial membrane and impact on staurosporine-induced apoptosis. Under physiological conditions (top), staurosporine treatment induces Bax translocation to the mitochondrial membrane. Because Bcl-xL is constitutively transported to the MOM, Bax pore formation is inhibited and slowed by Bcl-xL, but when sufficient Bax pore formation occurs, Cyt *c* is released and apoptosis occurs. Upon VPS35 knockdown (bottom), there is impaired retromer complex generation and decreased constitutive transport of Bcl-xL to the MOM. Accordingly, upon staurosporine treatment there is less inhibition of Bax by Bcl-xL, leading to more rapid Bax pore formation and an increased rate of apoptosis. Used with permission from MBoC (Farmer et al., 2019).

Chapter IV

Summary and Future Directions

16. SUMMARY

Overall, my work has uncovered several novel functions for endocytic regulatory proteins in non-classical endocytic pathways and on organelle biogenesis/homeostasis. In my first body of work, we demonstrated that EHD1 and Rabankyrin-5 play a role in mitochondrial homeostasis. Depleting EHD1 or Rabankyrin-5 results in mitochondria that are significantly longer and more interconnected, similar to what is observed upon Drp1- or Dyn2-depletion. Given that EHD1 is an ATPase with functional and structural homology to the Drp1 and Dyn2 GTPases, we hypothesized that EHD1 plays a direct role in mitochondrial fission alongside Drp1 and Dyn2. However, we did not observe significant localization of EHD1 to the mitochondrial membrane, and upon EHD1-depletion, cells nevertheless underwent staurosporine-induced mitochondrial fission (as opposed to Drp1- and Dyn2-depletion). Prior studies had shown that VPS35, an interaction partner of EHD1 and Rabankyrin-5, plays a role in mitochondrial homeostasis through two potential pathways. The first one is by regulating the ubiquitin ligase Mul1. Mul1 interacts with VPS35 which must release Mul1 from this interaction in order to facilitate the trafficking of Mul1 to the mitochondrial membrane, where it ubiquitinates the fusion-promoting protein, Mfn2, and targets it for proteasomal degradation (Tang et al., 2015). If EHD1 and Rabankyrin-5 play a role in this pathway, a difference in Mfn2 protein levels would be expected upon EHD1- or Rabankyrin-5-depletion. However, upon EHD1- or Rabankyrin-5-depletion, Mfn2 protein expression remained unchanged. This suggested that EHD1 and Rabnakyin-5 most likely play an upstream regulatory roles. The second potential mechanism by which VPS35 may

regulate mitochondrial homeostasis is by interacting with and removing inactive Drp1 from the mitochondrial membrane and thus promoting mitochondrial fission by freeing up receptors for active Drp1 (W. Wang et al., 2017). Under this scenario, alterations in VPS35 function, potentially by depleting EHD1 or Rabankyrin-5, would result in impaired fission, resulting in an elongated and static mitochondrial network. Indeed, we demonstrated that upon EHD1-depletion, VPS35 protein levels were significantly reduced. Surprisingly, Rabankyrin-5-depletion did not result in the same reduction of VPS35 protein levels. However, we demonstrated that upon Rabankyrin-5 depletion, VPS35 becomes sequestered in the Golgi region. Regardless, in both cases, VPS35 was no longer capable of removing inactive Drp1 from the mitochondrial membrane, thus resulting in an elongated and static mitochondrial network. Overall, in this study we provide a mechanism by which EHD1 and Rabankyrin-5 play a regulatory role in mitochondrial fission upstream of Drp1 and Dyn2 by controlling VPS35 expression or localization, respectively.

In my second body of work, we found that the retromer plays a critical role in regulating the translocation of Bcl-xL to the mitochondrial membrane where it functions as an inhibitor of apoptosis. Despite the tight control that Bcl-xL exerts over Bax- and Bak-driven pore formation, few studies have previously studied the mechanisms by which it is translocated to the MOM. In this study, we demonstrated for the first time that Bcl-xL physically interacts with VPS35 and retromer subunits in a Drp1-independent manner. Furthermore, the retromer and Bcl-xL colocalize on vesicles that are distinct from the Bcl-xL that colocalizes with mitochondria. Significantly, the loss of

VPS35 via siRNA both reduces the mitochondrial-localized Bcl-xL, and as a result, increases the rate of Bax activation and cleavage of Parp1 upon staurosporine-induced apoptosis. While our studies suggest that only a portion of Bcl-xL is translocated to the MOM by the retromer, given the significance of Bcl-xL in the regulation of apoptosis, this previously uncharacterized pathway for the delivery of Bcl-xL to the MOM may have potentially significant consequences. Our data supports a mechanism in which depletion of the retromer complex subunit VPS35 leads to reduced Bcl-xL at the MOM, causing enhanced Bax-mediated pore formation and Cyt *c* release upon staurosporine treatment, and an enhanced rate of apoptosis. Overall, this study highlights a novel role for the retromer, traditionally known as an endocytic regulatory protein complex, in the localization of Bcl-xL to the MOM, thus generating a link between endocytic regulation and apoptosis.

17. FUTURE DIRECTIONS

17.1 Chapter II future directions

An increasing number of studies have begun to focus on the indirect regulation of mitochondrial homeostasis proteins, adding to the complexity of mitochondrial regulation in normal and disease state cells. Work from Chapter II further solidified the notion that endocytic regulatory proteins play a significant role in regulating mitochondrial fission. Specifically, EHD1 is responsible for stabilizing the protein expression of VPS35 and if EHD1 is depleted, VPS35 protein expression is significantly decreased. Previously, data published form our lab has identified a complex containing

the proteins EHD1, Rabankyrin-5, and the retromer components, VPS35 and VPS26 (Zhang, Reiling, et al., 2012). However, whether the interactions between EHD1 and the retromer are direct or mediated via other proteins, such as Rabankyrin-5, has yet to be determined. Moreover, our data indicates that Rabankyrin-5-depletion has a similar impact on mitochondrial morphology to that of EHD1-depletion, suggesting that both proteins are needed to regulate inactive Drp1 removal from MOM by vesicles containing VPS35 and the retromer (Farmer et al., 2017). We have shown that EHD1 interacts directly with Rabankyrin-5, and we predict that EHD1 interacts indirectly with the retromer, likely mediated by Rabankyrin-5 or potentially another direct EHD1 interaction partner such as MICAL-L1 or Syndapin2. First, to determine if the interaction between EHD1 and the retromer components, VPS26 and VPS35, is direct or indirect, we will use purified GST-EHD1 and HIS-tagged retromer proteins. A GST-pull down assay will be done incubating equimolar concentrations of purified GST-EHD1, with HIS-VPS35 or HIS-VPS26. Immunoblotting of precipitated samples will be done. If, as anticipated, no direct binding is observed, we will first test whether the interaction is mediated by Rabankyrin-5. To accomplish this, Rabankyrin-5-depleted cells will be used to perform pull-downs with GST-EHD1 to determine whether retromer subunits fail to precipitate. If the interaction of the upstream regulators of Drp1 can be elucidated, a better therapeutic approach can be used for controlling various disease states with upregulated Drp1 and therefore mitochondrial fission.

Additionally, it is believed that VPS35-containing mitochondrial-derived vesicles (MDVs) traffic inactive Drp1 from the mitochondrial membrane to the lysosome for

degradation, thus allowing active Drp1 and Dnm2 to catalyze fission. However, how these vesicles undergo fission from the MOM is currently unknown. Therefore, we predict that EHD1 will be needed to generate the MDVs required for Drp1 removal. To test this idea, we will use confocal microscopy to analyze changes in MDVs upon EHD1 KD. Cells will be subjected to either mock- or EHD1-siRNA transfection. We will measure the number of MDVs containing Drp1 and/or VPS35 upon EHD1 KD. Observing significantly fewer MDVs in the absence of EHD1 will provide additional support for the notion that EHD1 is needed for the fission and generation of MDVs to traffic inactive Drp1 away from the mitochondria.

17.2 Chapter III future directions

To continue our work on chapter III, we will work to determine if Bcl-xL interacts directly with the retromer or if the interaction is mediated by other endocytic or apoptotic related proteins. By accomplishing this, we will gain insight into what other proteins are present with the retromer and Bcl-xL that may also be playing a role in the translocation of Bcl-xL to the MOM. For example, we might gain insight into the mechanism required for fission of the budding vesicle containing the retromer and Bcl-xL, potentially by EHD1. In order to test this, we will use purified His-VPS35 or His-VPS26 and GST-Bcl-xL to perform pull-down experiments. In the event that this experiment does not work, we will examine other potential candidates that might be mediating the interaction between the retromer and Bcl-xL.

Furthermore, we will perform live-cell imaging to track the dynamics of the vesicles containing the retromer and Bcl-xL upon various treatments and conditions to see what impact they may have on the rate of Bax activation and apoptosis. In tandem with microscopic dynamic studies, single molecule imaging techniques, such as direct Stochastic Optical Reconstruction Microscopy (dSTORM) and/or electron microscopy will be used to perform a detailed analysis of the structure of the vesicles containing Bcl-xL and retromer to gain further insight into the morphology and mechanism behind apoptosis regulation by endocytic proteins.

REFERENCES

Adams, J. M., & Cory, S. (1998). The Bcl-2 protein family: arbiters of cell survival. *Science, 281*(5381), 1322-1326. Retrieved from https://www.ncbi.nlm.nih.gov/pubmed/9735050

Aderem, A., & Underhill, D. M. (1999). Mechanisms of phagocytosis in macrophages. *Annu Rev Immunol, 17*, 593-623. doi:10.1146/annurev.immunol.17.1.593

Ago, T., Kuroda, J., Pain, J., Fu, C., Li, H., & Sadoshima, J. (2010). Upregulation of Nox4 by hypertrophic stimuli promotes apoptosis and mitochondrial dysfunction in cardiac myocytes. *Circ Res, 106*(7), 1253-1264. doi:10.1161/CIRCRESAHA.109.213116

Alexander, C., Votruba, M., Pesch, U. E., Thiselton, D. L., Mayer, S., Moore, A., . . . Wissinger, B. (2000). OPA1, encoding a dynamin-related GTPase, is mutated in autosomal dominant optic atrophy linked to chromosome 3q28. *Nat Genet, 26*(2), 211-215. doi:10.1038/79944

Allaire, P. D., Marat, A. L., Dall'Armi, C., Di Paolo, G., McPherson, P. S., & Ritter, B. (2010). The Connecdenn DENN domain: a GEF for Rab35 mediating cargo-specific exit from early endosomes. *Mol Cell, 37*(3), 370-382. doi:10.1016/j.molcel.2009.12.037

Anderson, R. G. (1998). The caveolae membrane system. *Annu Rev Biochem, 67*, 199-225. doi:10.1146/annurev.biochem.67.1.199

Arighi, C. N., Hartnell, L. M., Aguilar, R. C., Haft, C. R., & Bonifacino, J. S. (2004). Role of the mammalian retromer in sorting of the cation-independent mannose 6-phosphate receptor. *J Cell Biol, 165*(1), 123-133. doi:10.1083/jcb.200312055

Babbey, C. M., Ahktar, N., Wang, E., Chen, C. C., Grant, B. D., & Dunn, K. W. (2006). Rab10 regulates membrane transport through early endosomes of polarized Madin-Darby canine kidney cells. *Mol Biol Cell, 17*(7), 3156-3175. doi:10.1091/mbc.e05-08-0799

Babst, M., Katzmann, D. J., Estepa-Sabal, E. J., Meerloo, T., & Emr, S. D. (2002). Escrt-III: an endosome-associated heterooligomeric protein complex required for mvb sorting. *Dev Cell, 3*(2), 271-282. doi:10.1016/s1534-5807(02)00220-4

Babst, M., Katzmann, D. J., Snyder, W. B., Wendland, B., & Emr, S. D. (2002). Endosome-associated complex, ESCRT-II, recruits transport machinery for protein sorting at the multivesicular body. *Dev Cell, 3*(2), 283-289. doi:10.1016/s1534-5807(02)00219-8

Bahl, K., Naslavsky, N., & Caplan, S. (2015). Role of the EHD2 unstructured loop in dimerization, protein binding and subcellular localization. *PLoS One, 10*(4), e0123710. doi:10.1371/journal.pone.0123710

Bahl, K., Xie, S., Spagnol, G., Sorgen, P., Naslavsky, N., & Caplan, S. (2016). EHD3 Protein Is Required for Tubular Recycling Endosome Stabilization, and an Asparagine-Glutamic Acid Residue Pair within Its Eps15 Homology (EH) Domain Dictates Its Selective Binding to NPF Peptides. *J Biol Chem, 291*(26), 13465-13478. doi:10.1074/jbc.M116.716407

Barbieri, M. A., Roberts, R. L., Mukhopadhyay, A., & Stahl, P. D. (1996). Rab5 regulates the dynamics of early endosome fusion. *Biocell, 20*(3), 331-338. Retrieved from https://www.ncbi.nlm.nih.gov/pubmed/9031602

Barcia, C., Ros, C. M., Annese, V., Gomez, A., Ros-Bernal, F., Aguado-Yera, D., . . . Herrero, M. T. (2011). IFN-gamma signaling, with the synergistic contribution of TNF-alpha, mediates cell specific microglial and astroglial activation in experimental models of Parkinson's disease. *Cell Death Dis, 2*, e142. doi:10.1038/cddis.2011.17

Basanez, G., Zhang, J., Chau, B. N., Maksaev, G. I., Frolov, V. A., Brandt, T. A., . . . Zimmerberg, J. (2001). Pro-apoptotic cleavage products of Bcl-xL form cytochrome c-conducting pores in pure lipid membranes. *J Biol Chem, 276*(33), 31083-31091. doi:10.1074/jbc.M103879200

Basquin, C., Malarde, V., Mellor, P., Anderson, D. H., Meas-Yedid, V., Olivo-Marin, J. C., . . . Sauvonnet, N. (2013). The signalling factor PI3K is a specific regulator of the clathrin-independent dynamin-dependent endocytosis of IL-2 receptors. *J Cell Sci, 126*(Pt 5), 1099-1108. doi:10.1242/jcs.110932

Basquin, C., & Sauvonnet, N. (2013). Phosphoinositide 3-kinase at the crossroad between endocytosis and signaling of cytokine receptors. *Commun Integr Biol, 6*(4), e24243. doi:10.4161/cib.24243

Belmokhtar, C. A., Hillion, J., & Segal-Bendirdjian, E. (2001). Staurosporine induces apoptosis through both caspase-dependent and caspase-independent mechanisms. *Oncogene, 20*(26), 3354-3362. doi:10.1038/sj.onc.1204436

Benard, G., Bellance, N., James, D., Parrone, P., Fernandez, H., Letellier, T., & Rossignol, R. (2007). Mitochondrial bioenergetics and structural network organization. *J Cell Sci, 120*(Pt 5), 838-848. doi:10.1242/jcs.03381

Benard, G., Faustin, B., Passerieux, E., Galinier, A., Rocher, C., Bellance, N., . . . Rossignol, R. (2006). Physiological diversity of mitochondrial oxidative phosphorylation. *Am J Physiol Cell Physiol, 291*(6), C1172-1182. doi:10.1152/ajpcell.00195.2006

Benjamin, S., Weidberg, H., Rapaport, D., Pekar, O., Nudelman, M., Segal, D., . . . Horowitz, M. (2011). EHD2 mediates trafficking from the plasma membrane by modulating Rac1 activity. *Biochem J, 439*(3), 433-442. doi:10.1042/BJ20111010

Bennett, M. K. (1995). SNAREs and the specificity of transport vesicle targeting. *Curr Opin Cell Biol, 7*(4), 581-586. doi:10.1016/0955-0674(95)80016-6

Berry, C., La Vecchia, C., & Nicotera, P. (2010). Paraquat and Parkinson's disease. *Cell Death Differ, 17*(7), 1115-1125. doi:10.1038/cdd.2009.217

Bleazard, W., McCaffery, J. M., King, E. J., Bale, S., Mozdy, A., Tieu, Q., . . . Shaw, J. M. (1999). The dynamin-related GTPase Dnm1 regulates mitochondrial fission in yeast. *Nat Cell Biol, 1*(5), 298-304. doi:10.1038/13014

Bleicken, S., Classen, M., Padmavathi, P. V., Ishikawa, T., Zeth, K., Steinhoff, H. J., & Bordignon, E. (2010). Molecular details of Bax activation, oligomerization, and membrane insertion. *J Biol Chem, 285*(9), 6636-6647. doi:10.1074/jbc.M109.081539

Bonifacino, J. S., & Hurley, J. H. (2008). Retromer. *Curr Opin Cell Biol, 20*(4), 427-436. doi:10.1016/j.ceb.2008.03.009

Bonifacino, J. S., & Rojas, R. (2006). Retrograde transport from endosomes to the trans-Golgi network. *Nat Rev Mol Cell Biol, 7*(8), 568-579. doi:10.1038/nrm1985

Bonifacino, J. S., & Traub, L. M. (2003). Signals for sorting of transmembrane proteins to endosomes and lysosomes. *Annu Rev Biochem, 72*, 395-447. doi:10.1146/annurev.biochem.72.121801.161800

Braell, W. A., Schlossman, D. M., Schmid, S. L., & Rothman, J. E. (1984). Dissociation of clathrin coats coupled to the hydrolysis of ATP: role of an uncoating ATPase. *J Cell Biol, 99*(2), 734-741. doi:10.1083/jcb.99.2.734

Brandhorst, D., Zwilling, D., Rizzoli, S. O., Lippert, U., Lang, T., & Jahn, R. (2006). Homotypic fusion of early endosomes: SNAREs do not determine fusion specificity. *Proc Natl Acad Sci U S A, 103*(8), 2701-2706. doi:10.1073/pnas.0511138103

Braschi, E., Goyon, V., Zunino, R., Mohanty, A., Xu, L., & McBride, H. M. (2010). Vps35 mediates vesicle transport between the mitochondria and peroxisomes. *Curr Biol, 20*(14), 1310-1315. doi:10.1016/j.cub.2010.05.066

Braun, A., Pinyol, R., Dahlhaus, R., Koch, D., Fonarev, P., Grant, B. D., . . . Qualmann, B. (2005). EHD proteins associate with syndapin I and II and such interactions play a crucial role in endosomal recycling. *Mol Biol Cell, 16*(8), 3642-3658. doi:10.1091/mbc.e05-01-0076

Brown, S. E., Campbell, R. D., & Sanderson, C. M. (2001). Novel NG36/G9a gene products encoded within the human and mouse MHC class III regions. *Mamm Genome, 12*(12), 916-924. doi:10.1007/s00335-001-3029-3

Bucci, C., Parton, R. G., Mather, I. H., Stunnenberg, H., Simons, K., Hoflack, B., & Zerial, M. (1992). The small GTPase rab5 functions as a regulatory factor in the early endocytic pathway. *Cell, 70*(5), 715-728. doi:10.1016/0092-8674(92)90306-w

Cadete, V. J., Deschenes, S., Cuillerier, A., Brisebois, F., Sugiura, A., Vincent, A., . . . Burelle, Y. (2016). Formation of mitochondrial-derived vesicles is an active and physiologically relevant mitochondrial quality control process in the cardiac system. *J Physiol, 594*(18), 5343-5362. doi:10.1113/JP272703

Cai, B., Caplan, S., & Naslavsky, N. (2012). cPLA2alpha and EHD1 interact and regulate the vesiculation of cholesterol-rich, GPI-anchored, protein-containing endosomes. *Mol Biol Cell, 23*(10), 1874-1888. doi:10.1091/mbc.E11-10-0881

Cai, B., Giridharan, S. S., Zhang, J., Saxena, S., Bahl, K., Schmidt, J. A., . . . Caplan, S. (2013). Differential roles of C-terminal Eps15 homology domain proteins as vesiculators and tubulators of recycling endosomes. *J Biol Chem, 288*(42), 30172-30180. doi:10.1074/jbc.M113.488627

Cai, B., Xie, S., Caplan, S., & Naslavsky, N. (2014). GRAF1 forms a complex with MICAL-L1 and EHD1 to cooperate in tubular recycling endosome vesiculation. *Front Cell Dev Biol, 2*, 22. doi:10.3389/fcell.2014.00022

Cantalupo, G., Alifano, P., Roberti, V., Bruni, C. B., & Bucci, C. (2001). Rab-interacting lysosomal protein (RILP): the Rab7 effector required for transport to lysosomes. *EMBO J, 20*(4), 683-693. doi:10.1093/emboj/20.4.683

Capaldi, R. A., Murray, J., Byrne, L., Janes, M. S., & Marusich, M. F. (2004). Immunological approaches to the characterization and diagnosis of

mitochondrial disease. *Mitochondrion, 4*(5-6), 417-426. doi:10.1016/j.mito.2004.07.006

Caplan, S., Hartnell, L. M., Aguilar, R. C., Naslavsky, N., & Bonifacino, J. S. (2001). Human Vam6p promotes lysosome clustering and fusion in vivo. *J Cell Biol, 154*(1), 109-122. doi:10.1083/jcb.200102142

Caplan, S., Naslavsky, N., Hartnell, L. M., Lodge, R., Polishchuk, R. S., Donaldson, J. G., & Bonifacino, J. S. (2002). A tubular EHD1-containing compartment involved in the recycling of major histocompatibility complex class I molecules to the plasma membrane. *EMBO J, 21*(11), 2557-2567. doi:10.1093/emboj/21.11.2557

Castellani, R., Hirai, K., Aliev, G., Drew, K. L., Nunomura, A., Takeda, A., . . . Smith, M. A. (2002). Role of mitochondrial dysfunction in Alzheimer's disease. *J Neurosci Res, 70*(3), 357-360. doi:10.1002/jnr.10389

Caswell, P., & Norman, J. (2008). Endocytic transport of integrins during cell migration and invasion. *Trends Cell Biol, 18*(6), 257-263. doi:10.1016/j.tcb.2008.03.004

Cendrowski, J., Maminska, A., & Miaczynska, M. (2016). Endocytic regulation of cytokine receptor signaling. *Cytokine Growth Factor Rev, 32*, 63-73. doi:10.1016/j.cytogfr.2016.07.002

Chan, D. C. (2012). Fusion and fission: interlinked processes critical for mitochondrial health. *Annu Rev Genet, 46*, 265-287. doi:10.1146/annurev-genet-110410-132529

Chandhok, G., Lazarou, M., & Neumann, B. (2017). Structure, function, and regulation of mitofusin-2 in health and disease. *Biol Rev Camb Philos Soc*. doi:10.1111/brv.12378

Chaudhuri, R., Lindwasser, O. W., Smith, W. J., Hurley, J. H., & Bonifacino, J. S. (2007). Downregulation of CD4 by human immunodeficiency virus type 1 Nef is dependent on clathrin and involves direct interaction of Nef with the AP2 clathrin adaptor. *J Virol, 81*(8), 3877-3890. doi:10.1128/JVI.02725-06

Chen, H., & Chan, D. C. (2005). Emerging functions of mammalian mitochondrial fusion and fission. *Hum Mol Genet, 14 Spec No. 2*, R283-289. doi:10.1093/hmg/ddi270

Chen, H., & Chan, D. C. (2009). Mitochondrial dynamics--fusion, fission, movement, and mitophagy--in neurodegenerative diseases. *Hum Mol Genet, 18*(R2), R169-176. doi:10.1093/hmg/ddp326

Chen, H., Chomyn, A., & Chan, D. C. (2005). Disruption of fusion results in mitochondrial heterogeneity and dysfunction. *J Biol Chem, 280*(28), 26185-26192. doi:10.1074/jbc.M503062200

Chen, H., Detmer, S. A., Ewald, A. J., Griffin, E. E., Fraser, S. E., & Chan, D. C. (2003). Mitofusins Mfn1 and Mfn2 coordinately regulate mitochondrial fusion and are essential for embryonic development. *J Cell Biol, 160*(2), 189-200. doi:10.1083/jcb.200211046

Chen, K. H., Guo, X., Ma, D., Guo, Y., Li, Q., Yang, D., . . . Tang, J. (2004). Dysregulation of HSG triggers vascular proliferative disorders. *Nat Cell Biol, 6*(9), 872-883. doi:10.1038/ncb1161

Chen, Y. A., & Scheller, R. H. (2001). SNARE-mediated membrane fusion. *Nat Rev Mol Cell Biol, 2*(2), 98-106. doi:10.1038/35052017

Cheng, Z. J., Singh, R. D., Marks, D. L., & Pagano, R. E. (2006). Membrane microdomains, caveolae, and caveolar endocytosis of sphingolipids. *Mol Membr Biol, 23*(1), 101-110. doi:10.1080/09687860500460041

Chi, X., Kale, J., Leber, B., & Andrews, D. W. (2014). Regulating cell death at, on, and in membranes. *Biochim Biophys Acta, 1843*(9), 2100-2113. doi:10.1016/j.bbamcr.2014.06.002

Cho, D. H., Nakamura, T., Fang, J., Cieplak, P., Godzik, A., Gu, Z., & Lipton, S. A. (2009). S-nitrosylation of Drp1 mediates beta-amyloid-related mitochondrial fission and neuronal injury. *Science, 324*(5923), 102-105. doi:10.1126/science.1171091

Choi, S., Chen, Z., Tang, L. H., Fang, Y., Shin, S. J., Panarelli, N. C., . . . Du, Y. C. (2016). Bcl-xL promotes metastasis independent of its anti-apoptotic activity. *Nat Commun, 7*, 10384. doi:10.1038/ncomms10384

Christoforidis, S., Miaczynska, M., Ashman, K., Wilm, M., Zhao, L., Yip, S. C., . . . Zerial, M. (1999). Phosphatidylinositol-3-OH kinases are Rab5 effectors. *Nat Cell Biol, 1*(4), 249-252. doi:10.1038/12075

Chung, H. J., Qian, X., Ehlers, M., Jan, Y. N., & Jan, L. Y. (2009). Neuronal activity regulates phosphorylation-dependent surface delivery of G protein-activated inwardly rectifying potassium channels. *Proc Natl Acad Sci U S A, 106*(2), 629-634. doi:10.1073/pnas.0811615106

Cipolat, S., Martins de Brito, O., Dal Zilio, B., & Scorrano, L. (2004). OPA1 requires mitofusin 1 to promote mitochondrial fusion. *Proc Natl Acad Sci U S A, 101*(45), 15927-15932. doi:10.1073/pnas.0407043101

Conner, S. D., & Schmid, S. L. (2003). Regulated portals of entry into the cell. *Nature, 422*(6927), 37-44. doi:10.1038/nature01451

Crews, L., Patrick, C., Adame, A., Rockenstein, E., & Masliah, E. (2011). Modulation of aberrant CDK5 signaling rescues impaired neurogenesis in models of Alzheimer's disease. *Cell Death Dis, 2*, e120. doi:10.1038/cddis.2011.2

Czabotar, P. E., Lessene, G., Strasser, A., & Adams, J. M. (2014). Control of apoptosis by the BCL-2 protein family: implications for physiology and therapy. *Nat Rev Mol Cell Biol, 15*(1), 49-63. doi:10.1038/nrm3722

Czabotar, P. E., Westphal, D., Dewson, G., Ma, S., Hockings, C., Fairlie, W. D., . . . Colman, P. M. (2013). Bax crystal structures reveal how BH3 domains activate Bax and nucleate its oligomerization to induce apoptosis. *Cell, 152*(3), 519-531. doi:10.1016/j.cell.2012.12.031

Czech, M. P. (2003). Dynamics of phosphoinositides in membrane retrieval and insertion. *Annu Rev Physiol, 65*, 791-815. doi:10.1146/annurev.physiol.65.092101.142522

D'Souza-Schorey, C., & Chavrier, P. (2006). ARF proteins: roles in membrane traffic and beyond. *Nat Rev Mol Cell Biol, 7*(5), 347-358. doi:10.1038/nrm1910

Danial, N. N., & Korsmeyer, S. J. (2004). Cell death: critical control points. *Cell, 116*(2), 205-219. doi:10.1016/s0092-8674(04)00046-7

Daumke, O., Lundmark, R., Vallis, Y., Martens, S., Butler, P. J., & McMahon, H. T. (2007). Architectural and mechanistic insights into an EHD ATPase involved in membrane remodelling. *Nature, 449*(7164), 923-927. doi:10.1038/nature06173

de Brito, O. M., & Scorrano, L. (2008). Mitofusin 2 tethers endoplasmic reticulum to mitochondria. *Nature, 456*(7222), 605-610. doi:10.1038/nature07534

de Brito, O. M., & Scorrano, L. (2010). An intimate liaison: spatial organization of the endoplasmic reticulum-mitochondria relationship. *EMBO J, 29*(16), 2715-2723. doi:10.1038/emboj.2010.177

Delettre, C., Lenaers, G., Griffoin, J. M., Gigarel, N., Lorenzo, C., Belenguer, P., . . . Hamel, C. P. (2000). Nuclear gene OPA1, encoding a mitochondrial dynamin-related protein, is mutated in dominant optic atrophy. *Nat Genet, 26*(2), 207-210. doi:10.1038/79936

Deo, R., Kushwah, M. S., Kamerkar, S. C., Kadam, N. Y., Dar, S., Babu, K., . . . Pucadyil, T. J. (2018). ATP-dependent membrane remodeling links EHD1 functions to endocytic recycling. *Nat Commun, 9*(1), 5187. doi:10.1038/s41467-018-07586-z

Desagher, S., Osen-Sand, A., Nichols, A., Eskes, R., Montessuit, S., Lauper, S., . . . Martinou, J. C. (1999). Bid-induced conformational change of Bax is responsible for mitochondrial cytochrome c release during apoptosis. *J Cell Biol, 144*(5), 891-901. Retrieved from https://www.ncbi.nlm.nih.gov/pubmed/10085289

Doherty, G. J., & McMahon, H. T. (2009). Mechanisms of endocytosis. *Annu Rev Biochem, 78*, 857-902. doi:10.1146/annurev.biochem.78.081307.110540

Doherty, K. R., Demonbreun, A. R., Wallace, G. Q., Cave, A., Posey, A. D., Heretis, K., . . . McNally, E. M. (2008). The endocytic recycling protein EHD2 interacts with myoferlin to regulate myoblast fusion. *J Biol Chem, 283*(29), 20252-20260. doi:10.1074/jbc.M802306200

Donaldson, J. G., & Jackson, C. L. (2000). Regulators and effectors of the ARF GTPases. *Curr Opin Cell Biol, 12*(4), 475-482. doi:10.1016/s0955-0674(00)00119-8

Doray, B., Lee, I., Knisely, J., Bu, G., & Kornfeld, S. (2007). The gamma/sigma1 and alpha/sigma2 hemicomplexes of clathrin adaptors AP-1 and AP-2 harbor the dileucine recognition site. *Mol Biol Cell, 18*(5), 1887-1896. doi:10.1091/mbc.e07-01-0012

Duchen, M. R. (2000). Mitochondria and calcium: from cell signalling to cell death. *J Physiol, 529 Pt 1*, 57-68. Retrieved from https://www.ncbi.nlm.nih.gov/pubmed/11080251

Eaton, S. (2008). Retromer retrieves wntless. *Dev Cell, 14*(1), 4-6. doi:10.1016/j.devcel.2007.12.014

Elmore, S. (2007). Apoptosis: a review of programmed cell death. *Toxicol Pathol, 35*(4), 495-516. doi:10.1080/01926230701320337

Eskes, R., Desagher, S., Antonsson, B., & Martinou, J. C. (2000). Bid induces the oligomerization and insertion of Bax into the outer mitochondrial membrane. *Mol Cell Biol, 20*(3), 929-935. Retrieved from https://www.ncbi.nlm.nih.gov/pubmed/10629050

Etoh, K., & Fukuda, M. (2019). Rab10 regulates tubular endosome formation through KIF13A and KIF13B motors. *J Cell Sci, 132*(5). doi:10.1242/jcs.226977

Fadeel, B., & Orrenius, S. (2005). Apoptosis: a basic biological phenomenon with wide-ranging implications in human disease. *J Intern Med, 258*(6), 479-517. doi:10.1111/j.1365-2796.2005.01570.x

Farmer, T., Naslavsky, N., & Caplan, S. (2018). Tying trafficking to fusion and fission at the mighty mitochondria. *Traffic, 19*(8), 569-577. doi:10.1111/tra.12573

Farmer, T., O'Neill, K. L., Naslavsky, N., Luo, X., & Caplan, S. (2019). Retromer facilitates the localization of Bcl-xL to the mitochondrial outer membrane. *Mol Biol Cell, 30*(10), 1138-1146. doi:10.1091/mbc.E19-01-0044

Farmer, T., Reinecke, J. B., Xie, S., Bahl, K., Naslavsky, N., & Caplan, S. (2017). Control of mitochondrial homeostasis by endocytic regulatory proteins. *J Cell Sci*. doi:10.1242/jcs.204537

Farrow, S. N., & Brown, R. (1996). New members of the Bcl-2 family and their protein partners. *Curr Opin Genet Dev, 6*(1), 45-49. Retrieved from https://www.ncbi.nlm.nih.gov/pubmed/8791486

Fasshauer, D. (2003). Structural insights into the SNARE mechanism. *Biochim Biophys Acta, 1641*(2-3), 87-97. doi:10.1016/s0167-4889(03)00090-9

Ferguson, S. M., & De Camilli, P. (2012). Dynamin, a membrane-remodelling GTPase. *Nat Rev Mol Cell Biol, 13*(2), 75-88. doi:10.1038/nrm3266

Flippo, K. H., & Strack, S. (2017). Mitochondrial dynamics in neuronal injury, development and plasticity. *J Cell Sci, 130*(4), 671-681. doi:10.1242/jcs.171017

Follett, J., Bugarcic, A., Collins, B. M., & Teasdale, R. D. (2017). Retromer's Role in Endosomal Trafficking and Impaired Function in Neurodegenerative Diseases. *Curr Protein Pept Sci, 18*(7), 687-701. doi:10.2174/1389203717666160311121246

Follett, J., Norwood, S. J., Hamilton, N. A., Mohan, M., Kovtun, O., Tay, S., . . . Teasdale, R. D. (2014). The Vps35 D620N mutation linked to Parkinson's disease disrupts

the cargo sorting function of retromer. *Traffic, 15*(2), 230-244. doi:10.1111/tra.12136

Friedman, J. R., Lackner, L. L., West, M., DiBenedetto, J. R., Nunnari, J., & Voeltz, G. K. (2011). ER tubules mark sites of mitochondrial division. *Science, 334*(6054), 358-362. doi:10.1126/science.1207385

Friedman, J. R., Webster, B. M., Mastronarde, D. N., Verhey, K. J., & Voeltz, G. K. (2010). ER sliding dynamics and ER-mitochondrial contacts occur on acetylated microtubules. *J Cell Biol, 190*(3), 363-375. doi:10.1083/jcb.200911024

Frohlich, C., Grabiger, S., Schwefel, D., Faelber, K., Rosenbaum, E., Mears, J., . . . Daumke, O. (2013). Structural insights into oligomerization and mitochondrial remodelling of dynamin 1-like protein. *EMBO J, 32*(9), 1280-1292. doi:10.1038/emboj.2013.74

Fuchs, Y., & Steller, H. (2015). Live to die another way: modes of programmed cell death and the signals emanating from dying cells. *Nat Rev Mol Cell Biol, 16*(6), 329-344. doi:10.1038/nrm3999

Galperin, E., Benjamin, S., Rapaport, D., Rotem-Yehudar, R., Tolchinsky, S., & Horowitz, M. (2002). EHD3: a protein that resides in recycling tubular and vesicular membrane structures and interacts with EHD1. *Traffic, 3*(8), 575-589. doi:10.1034/j.1600-0854.2002.30807.x

Gao, Y., Balut, C. M., Bailey, M. A., Patino-Lopez, G., Shaw, S., & Devor, D. C. (2010). Recycling of the Ca2+-activated K+ channel, KCa2.3, is dependent upon RME-1,

Rab35/EPI64C, and an N-terminal domain. *J Biol Chem, 285*(23), 17938-17953. doi:10.1074/jbc.M109.086553

George, M., Ying, G., Rainey, M. A., Solomon, A., Parikh, P. T., Gao, Q., . . . Band, H. (2007). Shared as well as distinct roles of EHD proteins revealed by biochemical and functional comparisons in mammalian cells and C. elegans. *BMC Cell Biol, 8*, 3. doi:10.1186/1471-2121-8-3

George, N. M., Targy, N., Evans, J. J., Zhang, L., & Luo, X. (2010). Bax contains two functional mitochondrial targeting sequences and translocates to mitochondria in a conformational change- and homo-oligomerization-driven process. *J Biol Chem, 285*(2), 1384-1392. doi:10.1074/jbc.M109.049924

Gesbert, F., Sauvonnet, N., & Dautry-Varsat, A. (2004). Clathrin-lndependent endocytosis and signalling of interleukin 2 receptors IL-2R endocytosis and signalling. *Curr Top Microbiol Immunol, 286*, 119-148. Retrieved from https://www.ncbi.nlm.nih.gov/pubmed/15645712

Gillooly, D. J., Morrow, I. C., Lindsay, M., Gould, R., Bryant, N. J., Gaullier, J. M., . . . Stenmark, H. (2000). Localization of phosphatidylinositol 3-phosphate in yeast and mammalian cells. *EMBO J, 19*(17), 4577-4588. doi:10.1093/emboj/19.17.4577

Gilmore, A. P., Metcalfe, A. D., Romer, L. H., & Streuli, C. H. (2000). Integrin-mediated survival signals regulate the apoptotic function of Bax through its conformation and subcellular localization. *J Cell Biol, 149*(2), 431-446. Retrieved from https://www.ncbi.nlm.nih.gov/pubmed/10769034

Giridharan, S. S., Cai, B., Naslavsky, N., & Caplan, S. (2012). Trafficking cascades mediated by Rab35 and its membrane hub effector, MICAL-L1. *Commun Integr Biol, 5*(4), 384-387. doi:10.4161/cib.20064

Giridharan, S. S., Cai, B., Vitale, N., Naslavsky, N., & Caplan, S. (2013). Cooperation of MICAL-L1, syndapin2, and phosphatidic acid in tubular recycling endosome biogenesis. *Mol Biol Cell, 24*(11), 1776-1790, S1771-1715. doi:10.1091/mbc.E13-01-0026

Gokool, S., Tattersall, D., & Seaman, M. N. (2007). EHD1 interacts with retromer to stabilize SNX1 tubules and facilitate endosome-to-Golgi retrieval. *Traffic, 8*(12), 1873-1886. doi:10.1111/j.1600-0854.2007.00652.x

Gonzalez-Jamett, A. M., Momboisse, F., Haro-Acuna, V., Bevilacqua, J. A., Caviedes, P., & Cardenas, A. M. (2013). Dynamin-2 function and dysfunction along the secretory pathway. *Front Endocrinol (Lausanne), 4*, 126. doi:10.3389/fendo.2013.00126

Goping, I. S., Gross, A., Lavoie, J. N., Nguyen, M., Jemmerson, R., Roth, K., . . . Shore, G. C. (1998). Regulated targeting of BAX to mitochondria. *J Cell Biol, 143*(1), 207-215. Retrieved from https://www.ncbi.nlm.nih.gov/pubmed/9763432

Gorvel, J. P., Chavrier, P., Zerial, M., & Gruenberg, J. (1991). rab5 controls early endosome fusion in vitro. *Cell, 64*(5), 915-925. doi:10.1016/0092-8674(91)90316-q

Grant, B., Zhang, Y., Paupard, M. C., Lin, S. X., Hall, D. H., & Hirsh, D. (2001). Evidence that RME-1, a conserved C. elegans EH-domain protein, functions in endocytic recycling. *Nat Cell Biol, 3*(6), 573-579. doi:10.1038/35078549

Grant, B. D., & Caplan, S. (2008). Mechanisms of EHD/RME-1 protein function in endocytic transport. *Traffic, 9*(12), 2043-2052. doi:10.1111/j.1600-0854.2008.00834.x

Grant, B. D., & Donaldson, J. G. (2009). Pathways and mechanisms of endocytic recycling. *Nat Rev Mol Cell Biol, 10*(9), 597-608. doi:10.1038/nrm2755

Grassart, A., Dujeancourt, A., Lazarow, P. B., Dautry-Varsat, A., & Sauvonnet, N. (2008). Clathrin-independent endocytosis used by the IL-2 receptor is regulated by Rac1, Pak1 and Pak2. *EMBO Rep, 9*(4), 356-362. doi:10.1038/embor.2008.28

Griffiths, G. J., Dubrez, L., Morgan, C. P., Jones, N. A., Whitehouse, J., Corfe, B. M., . . . Hickman, J. A. (1999). Cell damage-induced conformational changes of the pro-apoptotic protein Bak in vivo precede the onset of apoptosis. *J Cell Biol, 144*(5), 903-914. Retrieved from https://www.ncbi.nlm.nih.gov/pubmed/10085290

Griparic, L., van der Wel, N. N., Orozco, I. J., Peters, P. J., & van der Bliek, A. M. (2004). Loss of the intermembrane space protein Mgm1/OPA1 induces swelling and localized constrictions along the lengths of mitochondria. *J Biol Chem, 279*(18), 18792-18798. doi:10.1074/jbc.M400920200

Grosshans, B. L., Ortiz, D., & Novick, P. (2006). Rabs and their effectors: achieving specificity in membrane traffic. *Proc Natl Acad Sci U S A, 103*(32), 11821-11827. doi:10.1073/pnas.0601617103

Guilherme, A., Soriano, N. A., Furcinitti, P. S., & Czech, M. P. (2004). Role of EHD1 and EHBP1 in perinuclear sorting and insulin-regulated GLUT4 recycling in 3T3-L1 adipocytes. *J Biol Chem, 279*(38), 40062-40075. doi:10.1074/jbc.M401918200

Hackenbrock, C. R. (1966). Ultrastructural bases for metabolically linked mechanical activity in mitochondria. I. Reversible ultrastructural changes with change in metabolic steady state in isolated liver mitochondria. *J Cell Biol, 30*(2), 269-297. doi:10.1083/jcb.30.2.269

Haglund, K., Sigismund, S., Polo, S., Szymkiewicz, I., Di Fiore, P. P., & Dikic, I. (2003). Multiple monoubiquitination of RTKs is sufficient for their endocytosis and degradation. *Nat Cell Biol, 5*(5), 461-466. doi:10.1038/ncb983

Hamanaka, R. B., & Chandel, N. S. (2010). Mitochondrial reactive oxygen species regulate cellular signaling and dictate biological outcomes. *Trends Biochem Sci, 35*(9), 505-513. doi:10.1016/j.tibs.2010.04.002

Han, H., Landreneau, R. J., Santucci, T. S., Tung, M. Y., Macherey, R. S., Shackney, S. E., . . . Silverman, J. F. (2002). Prognostic value of immunohistochemical expressions of p53, HER-2/neu, and bcl-2 in stage I non-small-cell lung cancer. *Hum Pathol, 33*(1), 105-110. Retrieved from https://www.ncbi.nlm.nih.gov/pubmed/11823980

Hansen, C. G., Bright, N. A., Howard, G., & Nichols, B. J. (2009). SDPR induces membrane curvature and functions in the formation of caveolae. *Nat Cell Biol, 11*(7), 807-814. doi:10.1038/ncb1887

Hanson, P. I., & Whiteheart, S. W. (2005). AAA+ proteins: have engine, will work. *Nat Rev Mol Cell Biol, 6*(7), 519-529. doi:10.1038/nrm1684

Hardel, N., Harmel, N., Zolles, G., Fakler, B., & Klocker, N. (2008). Recycling endosomes supply cardiac pacemaker channels for regulated surface expression. *Cardiovasc Res, 79*(1), 52-60. doi:10.1093/cvr/cvn062

Hausmann, G., O'Reilly, L. A., van Driel, R., Beaumont, J. G., Strasser, A., Adams, J. M., & Huang, D. C. (2000). Pro-apoptotic apoptosis protease-activating factor 1 (Apaf-1) has a cytoplasmic localization distinct from Bcl-2 or Bcl-x(L). *J Cell Biol, 149*(3), 623-634. Retrieved from https://www.ncbi.nlm.nih.gov/pubmed/10791976

Henry, G. D., Corrigan, D. J., Dineen, J. V., & Baleja, J. D. (2010). Charge effects in the selection of NPF motifs by the EH domain of EHD1. *Biochemistry, 49*(16), 3381-3392. doi:10.1021/bi100065r

Hill, M. M., Bastiani, M., Luetterforst, R., Kirkham, M., Kirkham, A., Nixon, S. J., . . . Parton, R. G. (2008). PTRF-Cavin, a conserved cytoplasmic protein required for caveola formation and function. *Cell, 132*(1), 113-124. doi:10.1016/j.cell.2007.11.042

Hirabayashi, Y., Kwon, S. K., Paek, H., Pernice, W. M., Paul, M. A., Lee, J., . . . Polleux, F. (2017). ER-mitochondria tethering by PDZD8 regulates Ca(2+) dynamics in mammalian neurons. *Science, 358*(6363), 623-630. doi:10.1126/science.aan6009

Horiuchi, H., Lippe, R., McBride, H. M., Rubino, M., Woodman, P., Stenmark, H., . . . Zerial, M. (1997). A novel Rab5 GDP/GTP exchange factor complexed to Rabaptin-5 links nucleotide exchange to effector recruitment and function. *Cell, 90*(6), 1149-1159. doi:10.1016/s0092-8674(00)80380-3

Horowitz, M. P., & Greenamyre, J. T. (2010). Mitochondrial iron metabolism and its role in neurodegeneration. *J Alzheimers Dis, 20 Suppl 2*, S551-568. doi:10.3233/JAD-2010-100354

Houndolo, T., Boulay, P. L., & Claing, A. (2005). G protein-coupled receptor endocytosis in ADP-ribosylation factor 6-depleted cells. *J Biol Chem, 280*(7), 5598-5604. doi:10.1074/jbc.M411456200

Howells, C. C., Baumann, W. T., Samuels, D. C., & Finkielstein, C. V. (2011). The Bcl-2-associated death promoter (BAD) lowers the threshold at which the Bcl-2-interacting domain death agonist (BID) triggers mitochondria disintegration. *J Theor Biol, 271*(1), 114-123. doi:10.1016/j.jtbi.2010.11.040

Hsu, V. W., & Prekeris, R. (2010). Transport at the recycling endosome. *Curr Opin Cell Biol, 22*(4), 528-534. doi:10.1016/j.ceb.2010.05.008

Hsu, Y. T., Wolter, K. G., & Youle, R. J. (1997). Cytosol-to-membrane redistribution of Bax and Bcl-X(L) during apoptosis. *Proc Natl Acad Sci U S A, 94*(8), 3668-3672. Retrieved from https://www.ncbi.nlm.nih.gov/pubmed/9108035

Huang, F., Kirkpatrick, D., Jiang, X., Gygi, S., & Sorkin, A. (2006). Differential regulation of EGF receptor internalization and degradation by multiubiquitination within the kinase domain. *Mol Cell, 21*(6), 737-748. doi:10.1016/j.molcel.2006.02.018

Huber, L. A., Pimplikar, S., Parton, R. G., Virta, H., Zerial, M., & Simons, K. (1993). Rab8, a small GTPase involved in vesicular traffic between the TGN and the basolateral plasma membrane. *J Cell Biol, 123*(1), 35-45. doi:10.1083/jcb.123.1.35

Huotari, J., & Helenius, A. (2011). Endosome maturation. *EMBO J, 30*(17), 3481-3500. doi:10.1038/emboj.2011.286

Ishihara, N., Fujita, Y., Oka, T., & Mihara, K. (2006). Regulation of mitochondrial morphology through proteolytic cleavage of OPA1. *EMBO J, 25*(13), 2966-2977. doi:10.1038/sj.emboj.7601184

Jakobsson, J., Ackermann, F., Andersson, F., Larhammar, D., Low, P., & Brodin, L. (2011). Regulation of synaptic vesicle budding and dynamin function by an EHD ATPase. *J Neurosci, 31*(39), 13972-13980. doi:10.1523/JNEUROSCI.1289-11.2011

Janvier, K., Kato, Y., Boehm, M., Rose, J. R., Martina, J. A., Kim, B. Y., . . . Bonifacino, J. S. (2003). Recognition of dileucine-based sorting signals from HIV-1 Nef and LIMP-II by the AP-1 gamma-sigma1 and AP-3 delta-sigma3 hemicomplexes. *J Cell Biol, 163*(6), 1281-1290. doi:10.1083/jcb.200307157

Jeong, S. Y., Gaume, B., Lee, Y. J., Hsu, Y. T., Ryu, S. W., Yoon, S. H., & Youle, R. J. (2004). Bcl-x(L) sequesters its C-terminal membrane anchor in soluble, cytosolic homodimers. *EMBO J, 23*(10), 2146-2155. doi:10.1038/sj.emboj.7600225

Johannes, L., & Popoff, V. (2008). Tracing the retrograde route in protein trafficking. *Cell, 135*(7), 1175-1187. doi:10.1016/j.cell.2008.12.009

Joset, A., Dodd, D. A., Halegoua, S., & Schwab, M. E. (2010). Pincher-generated Nogo-A endosomes mediate growth cone collapse and retrograde signaling. *J Cell Biol, 188*(2), 271-285. doi:10.1083/jcb.200906089

Jovic, M., Kieken, F., Naslavsky, N., Sorgen, P. L., & Caplan, S. (2009). Eps15 homology domain 1-associated tubules contain phosphatidylinositol-4-phosphate and phosphatidylinositol-(4,5)-bisphosphate and are required for efficient recycling. *Mol Biol Cell, 20*(11), 2731-2743. doi:10.1091/mbc.E08-11-1102

Jovic, M., Sharma, M., Rahajeng, J., & Caplan, S. (2010). The early endosome: a busy sorting station for proteins at the crossroads. *Histol Histopathol, 25*(1), 99-112. doi:10.14670/HH-25.99

Kale, J., Osterlund, E. J., & Andrews, D. W. (2018). BCL-2 family proteins: changing partners in the dance towards death. *Cell Death Differ, 25*(1), 65-80. doi:10.1038/cdd.2017.186

Kaufmann, S. H., Desnoyers, S., Ottaviano, Y., Davidson, N. E., & Poirier, G. G. (1993). Specific proteolytic cleavage of poly(ADP-ribose) polymerase: an early marker of chemotherapy-induced apoptosis. *Cancer Res, 53*(17), 3976-3985. Retrieved from https://www.ncbi.nlm.nih.gov/pubmed/8358726

Kaufmann, T., Schlipf, S., Sanz, J., Neubert, K., Stein, R., & Borner, C. (2003). Characterization of the signal that directs Bcl-x(L), but not Bcl-2, to the mitochondrial outer membrane. *J Cell Biol, 160*(1), 53-64. doi:10.1083/jcb.200210084

Kieken, F., Jovic, M., Naslavsky, N., Caplan, S., & Sorgen, P. L. (2007). EH domain of EHD1. *J Biomol NMR, 39*(4), 323-329. doi:10.1007/s10858-007-9196-0

Kieken, F., Sharma, M., Jovic, M., Giridharan, S. S., Naslavsky, N., Caplan, S., & Sorgen, P. L. (2010). Mechanism for the selective interaction of C-terminal Eps15 homology domain proteins with specific Asn-Pro-Phe-containing partners. *J Biol Chem, 285*(12), 8687-8694. doi:10.1074/jbc.M109.045666

Kirchhausen, T. (2000). Clathrin. *Annu Rev Biochem, 69*, 699-727. doi:10.1146/annurev.biochem.69.1.699

Kirkham, M., Fujita, A., Chadda, R., Nixon, S. J., Kurzchalia, T. V., Sharma, D. K., . . . Parton, R. G. (2005). Ultrastructural identification of uncoated caveolin-independent early endocytic vehicles. *J Cell Biol, 168*(3), 465-476. doi:10.1083/jcb.200407078

Kjaerulff, O., Verstreken, P., & Bellen, H. J. (2002). Synaptic vesicle retrieval: still time for a kiss. *Nat Cell Biol, 4*(11), E245-248. doi:10.1038/ncb1102-e245

Koch, D., Westermann, M., Kessels, M. M., & Qualmann, B. (2012). Ultrastructural freeze-fracture immunolabeling identifies plasma membrane-localized syndapin II as a crucial factor in shaping caveolae. *Histochem Cell Biol, 138*(2), 215-230. doi:10.1007/s00418-012-0945-0

Koopman, W. J., Visch, H. J., Verkaart, S., van den Heuvel, L. W., Smeitink, J. A., & Willems, P. H. (2005). Mitochondrial network complexity and pathological decrease in complex I activity are tightly correlated in isolated human complex I deficiency. *Am J Physiol Cell Physiol, 289*(4), C881-890. doi:10.1152/ajpcell.00104.2005

Kornmann, B., Currie, E., Collins, S. R., Schuldiner, M., Nunnari, J., Weissman, J. S., & Walter, P. (2009). An ER-mitochondria tethering complex revealed by a synthetic biology screen. *Science, 325*(5939), 477-481. doi:10.1126/science.1175088

Korobova, F., Ramabhadran, V., & Higgs, H. N. (2013). An actin-dependent step in mitochondrial fission mediated by the ER-associated formin INF2. *Science, 339*(6118), 464-467. doi:10.1126/science.1228360

Koshiba, T., Detmer, S. A., Kaiser, J. T., Chen, H., McCaffery, J. M., & Chan, D. C. (2004). Structural basis of mitochondrial tethering by mitofusin complexes. *Science, 305*(5685), 858-862. doi:10.1126/science.1099793

Kovtun, O., Leneva, N., Bykov, Y. S., Ariotti, N., Teasdale, R. D., Schaffer, M., . . . Collins, B. M. (2018). Structure of the membrane-assembled retromer coat determined by cryo-electron tomography. *Nature, 561*(7724), 561-564. doi:10.1038/s41586-018-0526-z

Ku, B., Liang, C., Jung, J. U., & Oh, B. H. (2011). Evidence that inhibition of BAX activation by BCL-2 involves its tight and preferential interaction with the BH3 domain of BAX. *Cell Res, 21*(4), 627-641. doi:10.1038/cr.2010.149

Kumar, K. R., Weissbach, A., Heldmann, M., Kasten, M., Tunc, S., Sue, C. M., . . . Lohmann, K. (2012). Frequency of the D620N mutation in VPS35 in Parkinson disease. *Arch Neurol, 69*(10), 1360-1364. doi:10.1001/archneurol.2011.3367

Kumari, S., & Mayor, S. (2008). ARF1 is directly involved in dynamin-independent endocytosis. *Nat Cell Biol, 10*(1), 30-41. doi:10.1038/ncb1666

Labrousse, A. M., Zappaterra, M. D., Rube, D. A., & van der Bliek, A. M. (1999). C. elegans dynamin-related protein DRP-1 controls severing of the mitochondrial outer membrane. *Mol Cell, 4*(5), 815-826. doi:10.1016/s1097-2765(00)80391-3

Lakhan, S. E., Sabharanjak, S., & De, A. (2009). Endocytosis of glycosylphosphatidylinositol-anchored proteins. *J Biomed Sci, 16*, 93. doi:10.1186/1423-0127-16-93

Lamaze, C., Dujeancourt, A., Baba, T., Lo, C. G., Benmerah, A., & Dautry-Varsat, A. (2001). Interleukin 2 receptors and detergent-resistant membrane domains define a clathrin-independent endocytic pathway. *Mol Cell, 7*(3), 661-671. doi:10.1016/s1097-2765(01)00212-x

Lee, A., Frank, D. W., Marks, M. S., & Lemmon, M. A. (1999). Dominant-negative inhibition of receptor-mediated endocytosis by a dynamin-1 mutant with a defective pleckstrin homology domain. *Curr Biol, 9*(5), 261-264. doi:10.1016/s0960-9822(99)80115-8

Lee, D. W., Zhao, X., Scarselletta, S., Schweinsberg, P. J., Eisenberg, E., Grant, B. D., & Greene, L. E. (2005). ATP binding regulates oligomerization and endosome association of RME-1 family proteins. *J Biol Chem, 280*(17), 17213-17220. doi:10.1074/jbc.M412751200

Lee, J. E., Westrate, L. M., Wu, H., Page, C., & Voeltz, G. K. (2016). Multiple dynamin family members collaborate to drive mitochondrial division. *Nature, 540*(7631), 139-143. doi:10.1038/nature20555

Lee, M. H., Lin, S. R., Chang, J. Y., Schultz, L., Heath, J., Hsu, L. J., . . . Chang, N. S. (2010). TGF-beta induces TIAF1 self-aggregation via type II receptor-independent signaling that leads to generation of amyloid beta plaques in Alzheimer's disease. *Cell Death Dis, 1*, e110. doi:10.1038/cddis.2010.83

Levkowitz, G., Waterman, H., Zamir, E., Kam, Z., Oved, S., Langdon, W. Y., . . . Yarden, Y. (1998). c-Cbl/Sli-1 regulates endocytic sorting and ubiquitination of the

epidermal growth factor receptor. *Genes Dev, 12*(23), 3663-3674. doi:10.1101/gad.12.23.3663

Li, H., Alavian, K. N., Lazrove, E., Mehta, N., Jones, A., Zhang, P., . . . Jonas, E. A. (2013). A Bcl-xL-Drp1 complex regulates synaptic vesicle membrane dynamics during endocytosis. *Nat Cell Biol, 15*(7), 773-785. doi:10.1038/ncb2791

Liesa, M., Palacin, M., & Zorzano, A. (2009). Mitochondrial dynamics in mammalian health and disease. *Physiol Rev, 89*(3), 799-845. doi:10.1152/physrev.00030.2008

Lin, S. X., Grant, B., Hirsh, D., & Maxfield, F. R. (2001). Rme-1 regulates the distribution and function of the endocytic recycling compartment in mammalian cells. *Nat Cell Biol, 3*(6), 567-572. doi:10.1038/35078543

Liu, Q., Moldoveanu, T., Sprules, T., Matta-Camacho, E., Mansur-Azzam, N., & Gehring, K. (2010). Apoptotic regulation by MCL-1 through heterodimerization. *J Biol Chem, 285*(25), 19615-19624. doi:10.1074/jbc.M110.105452

Lomonosova, E., & Chinnadurai, G. (2008). BH3-only proteins in apoptosis and beyond: an overview. *Oncogene, 27 Suppl 1*, S2-19. doi:10.1038/onc.2009.39

Loson, O. C., Song, Z., Chen, H., & Chan, D. C. (2013). Fis1, Mff, MiD49, and MiD51 mediate Drp1 recruitment in mitochondrial fission. *Mol Biol Cell, 24*(5), 659-667. doi:10.1091/mbc.E12-10-0721

Lu, Q., Insinna, C., Ott, C., Stauffer, J., Pintado, P. A., Rahajeng, J., . . . Westlake, C. J. (2015). Early steps in primary cilium assembly require EHD1/EHD3-dependent ciliary vesicle formation. *Nat Cell Biol, 17*(4), 531. doi:10.1038/ncb3155

Lundmark, R., Doherty, G. J., Howes, M. T., Cortese, K., Vallis, Y., Parton, R. G., & McMahon, H. T. (2008). The GTPase-activating protein GRAF1 regulates the CLIC/GEEC endocytic pathway. *Curr Biol, 18*(22), 1802-1808. doi:10.1016/j.cub.2008.10.044

MacLeod, D. A., Rhinn, H., Kuwahara, T., Zolin, A., Di Paolo, G., McCabe, B. D., . . . Abeliovich, A. (2013). RAB7L1 interacts with LRRK2 to modify intraneuronal protein sorting and Parkinson's disease risk. *Neuron, 77*(3), 425-439. doi:10.1016/j.neuron.2012.11.033

Magadan, J. G., Barbieri, M. A., Mesa, R., Stahl, P. D., & Mayorga, L. S. (2006). Rab22a regulates the sorting of transferrin to recycling endosomes. *Mol Cell Biol, 26*(7), 2595-2614. doi:10.1128/MCB.26.7.2595-2614.2006

Manon, S., Chaudhuri, B., & Guerin, M. (1997). Release of cytochrome c and decrease of cytochrome c oxidase in Bax-expressing yeast cells, and prevention of these effects by coexpression of Bcl-xL. *FEBS Lett, 415*(1), 29-32. Retrieved from https://www.ncbi.nlm.nih.gov/pubmed/9326363

Maxfield, F. R., & McGraw, T. E. (2004). Endocytic recycling. *Nat Rev Mol Cell Biol, 5*(2), 121-132. doi:10.1038/nrm1315

Mayer, A., Wickner, W., & Haas, A. (1996). Sec18p (NSF)-driven release of Sec17p (alpha-SNAP) can precede docking and fusion of yeast vacuoles. *Cell, 85*(1), 83-94. doi:10.1016/s0092-8674(00)81084-3

Mayor, S., & Pagano, R. E. (2007). Pathways of clathrin-independent endocytosis. *Nat Rev Mol Cell Biol, 8*(8), 603-612. doi:10.1038/nrm2216

Mayor, S., Parton, R. G., & Donaldson, J. G. (2014). Clathrin-independent pathways of endocytosis. *Cold Spring Harb Perspect Biol, 6*(6). doi:10.1101/cshperspect.a016758

Mayor, S., Presley, J. F., & Maxfield, F. R. (1993). Sorting of membrane components from endosomes and subsequent recycling to the cell surface occurs by a bulk flow process. *J Cell Biol, 121*(6), 1257-1269. doi:10.1083/jcb.121.6.1257

McBride, H. M., Rybin, V., Murphy, C., Giner, A., Teasdale, R., & Zerial, M. (1999). Oligomeric complexes link Rab5 effectors with NSF and drive membrane fusion via interactions between EEA1 and syntaxin 13. *Cell, 98*(3), 377-386. doi:10.1016/s0092-8674(00)81966-2

McKenzie, J. E., Raisley, B., Zhou, X., Naslavsky, N., Taguchi, T., Caplan, S., & Sheff, D. (2012). Retromer guides STxB and CD8-M6PR from early to recycling endosomes, EHD1 guides STxB from recycling endosome to Golgi. *Traffic, 13*(8), 1140-1159. doi:10.1111/j.1600-0854.2012.01374.x

McLelland, G. L., Soubannier, V., Chen, C. X., McBride, H. M., & Fon, E. A. (2014). Parkin and PINK1 function in a vesicular trafficking pathway regulating mitochondrial quality control. *EMBO J, 33*(4), 282-295. doi:10.1002/embj.201385902

McMahon, H. T., & Gallop, J. L. (2005). Membrane curvature and mechanisms of dynamic cell membrane remodelling. *Nature, 438*(7068), 590-596. doi:10.1038/nature04396

Mears, J. A., Lackner, L. L., Fang, S., Ingerman, E., Nunnari, J., & Hinshaw, J. E. (2011). Conformational changes in Dnm1 support a contractile mechanism for mitochondrial fission. *Nat Struct Mol Biol, 18*(1), 20-26. doi:10.1038/nsmb.1949

Mellman, I. (1996a). Endocytosis and molecular sorting. *Annu Rev Cell Dev Biol, 12*, 575-625. doi:10.1146/annurev.cellbio.12.1.575

Mellman, I. (1996b). Membranes and sorting. *Curr Opin Cell Biol, 8*(4), 497-498. doi:10.1016/s0955-0674(96)80026-3

Melo, A. A., Hegde, B. G., Shah, C., Larsson, E., Isas, J. M., Kunz, S., . . . Daumke, O. (2017). Structural insights into the activation mechanism of dynamin-like EHD ATPases. *Proc Natl Acad Sci U S A, 114*(22), 5629-5634. doi:10.1073/pnas.1614075114

Mercer, J., Knebel, S., Schmidt, F. I., Crouse, J., Burkard, C., & Helenius, A. (2010). Vaccinia virus strains use distinct forms of macropinocytosis for host-cell entry. *Proc Natl Acad Sci U S A, 107*(20), 9346-9351. doi:10.1073/pnas.1004618107

Merithew, E., Stone, C., Eathiraj, S., & Lambright, D. G. (2003). Determinants of Rab5 interaction with the N terminus of early endosome antigen 1. *J Biol Chem, 278*(10), 8494-8500. doi:10.1074/jbc.M211514200

Miaczynska, M., Christoforidis, S., Giner, A., Shevchenko, A., Uttenweiler-Joseph, S., Habermann, B., . . . Zerial, M. (2004). APPL proteins link Rab5 to nuclear signal transduction via an endosomal compartment. *Cell, 116*(3), 445-456. doi:10.1016/s0092-8674(04)00117-5

Moldoveanu, T., Grace, C. R., Llambi, F., Nourse, A., Fitzgerald, P., Gehring, K., . . . Green, D. R. (2013). BID-induced structural changes in BAK promote apoptosis. *Nat Struct Mol Biol, 20*(5), 589-597. doi:10.1038/nsmb.2563

Moreira, P. I., Cardoso, S. M., Santos, M. S., & Oliveira, C. R. (2006). The key role of mitochondria in Alzheimer's disease. *J Alzheimers Dis, 9*(2), 101-110. Retrieved from https://www.ncbi.nlm.nih.gov/pubmed/16873957

Moren, B., Shah, C., Howes, M. T., Schieber, N. L., McMahon, H. T., Parton, R. G., . . . Lundmark, R. (2012). EHD2 regulates caveolar dynamics via ATP-driven targeting and oligomerization. *Mol Biol Cell, 23*(7), 1316-1329. doi:10.1091/mbc.E11-09-0787

Murray, J. T., Panaretou, C., Stenmark, H., Miaczynska, M., & Backer, J. M. (2002). Role of Rab5 in the recruitment of hVps34/p150 to the early endosome. *Traffic, 3*(6), 416-427. doi:10.1034/j.1600-0854.2002.30605.x

Naslavsky, N., & Caplan, S. (2011). EHD proteins: key conductors of endocytic transport. *Trends Cell Biol, 21*(2), 122-131. doi:10.1016/j.tcb.2010.10.003

Naslavsky, N., & Caplan, S. (2018). The enigmatic endosome - sorting the ins and outs of endocytic trafficking. *J Cell Sci, 131*(13). doi:10.1242/jcs.216499

Naslavsky, N., McKenzie, J., Altan-Bonnet, N., Sheff, D., & Caplan, S. (2009). EHD3 regulates early-endosome-to-Golgi transport and preserves Golgi morphology. *J Cell Sci, 122*(Pt 3), 389-400. doi:10.1242/jcs.037051

Naslavsky, N., Rahajeng, J., Sharma, M., Jovic, M., & Caplan, S. (2006). Interactions between EHD proteins and Rab11-FIP2: a role for EHD3 in early endosomal transport. *Mol Biol Cell, 17*(1), 163-177. doi:10.1091/mbc.e05-05-0466

Naslavsky, N., Weigert, R., & Donaldson, J. G. (2003). Convergence of non-clathrin- and clathrin-derived endosomes involves Arf6 inactivation and changes in phosphoinositides. *Mol Biol Cell, 14*(2), 417-431. doi:10.1091/mbc.02-04-0053

Neuspiel, M., Schauss, A. C., Braschi, E., Zunino, R., Rippstein, P., Rachubinski, R. A., . . . McBride, H. M. (2008). Cargo-selected transport from the mitochondria to peroxisomes is mediated by vesicular carriers. *Curr Biol, 18*(2), 102-108. doi:10.1016/j.cub.2007.12.038

Ni, H. M., Williams, J. A., & Ding, W. X. (2015). Mitochondrial dynamics and mitochondrial quality control. *Redox Biol, 4*, 6-13. doi:10.1016/j.redox.2014.11.006

Nicholls, D. G. (2005). Mitochondria and calcium signaling. *Cell Calcium, 38*(3-4), 311-317. doi:10.1016/j.ceca.2005.06.011

Nielsen, E., Christoforidis, S., Uttenweiler-Joseph, S., Miaczynska, M., Dewitte, F., Wilm, M., . . . Zerial, M. (2000). Rabenosyn-5, a novel Rab5 effector, is complexed with hVPS45 and recruited to endosomes through a FYVE finger domain. *J Cell Biol, 151*(3), 601-612. doi:10.1083/jcb.151.3.601

Nielsen, E., Severin, F., Backer, J. M., Hyman, A. A., & Zerial, M. (1999). Rab5 regulates motility of early endosomes on microtubules. *Nat Cell Biol, 1*(6), 376-382. doi:10.1038/14075

Nijhawan, D., Fang, M., Traer, E., Zhong, Q., Gao, W., Du, F., & Wang, X. (2003). Elimination of Mcl-1 is required for the initiation of apoptosis following ultraviolet irradiation. *Genes Dev, 17*(12), 1475-1486. doi:10.1101/gad.1093903

Nordmann, M., Cabrera, M., Perz, A., Brocker, C., Ostrowicz, C., Engelbrecht-Vandre, S., & Ungermann, C. (2010). The Mon1-Ccz1 complex is the GEF of the late endosomal Rab7 homolog Ypt7. *Curr Biol, 20*(18), 1654-1659. doi:10.1016/j.cub.2010.08.002

O'Neill, J. W., Manion, M. K., Maguire, B., & Hockenbery, D. M. (2006). BCL-XL dimerization by three-dimensional domain swapping. *J Mol Biol, 356*(2), 367-381. doi:10.1016/j.jmb.2005.11.032

O'Neill, K. L., Huang, K., Zhang, J., Chen, Y., & Luo, X. (2016). Inactivation of prosurvival Bcl-2 proteins activates Bax/Bak through the outer mitochondrial membrane. *Genes Dev, 30*(8), 973-988. doi:10.1101/gad.276725.115

Ohno, H., Stewart, J., Fournier, M. C., Bosshart, H., Rhee, I., Miyatake, S., . . . Bonifacino, J. S. (1995). Interaction of tyrosine-based sorting signals with clathrin-associated proteins. *Science, 269*(5232), 1872-1875. doi:10.1126/science.7569928

Oltvai, Z. N., Milliman, C. L., & Korsmeyer, S. J. (1993). Bcl-2 heterodimerizes in vivo with a conserved homolog, Bax, that accelerates programmed cell death. *Cell, 74*(4), 609-619. Retrieved from https://www.ncbi.nlm.nih.gov/pubmed/8358790

Otera, H., Wang, C., Cleland, M. M., Setoguchi, K., Yokota, S., Youle, R. J., & Mihara, K. (2010). Mff is an essential factor for mitochondrial recruitment of Drp1 during

mitochondrial fission in mammalian cells. *J Cell Biol, 191*(6), 1141-1158. doi:10.1083/jcb.201007152

Owen, D. J., Collins, B. M., & Evans, P. R. (2004). Adaptors for clathrin coats: structure and function. *Annu Rev Cell Dev Biol, 20*, 153-191. doi:10.1146/annurev.cellbio.20.010403.104543

Pagliuso, A., Cossart, P., & Stavru, F. (2018). The ever-growing complexity of the mitochondrial fission machinery. *Cell Mol Life Sci, 75*(3), 355-374. doi:10.1007/s00018-017-2603-0

Pal, A., Severin, F., Lommer, B., Shevchenko, A., & Zerial, M. (2006). Huntingtin-HAP40 complex is a novel Rab5 effector that regulates early endosome motility and is up-regulated in Huntington's disease. *J Cell Biol, 172*(4), 605-618. doi:10.1083/jcb.200509091

Palmer, C. S., Elgass, K. D., Parton, R. G., Osellame, L. D., Stojanovski, D., & Ryan, M. T. (2013). Adaptor proteins MiD49 and MiD51 can act independently of Mff and Fis1 in Drp1 recruitment and are specific for mitochondrial fission. *J Biol Chem, 288*(38), 27584-27593. doi:10.1074/jbc.M113.479873

Palmer, C. S., Osellame, L. D., Laine, D., Koutsopoulos, O. S., Frazier, A. E., & Ryan, M. T. (2011). MiD49 and MiD51, new components of the mitochondrial fission machinery. *EMBO Rep, 12*(6), 565-573. doi:10.1038/embor.2011.54

Pant, S., Sharma, M., Patel, K., Caplan, S., Carr, C. M., & Grant, B. D. (2009). AMPH-1/Amphiphysin/Bin1 functions with RME-1/Ehd1 in endocytic recycling. *Nat Cell Biol, 11*(12), 1399-1410. doi:10.1038/ncb1986

Park, M., Penick, E. C., Edwards, J. G., Kauer, J. A., & Ehlers, M. D. (2004). Recycling endosomes supply AMPA receptors for LTP. *Science, 305*(5692), 1972-1975. doi:10.1126/science.1102026

Parton, R. G., & Simons, K. (2007). The multiple faces of caveolae. *Nat Rev Mol Cell Biol, 8*(3), 185-194. doi:10.1038/nrm2122

Pearse, B. M., & Crowther, R. A. (1987). Structure and assembly of coated vesicles. *Annu Rev Biophys Biophys Chem, 16*, 49-68. doi:10.1146/annurev.bb.16.060187.000405

Pennanen, C., Parra, V., Lopez-Crisosto, C., Morales, P. E., Del Campo, A., Gutierrez, T., . . . Lavandero, S. (2014). Mitochondrial fission is required for cardiomyocyte hypertrophy mediated by a Ca2+-calcineurin signaling pathway. *J Cell Sci, 127*(Pt 12), 2659-2671. doi:10.1242/jcs.139394

Peralta, E. R., Martin, B. C., & Edinger, A. L. (2010). Differential effects of TBC1D15 and mammalian Vps39 on Rab7 activation state, lysosomal morphology, and growth factor dependence. *J Biol Chem, 285*(22), 16814-16821. doi:10.1074/jbc.M110.111633

Petros, A. M., Nettesheim, D. G., Wang, Y., Olejniczak, E. T., Meadows, R. P., Mack, J., . . . Fesik, S. W. (2000). Rationale for Bcl-xL/Bad peptide complex formation from structure, mutagenesis, and biophysical studies. *Protein Sci, 9*(12), 2528-2534. doi:10.1110/ps.9.12.2528

Pfeffer, S., & Aivazian, D. (2004). Targeting Rab GTPases to distinct membrane compartments. *Nat Rev Mol Cell Biol, 5*(11), 886-896. doi:10.1038/nrm1500

Pitto, M., Brunner, J., Ferraretto, A., Ravasi, D., Palestini, P., & Masserini, M. (2000). Use of a photoactivable GM1 ganglioside analogue to assess lipid distribution in caveolae bilayer. *Glycoconj J, 17*(3 -4), 215-222. doi:10.1023/a:1026593307882

Pitts, K. R., Yoon, Y., Krueger, E. W., & McNiven, M. A. (1999). The dynamin-like protein DLP1 is essential for normal distribution and morphology of the endoplasmic reticulum and mitochondria in mammalian cells. *Mol Biol Cell, 10*(12), 4403-4417. doi:10.1091/mbc.10.12.4403

Placzek, W. J., Wei, J., Kitada, S., Zhai, D., Reed, J. C., & Pellecchia, M. (2010). A survey of the anti-apoptotic Bcl-2 subfamily expression in cancer types provides a platform to predict the efficacy of Bcl-2 antagonists in cancer therapy. *Cell Death Dis, 1*, e40. doi:10.1038/cddis.2010.18

Pohl, U., Smith, J. S., Tachibana, I., Ueki, K., Lee, H. K., Ramaswamy, S., . . . Louis, D. N. (2000). EHD2, EHD3, and EHD4 encode novel members of a highly conserved family of EH domain-containing proteins. *Genomics, 63*(2), 255-262. doi:10.1006/geno.1999.6087

Posey, A. D., Jr., Pytel, P., Gardikiotes, K., Demonbreun, A. R., Rainey, M., George, M., . . . McNally, E. M. (2011). Endocytic recycling proteins EHD1 and EHD2 interact with fer-1-like-5 (Fer1L5) and mediate myoblast fusion. *J Biol Chem, 286*(9), 7379-7388. doi:10.1074/jbc.M110.157222

Prasad, K., Barouch, W., Greene, L., & Eisenberg, E. (1993). A protein cofactor is required for uncoating of clathrin baskets by uncoating ATPase. *J Biol Chem, 268*(32), 23758-23761. Retrieved from https://www.ncbi.nlm.nih.gov/pubmed/8226905

Radhakrishna, H., & Donaldson, J. G. (1997). ADP-ribosylation factor 6 regulates a novel plasma membrane recycling pathway. *J Cell Biol, 139*(1), 49-61. doi:10.1083/jcb.139.1.49

Rahajeng, J., Giridharan, S. S., Cai, B., Naslavsky, N., & Caplan, S. (2012). MICAL-L1 is a tubular endosomal membrane hub that connects Rab35 and Arf6 with Rab8a. *Traffic, 13*(1), 82-93. doi:10.1111/j.1600-0854.2011.01294.x

Rahajeng, J., Giridharan, S. S., Naslavsky, N., & Caplan, S. (2010). Collapsin response mediator protein-2 (Crmp2) regulates trafficking by linking endocytic regulatory proteins to dynein motors. *J Biol Chem, 285*(42), 31918-31922. doi:10.1074/jbc.C110.166066

Raiborg, C., & Stenmark, H. (2002). Hrs and endocytic sorting of ubiquitinated membrane proteins. *Cell Struct Funct, 27*(6), 403-408. doi:10.1247/csf.27.403

Reinecke, J. B., Katafiasz, D., Naslavsky, N., & Caplan, S. (2015). Novel functions for the endocytic regulatory proteins MICAL-L1 and EHD1 in mitosis. *Traffic, 16*(1), 48-67. doi:10.1111/tra.12234

Richardson, D. R., Lane, D. J., Becker, E. M., Huang, M. L., Whitnall, M., Suryo Rahmanto, Y., . . . Ponka, P. (2010). Mitochondrial iron trafficking and the integration of iron metabolism between the mitochondrion and cytosol. *Proc Natl Acad Sci U S A, 107*(24), 10775-10782. doi:10.1073/pnas.0912925107

Robinson, M. S. (2015). Forty Years of Clathrin-coated Vesicles. *Traffic, 16*(12), 1210-1238. doi:10.1111/tra.12335

Rojas, R., van Vlijmen, T., Mardones, G. A., Prabhu, Y., Rojas, A. L., Mohammed, S., . . . Bonifacino, J. S. (2008). Regulation of retromer recruitment to endosomes by sequential action of Rab5 and Rab7. *J Cell Biol, 183*(3), 513-526. doi:10.1083/jcb.200804048

Rojo, M., Legros, F., Chateau, D., & Lombes, A. (2002). Membrane topology and mitochondrial targeting of mitofusins, ubiquitous mammalian homologs of the transmembrane GTPase Fzo. *J Cell Sci, 115*(Pt 8), 1663-1674. Retrieved from https://www.ncbi.nlm.nih.gov/pubmed/11950885

Roland, J. T., Kenworthy, A. K., Peranen, J., Caplan, S., & Goldenring, J. R. (2007). Myosin Vb interacts with Rab8a on a tubular network containing EHD1 and EHD3. *Mol Biol Cell, 18*(8), 2828-2837. doi:10.1091/mbc.e07-02-0169

Sandvig, K., & van Deurs, B. (1994). Endocytosis without clathrin. *Trends Cell Biol, 4*(8), 275-277. doi:10.1016/0962-8924(94)90211-9

Santel, A., & Frank, S. (2008). Shaping mitochondria: The complex posttranslational regulation of the mitochondrial fission protein DRP1. *IUBMB Life, 60*(7), 448-455. doi:10.1002/iub.71

Santel, A., & Fuller, M. T. (2001). Control of mitochondrial morphology by a human mitofusin. *J Cell Sci, 114*(Pt 5), 867-874. Retrieved from https://www.ncbi.nlm.nih.gov/pubmed/11181170

Sato, M., Sato, K., Liou, W., Pant, S., Harada, A., & Grant, B. D. (2008). Regulation of endocytic recycling by C. elegans Rab35 and its regulator RME-4, a coated-pit protein. *EMBO J, 27*(8), 1183-1196. doi:10.1038/emboj.2008.54

Scherr, A. L., Gdynia, G., Salou, M., Radhakrishnan, P., Duglova, K., Heller, A., . . . Koehler, B. C. (2016). Bcl-xL is an oncogenic driver in colorectal cancer. *Cell Death Dis, 7*(8), e2342. doi:10.1038/cddis.2016.233

Schinzel, A., Kaufmann, T., & Borner, C. (2004). Bcl-2 family members: integrators of survival and death signals in physiology and pathology [corrected]. *Biochim Biophys Acta, 1644*(2-3), 95-105. doi:10.1016/j.bbamcr.2003.09.006

Schonteich, E., Wilson, G. M., Burden, J., Hopkins, C. R., Anderson, K., Goldenring, J. R., & Prekeris, R. (2008). The Rip11/Rab11-FIP5 and kinesin II complex regulates endocytic protein recycling. *J Cell Sci, 121*(Pt 22), 3824-3833. doi:10.1242/jcs.032441

Seaman, M. N. (2004). Cargo-selective endosomal sorting for retrieval to the Golgi requires retromer. *J Cell Biol, 165*(1), 111-122. doi:10.1083/jcb.200312034

Seaman, M. N. (2005). Recycle your receptors with retromer. *Trends Cell Biol, 15*(2), 68-75. doi:10.1016/j.tcb.2004.12.004

Seaman, M. N., McCaffery, J. M., & Emr, S. D. (1998). A membrane coat complex essential for endosome-to-Golgi retrograde transport in yeast. *J Cell Biol, 142*(3), 665-681. Retrieved from https://www.ncbi.nlm.nih.gov/pubmed/9700157

Senju, Y., Itoh, Y., Takano, K., Hamada, S., & Suetsugu, S. (2011). Essential role of PACSIN2/syndapin-II in caveolae membrane sculpting. *J Cell Sci, 124*(Pt 12), 2032-2040. doi:10.1242/jcs.086264

Shamas-Din, A., Bindner, S., Zhu, W., Zaltsman, Y., Campbell, C., Gross, A., . . . Fradin, C. (2013). tBid undergoes multiple conformational changes at the membrane

required for Bax activation. *J Biol Chem, 288*(30), 22111-22127. doi:10.1074/jbc.M113.482109

Shamas-Din, A., Brahmbhatt, H., Leber, B., & Andrews, D. W. (2011). BH3-only proteins: Orchestrators of apoptosis. *Biochim Biophys Acta, 1813*(4), 508-520. doi:10.1016/j.bbamcr.2010.11.024

Shao, Y., Akmentin, W., Toledo-Aral, J. J., Rosenbaum, J., Valdez, G., Cabot, J. B., . . . Halegoua, S. (2002). Pincher, a pinocytic chaperone for nerve growth factor/TrkA signaling endosomes. *J Cell Biol, 157*(4), 679-691. doi:10.1083/jcb.200201063

Sharma, M., Giridharan, S. S., Rahajeng, J., Naslavsky, N., & Caplan, S. (2009). MICAL-L1 links EHD1 to tubular recycling endosomes and regulates receptor recycling. *Mol Biol Cell, 20*(24), 5181-5194. doi:10.1091/mbc.E09-06-0535

Sharma, M., Ioannidis, J. P., Aasly, J. O., Annesi, G., Brice, A., Bertram, L., . . . consortium, G. (2012). A multi-centre clinico-genetic analysis of the VPS35 gene in Parkinson disease indicates reduced penetrance for disease-associated variants. *J Med Genet, 49*(11), 721-726. doi:10.1136/jmedgenet-2012-101155

Sharma, M., Jovic, M., Kieken, F., Naslavsky, N., Sorgen, P., & Caplan, S. (2009). A model for the role of EHD1-containing membrane tubules in endocytic recycling. *Commun Integr Biol, 2*(5), 431-433. Retrieved from https://www.ncbi.nlm.nih.gov/pubmed/19907710

Sharma, M., Naslavsky, N., & Caplan, S. (2008). A role for EHD4 in the regulation of early endosomal transport. *Traffic, 9*(6), 995-1018. doi:10.1111/j.1600-0854.2008.00732.x

Sheff, D. R., Daro, E. A., Hull, M., & Mellman, I. (1999). The receptor recycling pathway contains two distinct populations of early endosomes with different sorting functions. *J Cell Biol, 145*(1), 123-139. doi:10.1083/jcb.145.1.123

Shestakova, A., Hanono, A., Drosner, S., Curtiss, M., Davies, B. A., Katzmann, D. J., & Babst, M. (2010). Assembly of the AAA ATPase Vps4 on ESCRT-III. *Mol Biol Cell, 21*(6), 1059-1071. doi:10.1091/mbc.E09-07-0572

Shimizu, S., Eguchi, Y., Kosaka, H., Kamiike, W., Matsuda, H., & Tsujimoto, Y. (1995). Prevention of hypoxia-induced cell death by Bcl-2 and Bcl-xL. *Nature, 374*(6525), 811-813. doi:10.1038/374811a0

Siddhanta, A., & Shields, D. (1998). Secretory vesicle budding from the trans-Golgi network is mediated by phosphatidic acid levels. *J Biol Chem, 273*(29), 17995-17998. doi:10.1074/jbc.273.29.17995

Simone, L. C., Caplan, S., & Naslavsky, N. (2013). Role of phosphatidylinositol 4,5-bisphosphate in regulating EHD2 plasma membrane localization. *PLoS One, 8*(9), e74519. doi:10.1371/journal.pone.0074519

Simonsen, A., Gaullier, J. M., D'Arrigo, A., & Stenmark, H. (1999). The Rab5 effector EEA1 interacts directly with syntaxin-6. *J Biol Chem, 274*(41), 28857-28860. doi:10.1074/jbc.274.41.28857

Skop, A. R., Bergmann, D., Mohler, W. A., & White, J. G. (2001). Completion of cytokinesis in C. elegans requires a brefeldin A-sensitive membrane accumulation at the cleavage furrow apex. *Curr Biol, 11*(10), 735-746. doi:10.1016/s0960-9822(01)00231-7

Slomp, A., & Peperzak, V. (2018). Role and Regulation of Pro-survival BCL-2 Proteins in Multiple Myeloma. *Front Oncol, 8*, 533. doi:10.3389/fonc.2018.00533

Smirnova, E., Griparic, L., Shurland, D. L., & van der Bliek, A. M. (2001). Dynamin-related protein Drp1 is required for mitochondrial division in mammalian cells. *Mol Biol Cell, 12*(8), 2245-2256. Retrieved from https://www.ncbi.nlm.nih.gov/pubmed/11514614

Sollner, T. (1995). SNAREs and targeted membrane fusion. *FEBS Lett, 369*(1), 80-83. doi:10.1016/0014-5793(95)00594-y

Song, Z., Chen, H., Fiket, M., Alexander, C., & Chan, D. C. (2007). OPA1 processing controls mitochondrial fusion and is regulated by mRNA splicing, membrane potential, and Yme1L. *J Cell Biol, 178*(5), 749-755. doi:10.1083/jcb.200704110

Sonnichsen, B., De Renzis, S., Nielsen, E., Rietdorf, J., & Zerial, M. (2000). Distinct membrane domains on endosomes in the recycling pathway visualized by multicolor imaging of Rab4, Rab5, and Rab11. *J Cell Biol, 149*(4), 901-914. doi:10.1083/jcb.149.4.901

Sorkin, A. (2004). Cargo recognition during clathrin-mediated endocytosis: a team effort. *Curr Opin Cell Biol, 16*(4), 392-399. doi:10.1016/j.ceb.2004.06.001

Soubannier, V., McLelland, G. L., Zunino, R., Braschi, E., Rippstein, P., Fon, E. A., & McBride, H. M. (2012). A vesicular transport pathway shuttles cargo from mitochondria to lysosomes. *Curr Biol, 22*(2), 135-141. doi:10.1016/j.cub.2011.11.057

Soubannier, V., Rippstein, P., Kaufman, B. A., Shoubridge, E. A., & McBride, H. M. (2012). Reconstitution of mitochondria derived vesicle formation demonstrates

selective enrichment of oxidized cargo. *PLoS One, 7*(12), e52830. doi:10.1371/journal.pone.0052830

Srivastava, S. (2017). The Mitochondrial Basis of Aging and Age-Related Disorders. *Genes (Basel), 8*(12). doi:10.3390/genes8120398

Stein, M. P., Dong, J., & Wandinger-Ness, A. (2003). Rab proteins and endocytic trafficking: potential targets for therapeutic intervention. *Adv Drug Deliv Rev, 55*(11), 1421-1437. doi:10.1016/j.addr.2003.07.009

Stenmark, H., Aasland, R., & Driscoll, P. C. (2002). The phosphatidylinositol 3-phosphate-binding FYVE finger. *FEBS Lett, 513*(1), 77-84. doi:10.1016/s0014-5793(01)03308-7

Stoeber, M., Stoeck, I. K., Hanni, C., Bleck, C. K., Balistreri, G., & Helenius, A. (2012). Oligomers of the ATPase EHD2 confine caveolae to the plasma membrane through association with actin. *EMBO J, 31*(10), 2350-2364. doi:10.1038/emboj.2012.98

Struhal, W., Presslauer, S., Spielberger, S., Zimprich, A., Auff, E., Bruecke, T., . . . Austrian, V. P. S. I. T. (2014). VPS35 Parkinson's disease phenotype resembles the sporadic disease. *J Neural Transm (Vienna), 121*(7), 755-759. doi:10.1007/s00702-014-1179-1

Subburaj, Y., Cosentino, K., Axmann, M., Pedrueza-Villalmanzo, E., Hermann, E., Bleicken, S., . . . Garcia-Saez, A. J. (2015). Bax monomers form dimer units in the membrane that further self-assemble into multiple oligomeric species. *Nat Commun, 6*, 8042. doi:10.1038/ncomms9042

Sun, N., Youle, R. J., & Finkel, T. (2016). The Mitochondrial Basis of Aging. *Mol Cell, 61*(5), 654-666. doi:10.1016/j.molcel.2016.01.028

Sutton, R. B., Fasshauer, D., Jahn, R., & Brunger, A. T. (1998). Crystal structure of a SNARE complex involved in synaptic exocytosis at 2.4 A resolution. *Nature, 395*(6700), 347-353. doi:10.1038/26412

Tabuchi, M., Yanatori, I., Kawai, Y., & Kishi, F. (2010). Retromer-mediated direct sorting is required for proper endosomal recycling of the mammalian iron transporter DMT1. *J Cell Sci, 123*(Pt 5), 756-766. doi:10.1242/jcs.060574

Taguchi, N., Ishihara, N., Jofuku, A., Oka, T., & Mihara, K. (2007). Mitotic phosphorylation of dynamin-related GTPase Drp1 participates in mitochondrial fission. *J Biol Chem, 282*(15), 11521-11529. doi:10.1074/jbc.M607279200

Tang, F. L., Liu, W., Hu, J. X., Erion, J. R., Ye, J., Mei, L., & Xiong, W. C. (2015). VPS35 Deficiency or Mutation Causes Dopaminergic Neuronal Loss by Impairing Mitochondrial Fusion and Function. *Cell Rep, 12*(10), 1631-1643. doi:10.1016/j.celrep.2015.08.001

Tawfik, K., Kimler, B. F., Davis, M. K., Fan, F., & Tawfik, O. (2012). Prognostic significance of Bcl-2 in invasive mammary carcinomas: a comparative clinicopathologic study between "triple-negative" and non-"triple-negative" tumors. *Hum Pathol, 43*(1), 23-30. doi:10.1016/j.humpath.2011.04.011

Tewari, M., Quan, L. T., O'Rourke, K., Desnoyers, S., Zeng, Z., Beidler, D. R., . . . Dixit, V. M. (1995). Yama/CPP32 beta, a mammalian homolog of CED-3, is a CrmA-inhibitable protease that cleaves the death substrate poly(ADP-ribose)

polymerase. *Cell, 81*(5), 801-809. Retrieved from https://www.ncbi.nlm.nih.gov/pubmed/7774019

Traub, L. M., & Bonifacino, J. S. (2013). Cargo recognition in clathrin-mediated endocytosis. *Cold Spring Harb Perspect Biol, 5*(11), a016790. doi:10.1101/cshperspect.a016790

Twig, G., & Shirihai, O. S. (2011). The interplay between mitochondrial dynamics and mitophagy. *Antioxid Redox Signal, 14*(10), 1939-1951. doi:10.1089/ars.2010.3779

Ullrich, O., Reinsch, S., Urbe, S., Zerial, M., & Parton, R. G. (1996). Rab11 regulates recycling through the pericentriolar recycling endosome. *J Cell Biol, 135*(4), 913-924. doi:10.1083/jcb.135.4.913

Umebayashi, K., Stenmark, H., & Yoshimori, T. (2008). Ubc4/5 and c-Cbl continue to ubiquitinate EGF receptor after internalization to facilitate polyubiquitination and degradation. *Mol Biol Cell, 19*(8), 3454-3462. doi:10.1091/mbc.E07-10-0988

Ungewickell, E. (1999). Clathrin: a good view of a shapely leg. *Curr Biol, 9*(1), R32-35. doi:10.1016/s0960-9822(99)80040-2

Valdez, G., Akmentin, W., Philippidou, P., Kuruvilla, R., Ginty, D. D., & Halegoua, S. (2005). Pincher-mediated macroendocytosis underlies retrograde signaling by neurotrophin receptors. *J Neurosci, 25*(21), 5236-5247. doi:10.1523/JNEUROSCI.5104-04.2005

Vallis, Y., Wigge, P., Marks, B., Evans, P. R., & McMahon, H. T. (1999). Importance of the pleckstrin homology domain of dynamin in clathrin-mediated endocytosis. *Curr Biol, 9*(5), 257-260. doi:10.1016/s0960-9822(99)80114-6

van der Bliek, A. M., Redelmeier, T. E., Damke, H., Tisdale, E. J., Meyerowitz, E. M., & Schmid, S. L. (1993). Mutations in human dynamin block an intermediate stage in coated vesicle formation. *J Cell Biol, 122*(3), 553-563. doi:10.1083/jcb.122.3.553

Van Der Sluijs, P., Hull, M., Zahraoui, A., Tavitian, A., Goud, B., & Mellman, I. (1991). The small GTP-binding protein rab4 is associated with early endosomes. *Proc Natl Acad Sci U S A, 88*(14), 6313-6317. doi:10.1073/pnas.88.14.6313

Viard-Leveugle, I., Veyrenc, S., French, L. E., Brambilla, C., & Brambilla, E. (2003). Frequent loss of Fas expression and function in human lung tumours with overexpression of FasL in small cell lung carcinoma. *J Pathol, 201*(2), 268-277. doi:10.1002/path.1428

Vilarino-Guell, C., Wider, C., Ross, O. A., Dachsel, J. C., Kachergus, J. M., Lincoln, S. J., . . . Farrer, M. J. (2011). VPS35 mutations in Parkinson disease. *Am J Hum Genet, 89*(1), 162-167. doi:10.1016/j.ajhg.2011.06.001

Walseng, E., Bakke, O., & Roche, P. A. (2008). Major histocompatibility complex class II-peptide complexes internalize using a clathrin- and dynamin-independent endocytosis pathway. *J Biol Chem, 283*(21), 14717-14727. doi:10.1074/jbc.M801070200

Wang, C., & Youle, R. J. (2009). The role of mitochondria in apoptosis*. *Annu Rev Genet, 43*, 95-118. doi:10.1146/annurev-genet-102108-134850

Wang, C. L., Tang, F. L., Peng, Y., Shen, C. Y., Mei, L., & Xiong, W. C. (2012). VPS35 regulates developing mouse hippocampal neuronal morphogenesis by

promoting retrograde trafficking of BACE1. *Biol Open, 1*(12), 1248-1257. doi:10.1242/bio.20122451

Wang, E., Brown, P. S., Aroeti, B., Chapin, S. J., Mostov, K. E., & Dunn, K. W. (2000). Apical and basolateral endocytic pathways of MDCK cells meet in acidic common endosomes distinct from a nearly-neutral apical recycling endosome. *Traffic, 1*(6), 480-493. doi:10.1034/j.1600-0854.2000.010606.x

Wang, W., Ma, X., Zhou, L., Liu, J., & Zhu, X. (2017). A conserved retromer sorting motif is essential for mitochondrial DLP1 recycling by VPS35 in Parkinson's disease model. *Hum Mol Genet, 26*(4), 781-789. doi:10.1093/hmg/ddw430

Wang, W., Wang, X., Fujioka, H., Hoppel, C., Whone, A. L., Caldwell, M. A., . . . Zhu, X. (2016). Parkinson's disease-associated mutant VPS35 causes mitochondrial dysfunction by recycling DLP1 complexes. *Nat Med, 22*(1), 54-63. doi:10.1038/nm.3983

Wei, M. C., Zong, W. X., Cheng, E. H., Lindsten, T., Panoutsakopoulou, V., Ross, A. J., . . . Korsmeyer, S. J. (2001). Proapoptotic BAX and BAK: a requisite gateway to mitochondrial dysfunction and death. *Science, 292*(5517), 727-730. doi:10.1126/science.1059108

Weigert, R., Yeung, A. C., Li, J., & Donaldson, J. G. (2004). Rab22a regulates the recycling of membrane proteins internalized independently of clathrin. *Mol Biol Cell, 15*(8), 3758-3770. doi:10.1091/mbc.e04-04-0342

Wolter, K. G., Hsu, Y. T., Smith, C. L., Nechushtan, A., Xi, X. G., & Youle, R. J. (1997). Movement of Bax from the cytosol to mitochondria during apoptosis. *J Cell Biol,*

139(5), 1281-1292. Retrieved from https://www.ncbi.nlm.nih.gov/pubmed/9382873

Woodman, P. G. (2000). Biogenesis of the sorting endosome: the role of Rab5. *Traffic, 1*(9), 695-701. doi:10.1034/j.1600-0854.2000.010902.x

Wurmser, A. E., Sato, T. K., & Emr, S. D. (2000). New component of the vacuolar class C-Vps complex couples nucleotide exchange on the Ypt7 GTPase to SNARE-dependent docking and fusion. *J Cell Biol, 151*(3), 551-562. doi:10.1083/jcb.151.3.551

Xie, S., Bahl, K., Reinecke, J. B., Hammond, G. R., Naslavsky, N., & Caplan, S. (2016). The endocytic recycling compartment maintains cargo segregation acquired upon exit from the sorting endosome. *Mol Biol Cell, 27*(1), 108-126. doi:10.1091/mbc.E15-07-0514

Xie, S., Reinecke, J. B., Farmer, T., Bahl, K., Yeow, I., Nichols, B. J., . . . Caplan, S. (2018). Vesicular trafficking plays a role in centriole disengagement and duplication. *Mol Biol Cell, 29*(22), 2622-2631. doi:10.1091/mbc.E18-04-0241

Xu, X. P., Zhai, D., Kim, E., Swift, M., Reed, J. C., Volkmann, N., & Hanein, D. (2013). Three-dimensional structure of Bax-mediated pores in membrane bilayers. *Cell Death Dis, 4*, e683. doi:10.1038/cddis.2013.210

Yang, E., Zha, J., Jockel, J., Boise, L. H., Thompson, C. B., & Korsmeyer, S. J. (1995). Bad, a heterodimeric partner for Bcl-XL and Bcl-2, displaces Bax and promotes cell death. *Cell, 80*(2), 285-291. Retrieved from https://www.ncbi.nlm.nih.gov/pubmed/7834748

Yin, H. L., & Janmey, P. A. (2003). Phosphoinositide regulation of the actin cytoskeleton. *Annu Rev Physiol, 65*, 761-789. doi:10.1146/annurev.physiol.65.092101.142517

Yoshida, Y., Kinuta, M., Abe, T., Liang, S., Araki, K., Cremona, O., . . . Takei, K. (2004). The stimulatory action of amphiphysin on dynamin function is dependent on lipid bilayer curvature. *EMBO J, 23*(17), 3483-3491. doi:10.1038/sj.emboj.7600355

Youle, R. J., & Strasser, A. (2008). The BCL-2 protein family: opposing activities that mediate cell death. *Nat Rev Mol Cell Biol, 9*(1), 47-59. doi:10.1038/nrm2308

Yun, J., Puri, R., Yang, H., Lizzio, M. A., Wu, C., Sheng, Z. H., & Guo, M. (2014). MUL1 acts in parallel to the PINK1/parkin pathway in regulating mitofusin and compensates for loss of PINK1/parkin. *Elife, 3*, e01958. doi:10.7554/eLife.01958

Zerial, M., & McBride, H. (2001). Rab proteins as membrane organizers. *Nat Rev Mol Cell Biol, 2*(2), 107-117. doi:10.1038/35052055

Zhang, J., Naslavsky, N., & Caplan, S. (2012). EHDs meet the retromer: Complex regulation of retrograde transport. *Cell Logist, 2*(3), 161-165. doi:10.4161/cl.20582

Zhang, J., Reiling, C., Reinecke, J. B., Prislan, I., Marky, L. A., Sorgen, P. L., . . . Caplan, S. (2012). Rabankyrin-5 interacts with EHD1 and Vps26 to regulate endocytic trafficking and retromer function. *Traffic, 13*(5), 745-757. doi:10.1111/j.1600-0854.2012.01334.x

Zhao, J., Liu, T., Jin, S., Wang, X., Qu, M., Uhlen, P., . . . Nister, M. (2011). Human MIEF1 recruits Drp1 to mitochondrial outer membranes and promotes mitochondrial fusion rather than fission. *EMBO J, 30*(14), 2762-2778. doi:10.1038/emboj.2011.198

Zimmerberg, J., & Kozlov, M. M. (2006). How proteins produce cellular membrane curvature. *Nat Rev Mol Cell Biol, 7*(1), 9-19. doi:10.1038/nrm1784

Zimprich, A., Benet-Pages, A., Struhal, W., Graf, E., Eck, S. H., Offman, M. N., . . . Strom, T. M. (2011). A mutation in VPS35, encoding a subunit of the retromer complex, causes late-onset Parkinson disease. *Am J Hum Genet, 89*(1), 168-175. doi:10.1016/j.ajhg.2011.06.008

Zwilling, D., Cypionka, A., Pohl, W. H., Fasshauer, D., Walla, P. J., Wahl, M. C., & Jahn, R. (2007). Early endosomal SNAREs form a structurally conserved SNARE complex and fuse liposomes with multiple topologies. *EMBO J, 26*(1), 9-18. doi:10.1038/sj.emboj.7601467